Ichnology and sedimentology of large tetrapod burrows in the latest Early Triassic Katberg Formation, south-eastern main Karoo Basin, South Africa

William Desmond Krummeck

Dissertation presented for the degree of Master of Science

Department of Geological Sciences

University of Cape Town

February 2013

DECLARATION

I hereby declare that all of the work presented in this thesis is my own, except where otherwise stated in the text

William Desmond Krummeck

11 February 2013

Abstract

Trace fossils in the form of large (~11 cm diameter and up to 2 m in length) burrows were studied at three localities in the Early Triassic Katberg Formation in the south-eastern and central parts of the main Karoo Basin, Eastern Cape, South Africa. The most interesting site, Hobbs Hill, north-west of Cathcart (Eastern Cape) has numerous burrows, contains an exceptionally well exposed sedimentary succession and bone beds. This site is also the type locality for the holotype of the parareptile *Kitchingnathus untabeni* (BP/1/1187).

The aims of this dissertation are to: 1) reconstruct the local paleoenvironments of the burrow localities; 2) determine the purpose of the burrows; 3) identify the possible burrow makers based on the sedimentology and burrow morphology and 4) attempt to use photogrammetry and low-cost hardware to produce 3D digital burrows for improved descriptions. Insights into the survival strategies and behaviours of organisms during the P/T extinction recovery period are explored. Detailed analysis is mainly done on observations from the Hobbs Hill site; the results and interpretations are important for and compatible with the entire Katberg Formation.

The interactions between the physical (sedimentary) and biological (animal behaviour) processes are important in ichnology and paleoenvironmental reconstruction. The analyses have therefore been undertaken through a multidisciplinary approach based on ichnological, sedimentological, petrographical, stratigraphic and paleontological evidence, gathered both in the field and laboratory.

At Hobbs Hill, the bilobate cross-sectional shape, scratch marks, low-angle ramp, sub-linear architecture and size of the burrows exclude invertebrates and aquatic organisms but favour tetrapods as possible trace makers. Comparative analysis and repeated associations suggests that *Procolophon trigoniceps* is the most likely producer. The palaeo-current indicators imply an ancient flow direction towards northwest, whereas the east dipping, shallow accretionary surfaces suggest lateral channel migration in low-sinuosity to braided, sandy river systems.

The study shows that semi-fossorial or fossorial behaviour was utilized by tetrapods, that protected them from the harsh environment, in riverbank or floodplain sub-environments of a low sinuosity to braided sandy river system. Early Triassic organisms in the Karoo Basin had to contend with a dynamic environment characterized by flooding and periods with high levels of evaporation.

Table of Contents

1. Introduction 1

Context of the research 3

2. Background 5

2.1. Karoo Basin stratigraphy 5

2.1.1. Dwyka Group 6

2.1.2. Ecca Group 7

2.1.3. The Beaufort Group 7

2.2. The Triassic 14

2.2.1. Triassic continental configuration 14

2.2.2. Tectonic setting of the Karoo Basin 16

2.2.3. Triassic climate 19

2.2.4. Triassic climate of the Karoo Basin 25

2.2.5. Triassic stratigraphy 27

2.2.6. *Lystrosaurus* Assemblage Zone 31

2.3. 3D digital burrows 32

3. Methodology 35

3.1. Introduction 35

3.2. The study area 35

3.3. Sedimentology 37

3.3.1. Observations 37

3.3.2. Facies Analysis 38

3.3.3. Architectural element analysis 39

3.4. Ichnology 40

3.4.1. Inorganic Origin 40

3.4.2. Field Techniques 40

3.4.3. Sample processing 44

3.5. Photogrammetry 46

3.5.1. Introduction 46
3.5.2. Definitions 46
3.5.3. Photogrammetry workflow 49
3.6. Palaeontology descriptions and analysis 51
4. Sedimentological Results 52
4.1. Introduction 52
4.2. Facies Descriptions and Assemblages 52
4.2.1. Sandstone facies assemblage 55
4.2.2. Fine-grained facies assemblage 66
4.3. Architectural Element Analysis 72
4.3.1. Channel elements (CH) 72
4.3.2. Sandy Bedforms (SB) 73
4.3.3. Lateral Accretion elements (LA) 73
4.3.4. Floodplain Fines Element (FF) 74
4.4. Sedimentology of the burrow fill 75
4.4.1. Displacive carbonate 76
5. Ichnological Results 79
5.1. Bioturbation 79
5.2. Architectural morphology 82
5.3. The burrow fill 87
5.4. Surficial Morphology 90
5.5. Digital 3D burrow sample 94
6. Interpretations 98
6.1. Sedimentary facies interpretations 98
6.1.1. The sandstone facies assemblage 98
6.1.2. The fine-grained facies assemblage 100
6.1.3. Sedimentary interpretations of the burrow fill 101
6.2. The Low sinuosity sand-bed River Fluvial Styles 105

7. Burrow Producer Identification 107
7.1. Possible Producers 107
7.1.1. Invertebrates (arthropods) 107
7.1.1. Lungfish 108
7.1.2. Tetrapods 108
7.2. Studies of fossils bearing-burrows 109
7.2.1. Late Permian spiralling burrows 109
7.2.2. *Trirachodon* complex burrow systems 114
7.2.3. *Thrinaxodon* containing burrow 116
7.3. Studies on burrows not containing fossil in "life position" 120
7.3.1. Burrow resembling *Spongeliomorpha* 120
7.3.2. Large burrow of the Palingkloof Member 121
7.3.3. Large Burrow in the Katberg Formation Bordy *et al*. (2011) 122
7.3.4. Ichnogenus A 123
7.3.5. Type G burrows of Miller 126
7.4. Fossils found in association with burrows 130
7.5. 3D digital burrows 132
8. Conclusions 136
9. Acknowledgements 142
10. References 143

1. Introduction

"Among one and another rock layers, there are the traces of the worms that crawled in them when they were not yet dry." - Leonardo Da Vinci (1452-1519) (Baucon, 2010)

Ichnology is the study of trace fossils. A trace fossil is the trace or impression made by an organism preserved in sediment, which can be used to infer the organism's behaviour (Seilacher, 1967). Preservation of evidence for behaviours of organisms is implicit of but not a defining characteristic of trace fossils. Trace fossils can therefore give an indication of the environmental conditions that influenced the behaviour of the organisms that created them (Seilacher, 1967). The focus of ichnology in the past has been on marine trace fossils, but in the last few decades there has been increased interest in large penetrative burrows in terrestrial environments as well (Smith, 1987; Groenewald, 1991; Groenewald *et al.*, 2001; Miller *et al.*, 2001; Damiani *et al.*, 2003; Hasiotis *et al.*, 2004; Abdala *et al.*, 2006; Sidor *et al.*, 2008; Bordy *et al.*, 2011).

The aim of this study is to determine the origin and the possible trace makers of burrow casts found in Lower Triassic rocks in South Africa (Figure 1). These rocks and their fossil content date back to the earliest Triassic when life was recovering after the Permo-Triassic extinction event during which nearly 90% of all life was wiped out (Ward *et al.*, 2000). The Hobbs Hill deposits are from the Olenekian (249.5-245.9 Ma) based on the occurrence of *Procolophon trigoniceps* (Neveling, 2004; Cisneros, 2008). With the Permo-Triassic exctinctions event occurring at 252.28±0.08Ma, these deposits record the conditions and processes taking place less than 3 million years after the biocrisis (Shen *et al.*, 2011). Several burrow casts of ~11 cm in diameter and up to 2 m in length, morphologically similar to those described from the Triassic of Antarctica, were found in the Katberg Formation (*Lystrosaurus* Assemblage Zone) in the Free State and Eastern Cape (South Africa, Figure 1) (Miller *et al.*, 2001; Rubidge, 2005). The Hobbs Hill locality, (Eastern Cape, NW of Cathcart) previously produced several vertebrate fossils and is the type locality for the holotype of *Kitchingnathus untabeni* (BP/1/1187).

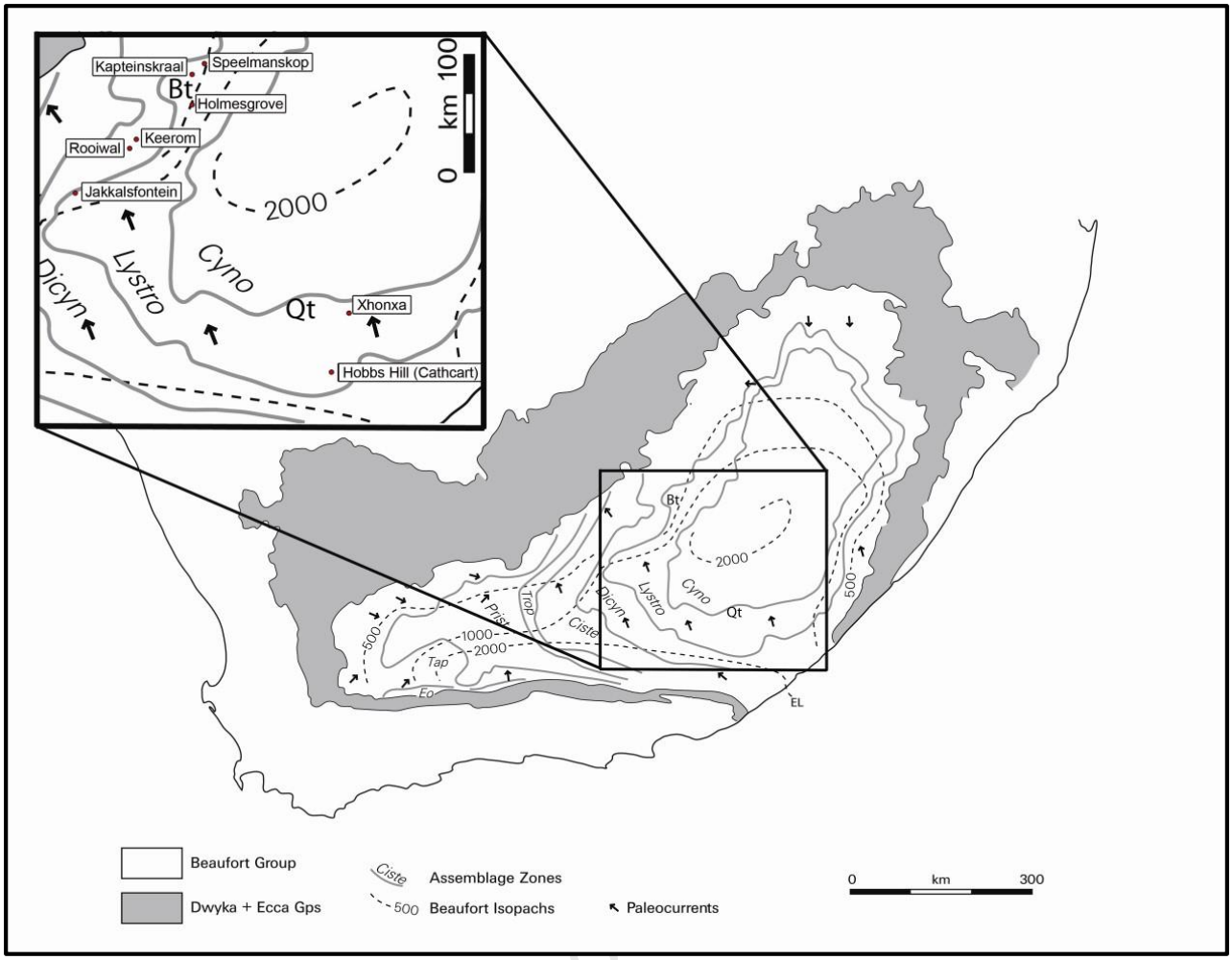

Figure 1. Schematic geological map of the Karoo Basin in South Africa showing the Beaufort Group (white) and its biostratigraphic assemblage zones. Inset shows the positions of the eight study sites. (EL = East London; Bt = Bethulie; Qt = Queenstown - modified from Tankard *et al.*, 2009).

The main research questions investigated in this study are:

1) What organisms created the trace fossils at Hobbs Hill?
2) Why were the burrows created?
3) What was the depositional environment at the study sites during the Early Triassic?
4) Can photogrammetry be used to create digital 3D copies of burrows for a more accurate description of these complex trace fossils?

To answer these questions, a multidisciplinary approach was employed incorporating field and laboratory methods and principles of ichnology, sedimentology, palaeontology petrography and stratigraphy. Although these fields are highly specialised, they share a common line of reasoning concerning the understanding of evidence of processes that occurred in the past by considering

those which occur in modern times. Uniformitarianism is one of the most fundamental concepts of geology and it supposes that the physical processes occurring today are very similar to those that occurred in the past or in other words "the present is key to the past", a concept defined by James Hutton in late 18th century (Boggs, 2006).

Context of the research

Because trace fossils provide a record of past organisms behaviour, they can be used to understand how organisms responded to changes in the environment. Trace fossils, in conjunction with physical sedimentary structures, may provide valuable insights into the physical, chemical and biological processes that occurred in the ecosystem at the time of deposition (Seilacher, 1967). Studies of large penetrative burrows in fluvial floodplain deposits are relatively rare, especially in comparison to other forms of trace fossils in similar non-marine environments (Miller *et al.*, 2001). Bone beds are sedimentary beds that contain large concentrations of fossils, belonging to more than one organism. Bone beds can form in a variety of ways, by studying the preservation and articulation of the fossils, the process by which the bone beds formed can be determined. The study of fossilized bone and its origin (palaeontology and taphonomy) can identify the species that occurred in association with the burrows and the processes that took place between death and mineralization (Efremov, 1940; Seilacher, 2007; Baucon, 2010).

The burrows are found in sedimentary sequences of the Katberg Formation (Figure 1), which were deposited during the delayed period of recovery of life after the largest mass extinction event in the Earth's history at the end of the Permian at 252.28±0.08Ma (Smith and Botha, 2005; Cisneros, 2008; Retallack *et al*., 2011; Shen *et al*., 2011). This event wiped out over 90% of marine species and 70% of terrestrial vertebrate families (Smith, 1995; Ward *et al.*, 2000; Rubidge, 2005). It is during this delayed recovery period when most vertebrate taxa were going extinct that procolophonoids were paradoxically radiating (Botha *et al*., 2007). The late Early Triassic is characterised by high levels of CO_2, high global temperatures, seasonal megamonsoons and no

permanent ice caps in the polar regions (Scotese and McKerrow, 1990; Dubiel *et al.*, 1991; Parrish, 1993; Wignall, 2001; Chumakov and Zharkov, 2002; Kidder and Worsley, 2004; Payne *et al.*, 2004; Royer *et al.*, 2004; Gradstein *et al.*, 2005; Kiehl and Shields, 2005; Beerling *et al.*, 2007; Svensen *et al.*, 2007, 2009a, 2009b; Preto *et al.*, 2010; Svensen and Jamtveit, 2010).

The Karoo Basin was experiencing similar conditions at the same time with increasingly arid conditions, seasonal climate and low water tables indicated by the sedimentary evidence (Johnson, 1976; Hiller and Stavrakis, 1984; Smith, 1990; Smith and Botha, 2005; Keyser, 1966 in Catuneanu *et al.*, 2005). The depositional environment was a alluvial fan with a system of braided and meander rivers draining into an area previously occupied by the Ecca sea, now silted up (Johnson, 1976; Hiller and Stavrakis, 1984; Neveling, 2004; Johnson *et al.*, 2006; Pace *et al.*, 2009; Bordy *et al.*, 2011). The fauna during the Early Triassic included temnospondyls, non-mammalian cynodonts, species of the dicynodont genus Lystrosaurus and the radiating procolophonoids (Rubidge, 2005; Botha *et al*., 2007).

Studying the behaviour of organisms during this exceptional period in the history of life on land could provide clues about how some life forms managed to survive and even thrive and whether burrowing strategies gave them an advantage over other vertebrate taxa (Erwin, 1998; Botha *et al*., 2007). This study may add to the understanding of the environmental conditions experienced by organisms during the Early Triassic of the southeastern part of South Africa.

2. Background

2.1. Karoo Basin stratigraphy

The Karoo Basin is part of an intracratonic retroarc foreland system that extended across the south-western margin of Gondwana from the Late Carboniferous to Jurassic (Lock, 1978; Tankard *et al.*, 1982; Cole, 1992; Duncan *et al.*, 1997; Turner, 1999; Neveling, 2004). The foreland system developed in response to the compression related to the subduction of the paleo-Pacific (or Panthalassian) plate along the south-western margin of Gondwana (Figure 2) (Lock, 1978; Tankard *et al.*, 1982; De Wit and Ransome, 1992; Catuneanu and Elango, 2001). It is preserved in the fragments of the supercontinent namely the Parana Basin in South America, the Beacon Basin in Antarctica, the Bowen Basin in Australia and the Karoo Basin in South Africa (Figure 2). The Karoo Basin is one of the largest, covering two thirds of the surface of South Africa, and the thickest, up to 12km in the southern parts (calculate by adding the thickest exposures; Johnson, 1976). It overlies the Kaapvaal Craton in the north, the Namaqua-Natal Mobile Belt in the south and the Cape Supergroup in the southwest; bounded by the Cape Fold Belt along its southern margin (Tankard *et al.*, 1982; Johnson *et al.*, 1996; Trouw and De Wit, 1999). The Karoo Supergroup was deposited after a ~30My hiatus subsequent to the termination of the deposition of the Cape Supergroup (Catuneanu *et al.*, 1998). It consists of primarily sedimentary groups and one final igneous group, in chronological order namely the Dwyka, Ecca, Beaufort, Stormberg and Drakensberg Groups, respectively (Johnson, 1976; Lock, 1978; Tankard *et al.*, 1982; Smith, 1990; Cole, 1992; Catuneanu *et al.*, 2005). The ages of the groups have been determined by radiometric dating of ash beds and biostratigraphic correlation of vertebrate assemblage zones (Cole, 1992; Rubidge *et al.*, 1995, 2013; Bangert *et al.*, 1999; Catuneanu *et al.*, 2005).

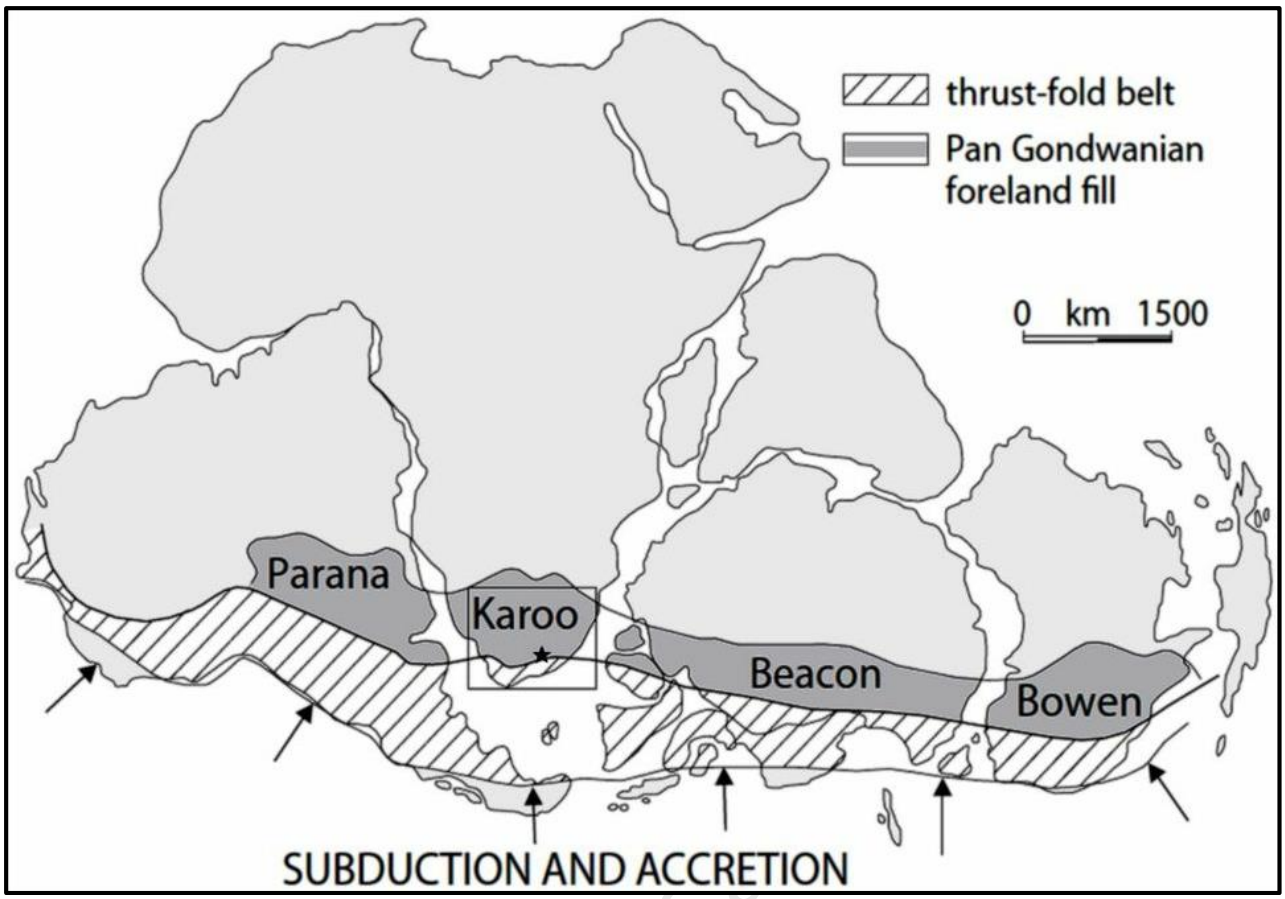

Figure 2. The foreland system along the paleo-Pacific margin of Gondwana that contained the Karoo Basin. The study area is indicated by a star (taken from Catuneanu and Elango, 2001).

2.1.1. Dwyka Group

The Dwyka Group has been dated 302-290Ma based on U-Pb radiometric dating of ash beds in the Dwyka in Namibia and near the base of the Ecca in South Africa (Bangert *et al.*, 1999). The base is generally unconformable, where it overlies the Cape Supergroup and the Natal Group, and conformable east of 23°E where the base is defined by the first occurrence of polymictic diamictites overlying the Miller Diamictite Formation of the Witteberg Group (Cape Supergroup) (Visser *et al.*, 1990). The top diachronous with the Ecca Group being deposited in the south (proximal) earlier than in the north (distal) (Cole, 1992; Catuneanu *et al.*, 2005). In the south the Dwyka Group is thicker (up to 700 m) consisting of mainly massive diamictites, while in the north is fine-grained dominated (42%) with lesser massive and laminated diamictites making up equal proportions of the sediments (Visser, 1989). The massive diamictites are poorly sorted and composed of clasts ranging from pebbles to boulder in a silty matrix (Tankard *et al.*, 1982; Visser, 1989).The uniformity and

lateral continuity of the massive diamictites suggests suspension settling in the south (Tankard *et al.*, 1982). In the north, the basement rocks have striations, grooves and friction cracks characteristic of a glacial pavement (Tankard *et al.*, 1982). During the Late Carboniferous, the Karoo Basin was situated near the South Pole and the global climate was cooling (Figures 1, 2, 3 and 6) (Scotese and McKerrow, 1990). The proximal Dwyka Group is considered to have been deposited in a glacio-marine environment with sediment transported from the south, in the northern parts of the basin the glaciers moved over land from the Cargonian Highlands in the north towards the marine environment in the south (Figure 3) (Visser, 1989).

2.1.2. Ecca Group

As Gondwana moved towards the equator, the location of the Karoo Basin migrated with it from the polar regions in the Late Carboniferous to between 50º and 70º latitude during the Permian. The basal units of the Ecca Group have been dated using zircons from two different ash tuff horizons, indicating its deposition was initiated by 288±3 and 289±3.8 Ma (Bangert *et al.*, 1999). In the south, the Ecca-Dwyka contact is gradual as the depositional environment changed from deep glacio-marine to marine; this change is marked by a decrease and eventual absence of dropstones. In the north, the contact is more obvious in places as the latest Dwyka contains coal deposits that are overlain by transgressive marine deposits of the Ecca Group (Smith *et al.*, 1993). The formations summarised in Figure 3 record the filling up of Ecca Sea, preserving sedimentary facies indicating deep marine, distal to proximal submarine fan, to shallow and marginal marine or deltaic depositional environments (Johnson, 1976; Catuneanu *et al.*, 2005). The Ecca Group represents the last marine deposits of the Karoo Basin.

2.1.3. The Beaufort Group

The non-marine Beaufort Group diachronously and conformably overlies the Ecca Group and was deposited from the Middle Permian to Early Triassic (Figure 3) (Johnson, 1976; Catuneanu *et al.*, 1998). It is subdivided into a lower and upper subgroup, the Adelaide and Tarkastad Subgroup

respectively (Johnson, 1976; Catuneanu *et al.*, 2005). In the south (proximal facies), the Adelaide Subgroup is divided into three formations, in chronological order: Koonap, Middleton and Balfour (Neveling, 2004). The Koonap Formation grades into the Abrahamskraal Formation towards the west; while the Middleton and Balfour Formation grade in to the Teekloof Formation correspondingly (Figure 3) (Smith, 1993; Catuneanu *et al.*, 2005). The Tarkastad Subgroup consists of the Katberg Formation at the base and the conformable Burgersdorp Formation at the top. Together these two form a single fining upwards sequence (Johnson, 1976; Neveling, 2004).

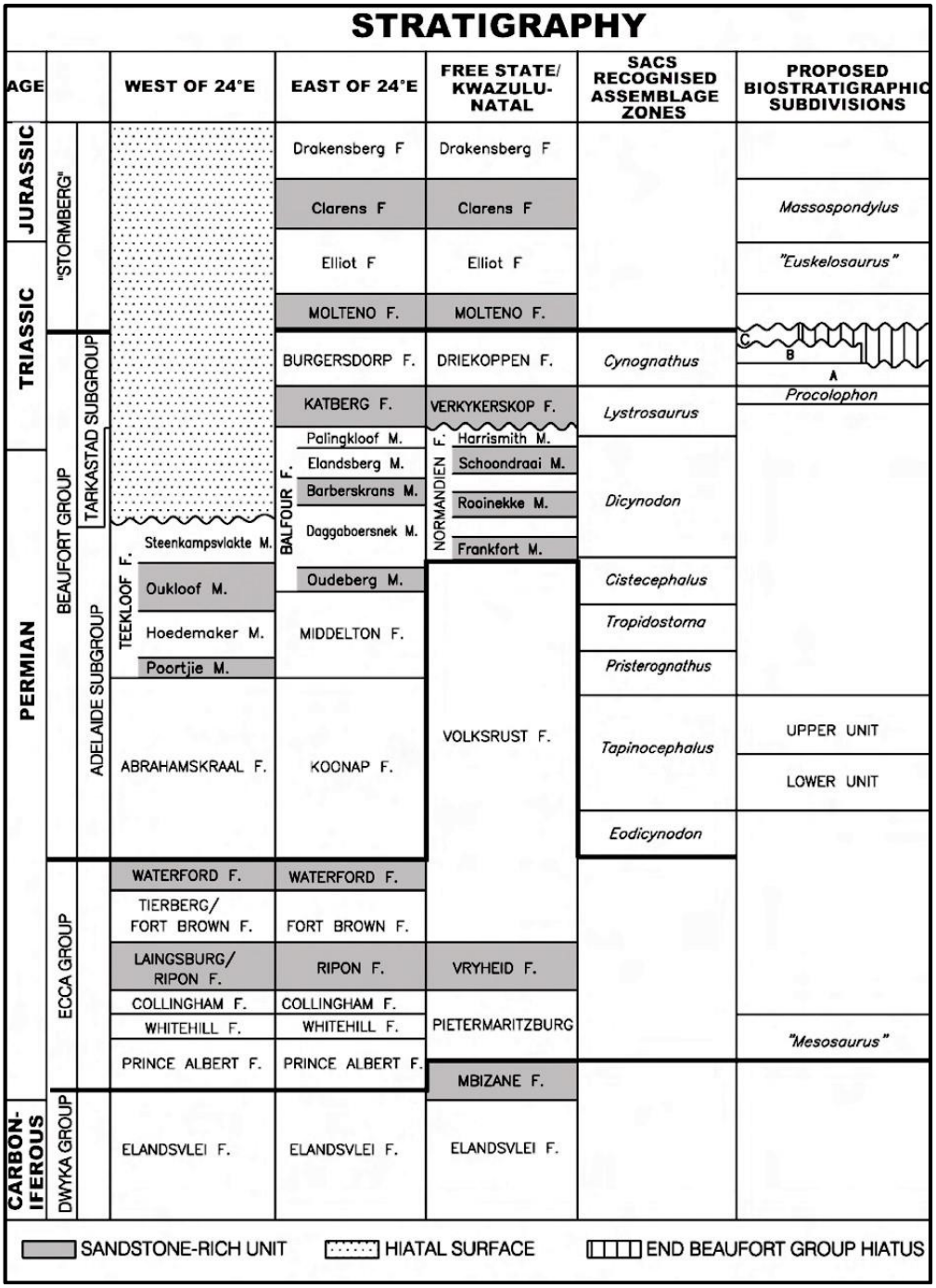

Figure 3. The lithostratigraphy and biostratigraphy of the Beaufort Group summarised for the different parts of the Karoo Basin (taken from Rubidge, 2005).

The Koonap Formation is dominated by dark grey siltstone and mudstone units with subordinate interbedded yellowish and bluish-greenish-grey lenticular sandstones (Johnson, 1976; Smith *et al.*, 1993). The mudstones and interbedded sandstones form fining upward cycles in the upper part of the formation (Smith *et al.*, 1993; Catuneanu *et al.*, 2005). The depositional environments have been interpreted to range from meandering to braided fluvial systems, draining into shallow lakes (Smith *et al.*, 1993; Catuneanu *et al.*, 2005). The overlying Middleton Formation contains greater

proportions of mudstone with interbedded sandstone units that are fining upwards (Smith *et al.*, 1993; Catuneanu *et al.*, 2005). The depositional environments are interpreted to change from meandering at the base to more lacustrine towards the top (Smith *et al.*, 1993; Catuneanu *et al.*, 2005). These first two formations can be considered to form a single fining upwards sequence (Smith *et al.*, 1993; Catuneanu *et al.*, 2005). The Balfour Formation unconformably overlies the Middleton Formation and is characterised by fining upward cycles consisting of erosive sandstones at the base and the dominant lithologies, mudstones and siltstones, towards the top (Smith *et al.*, 1993; Catuneanu and Elango, 2001; Catuneanu *et al.*, 2005). Three members worth mentioning are:

1) Oudeberg Member defines the base of the Balfour Formation and is dominated by fining upward sandstone sequences deposited in a low sinuosity system;
2) Baberskrans Member consists of subordinate laterally accreted sandstone packages;
3) Palingkloof Member 20m below the Katberg Formation is considered to contain the Permo-Triassic boundary (Johnson, 1976; Smith *et al.*, 1993; Catuneanu and Elango, 2001; Smith and Ward, 2001).

The depositional environments that are represented include braided to meandering fluvial systems within vast floodplains (Johnson, 1976; Visser and Dukas, 1979 in Catuneanu and Elango, 2001).

Tarkastad Subgroup

The (un)conformable nature of the contact between the Katberg Formation and the underlying Balfour Formation is debated (Catuneanu *et al.*, 1998; Neveling, 2004). The top of the Burgersdorp Formation is unconformably overlain by the Molteno Formation of the Stormberg Group (Hiller and Stavrakis, 1984; Catuneanu *et al.*, 1998, 2005). The Tarkastad Subgroup is particularly important as it records the period when life recovered after the Permo-Triassic extinction and contains the trace fossils of this study (Retallack *et al.*, 2003; Kidder and Worsley, 2004; Johnson *et al.*, 2006; Preto *et al.*, 2010).

The Katberg Formation was initially referred to as the Middle Beaufort Beds (Du Toit, 1917 in Johnson, 1976) and was first referred to as the Katberg Sandstones after the Katberg Pass in the Winterberg Range by Johnson in 1966 (Eastern Cape) (Du Toit, 1917 in Johnson, 1976; Neveling, 2004). It is an arenaceous unit with varying amounts of subordinate thin (2-10m) red, olive-yellow and greenish mudstones (Johnson, 1976; Hiller and Stavrakis, 1984; Neveling, 2004; Pace *et al.*, 2009). The sandstones are predominantly light olive grey, greenish grey or light brownish grey, predominantly fine- to medium-grained. Coarse to pebbly (up to 15 cm) sandstones occur in coastal exposures near East London where it consists of 90% sandstone (Johnson, 1976; Hiller and Stavrakis, 1984; Neveling, 2004; Johnson *et al.*, 2006). The sandstone-mudstone ratio decreases northward until it is difficult to distinguish the Katberg Formation from the conformably overlying Burgersdorp Formation. In the south, the sandstones are coarser grained, mudstones are less common, ripple cross-laminations are absent and massive beds are more common in the Katberg Formation (Hiller and Stavrakis, 1984; Neveling, 2004; Johnson *et al.*, 2006).

The Katberg Formation has a maximum thickness of 1238m near East London and thins out towards the north, to 760m at Groot Winterberg, to 370m at Graaff Reinet and to 70m at Inzicht (Johnson, 1976; Hiller and Stavrakis, 1984; Neveling, 2004; Johnson *et al.*, 2006). Similar to the

grain size, the thickness of the sandstone beds and packages of sandstone beds decrease northwards. The sandstone occur in thin (less than 1.5m), tabular sheets, bounded by sharp and erosional surfaces, which are laterally extensive and stacked vertically into multistory tabular forms 5-10m thick (Pace *et al.*, 2009). The term macroform refers to sandbar or barforms which have been deposited in multiple sedimentary events over tens to thousands of years and are those features of present day rivers which are visible at aerial photograph scale (Miall, 1985). The architectural elements of the sandstone bodies of the Katberg Formation include lateral, vertical and downstream accretion bars and forms or macroforms and sandy barforms (Pace *et al.*, 2009; Bordy *et al.*, 2011). Intra-formational mud clast and reworked pedogenic nodule conglomerate lenses are common; large, *in situ* brown-weathering calcareous concretions (3-10 cm) are also common (Hiller and Stavrakis, 1984; Neveling, 2004). The sedimentary structures in the sandstone are predominantly horizontal laminations and ripple cross-laminations, planar- and trough-cross bedding (Hiller and Stavrakis, 1984; Neveling, 2004; Johnson *et al.*, 2006).

The distinction between the Katberg and Burgersdorp Formations based on sandstone content becomes increasingly difficult north of 31ºS as the amount of sandstone in the Subgroup decreases (Johnson, 1976; Van Eeden, 1937 and Du Toit, 1954 in Neveling, 2004). Hiller and Stavrakis (1984) proposed that the Katberg Formation is the proximal higher energy equivalent of the Burgersdorp Formation, which was deposited under lower energy conditions, in a more distal fluvial environment. Neveling (2004) showed that the Katberg and Burgersdorp Formations are not lateral equivalents because arenaceous marker horizons are traceable throughout the proximal and distal parts of the Katberg and Burgersdorp Formations. Biostratigraphic investigations of the formations also do not support the supposition that the Katberg Formation is the proximal equivalent of the Burgersdorp Formation (Neveling, 2004).

The Katberg Formation in the south is considered to have been deposited in alluvial fan and braided stream environments, because of the relatively coarse grain size; the geometries, lateral extent and thickness of sandstone beds; the presence of up to 15 cm pebbles; the massive beds and the lack of well-developed fining upward sequences (Smith *et al.,* 1993; Catuneanu *et al.,* 1998; Catuneanu *et al.,* 2005; Johnson *et al.,* 2006). In the north, the presence of fining-upward cycles and the increase in mudstone layers indicate a decrease in energy levels in the depositional environment, and thus suggest the dominance of meandering fluvial systems (Johnson *et al.,* 2006). According to Neveling (2004), the pedogenic calcareous nodules formed in alkaline soils when the rate of evapotranspiration was much higher than the precipitation. Based on the lithofacies of the Katberg Formation and close analogies to sedimentary features of rivers in modern arid to semi-arid settings, it is believed that the fluvial systems of Early Triassic were non-perennial, but rather ephemeral (Neveling, 2004).

2.2. The Triassic

2.2.1. Triassic continental configuration

The geological history of global plate tectonics, including the continental configuration and movement of tectonic plates have been determined for the past 750 Ma based on evidence from linear magnetic anomalies produced by sea floor spreading, palaeomagnetism, hotspot tracks, large igneous provinces (LIPs), tectonic fabrics of the ocean floor, lithologic indicators of climate (e.g., coal, evaporites) (Scotese, 2004). The degree of uncertainty of these reconstructions increases with geological time as the rock record is less likely to survive or becomes distorted and thus less reliable (Scotese, 2004).

The Triassic Period represents a climax of aggregated continental crust and exposed land area in the form of the supercontinent Pangaea (Dubiel *et al.*, 1991). This continental aggregation started in the Carboniferous with the collision of Gondwana and Laurasia, and continued into the Triassic with the collision of Kazakhstan, Siberia, parts of China and southeastern Asia (Dubiel *et al.*, 1991). The supercontinent, possibly the largest ever, extended from 85^{o}N to 90^{o}S, was surrounded by the Panthalassian Ocean and cut into by the deep Tethys oceanic gulf. The Tethys was situated between 30^{o}N and 30^{o}S in the tropical (equatorial) to subtropical belt (Dubiel *et al.*, 1991; Ziegler *et al.*, 1993, 2003; Sun *et al.*, 2012).

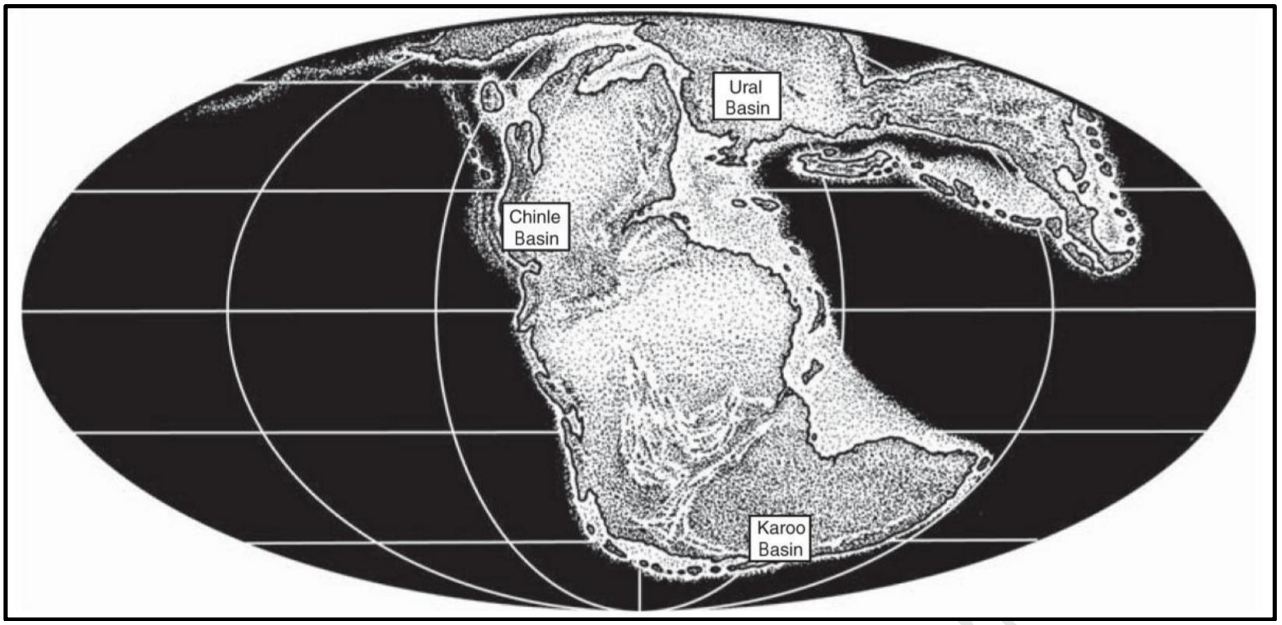

Figure 4. Map of Triassic Pangaea showing the continental configuration and the three areas that contain the land-vertebrate fossil assemblages that form the standards for the Triassic tetrapod timescale: Karoo Basin in South Africa (Lootsbergian and Nonesian); Urals Basin in Russia (Perovkan and Berdyankian) and Chinle Basin in USA (Otischalkian, Adamanian, Revueltian and Apachean) (taken from Lucas, 2010b).

This nearly pole-to-pole continental configuration resulted in few physical boundaries for biotic dispersal among terrestrial tetrapods allowing the subdivision of the Triassic Period based on terrestrial vertebrate faunal assemblages (Figure 4) (Dubiel *et al.*, 1991; Rubidge, 2005). Furthermore, the configuration of the supercontinent disrupted the atmospheric and oceanic circulation patterns and had a major impact on the global climate during the Triassic (Dubiel *et al.*, 1991; Scotese, 2004).

2.2.2. Tectonic setting of the Karoo Basin

In the southern part of the this supercontinent, in SW Gondwana, the tectonic mechanisms that produced and influenced the development of the Karoo Basin include flexural tectonics, dynamic subsidence, progradation and retrogradation of the foredeep (Catuneanu *et al.*, 1998; Catuneanu and Elango, 2001; Catuneanu, 2004a; Tankard *et al.*, 2009).

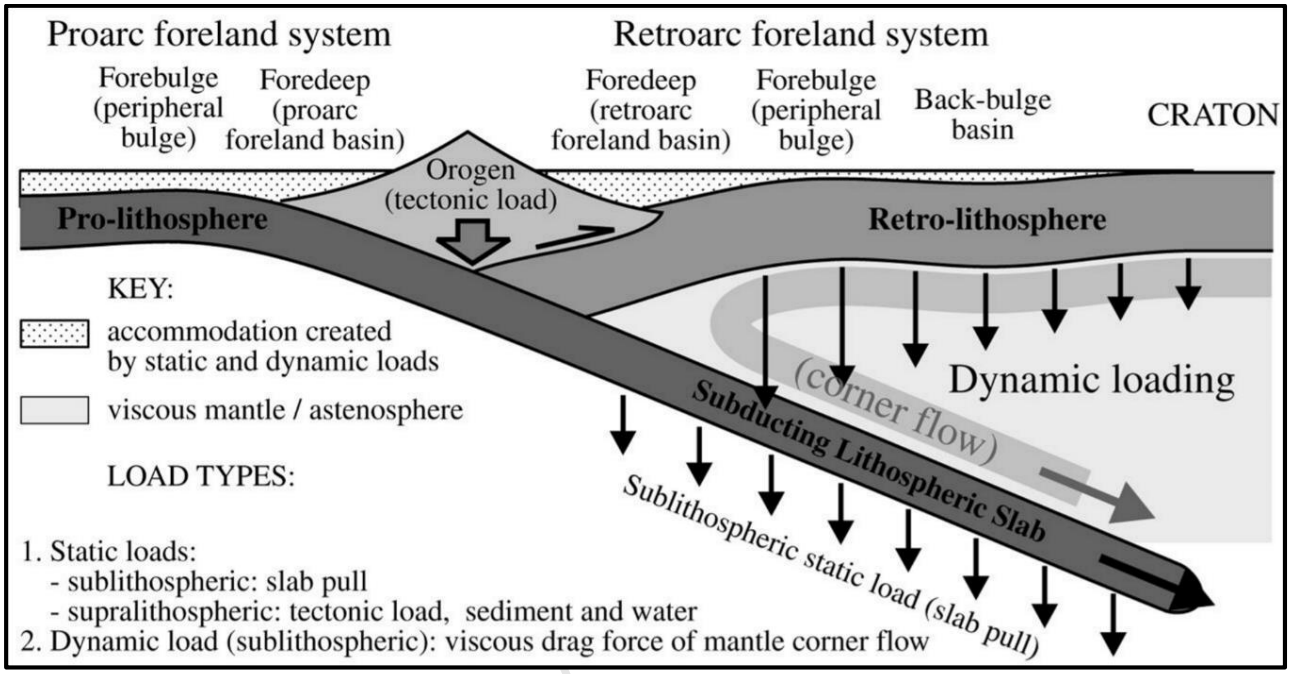

Figure 5. Schematic representation of the flexural response of the retro-lithosphere to orogenic loading, the sine shape of the continental crust, dynamic loading due to corner flow and the resulting basins and bulges (taken from Catuneanu, 2004b).

Flexural tectonics is the flexural response of the retro-lithosphere (Figure 5) to orogenic loading which produces a sine shaped deflection profile in an ideal homogeneous lithosphere (Figure 5) (Mitrovica *et al.*, 1989; Jordan, 1981 in Catuneanu, 2004). The deflected retrolithosphere is subdivided into the foredeep that experiences subsidence, the forebulge that experiences uplift and the back bulge basin that experience subsidence, during orogenic loading (DeCelles and Giles, 1996; Catuneanu *et al.*, 1998). During orogenic unloading, the opposite occurs and the foredeep becomes a foreslope while the forebulge becomes a foresag (Catuneanu *et al.*, 1998). Therefore, the distal and proximal parts of the basin experience erosion and deposition respectively at the same time during loading. This flexural behaviour explains the contrasting stratigraphies in the proximal and distal parts of the basin (Catuneanu *et al.*, 1998). The uplift and subsidence are directly

proportional to the mass of the orogenic load and inversely proportional to the flexural rigidity of the lithosphere (Catuneanu *et al.*, 1998, Catuneanu and Elango, 2001; Catuneanu, 2004b). The amplitude of the sine shaped profile decreases dramatically with distance from the orogenic load (Catuneanu *et al.*, 1998, Catuneanu and Elango, 2001; Catuneanu, 2004b). The subduction of the paleo-Pacific (or Panthalassian) plate along the southwestern margin of Gondwana resulted in viscous mantle corner flow (Figure 5), which dragged the overriding lithosphere downwards (Catuneanu, 2004b). During tectonic progradation, the depocenter migrated roughly northwards resulting in the reworking of sediments deposited in the foredeep earlier on. At the same time, the orogeny deformed and cannibalised the most proximal deposits, some of which are preserved in the Cape Fold Belt (CFB) (Catuneanu, *et al.*, 1998).

During the Early Triassic, the Karoo Basin was still in the compressive phase of the first order orogenic cycle terminating during the breakup of Gondwana (Middle Jurassic) (Catuneanu *et al.*, 1998). Second order orogenic cycles related to events such as folding, thrusting and supracrustal loading (paroxysms) are dated in the Cape Fold Belt, punctuate cycles of flexural tectonics that are recorded in the stratigraphic record (Catuneanu *et al.*, 1998). The Tarkastad Subgroup (Katberg and Burgersdorp Formations) was deposited during orogenic loading with the depocenter in the more proximal or southern part of the basin, orogenic unloading occurred directly before and after its deposition and may account for the unconformities at the upper and lower contacts (Catuneanu *et al.*, 1998). This model also explains the very large differences in formations moving from south to north (Catuneanu *et al.*, 1998).

Flexural tectonics is presented by Catuneanu (op. cit.) as one of the most important controls on the stratigraphy of the Karoo Basin and is described above for this reason. Tankard *et al.* (2009) however presents arguments to the contrary and they contend that the basement architecture, timing of the Cape Orogeny and the stratigraphic relationships of the Karoo Basin are atypical of a flexural

foreland basin. Tankard *et al.* (2009, 2012) propose that the subsidence in the Karoo Basin (from the Triassic onwards) and Karoo magmatism (Drakensberg Group) was controlled primarily by first order basement faults and the movements of the basement blocks between them. First-order basement faults refer to faults such as the Colesberg-Trompsburg Fault zone (east-dipping) which divides the eastern and western blocks of the Archaean Kaapvaal Craton; the Doringberg fault along the southern margin of the Kaapvaal Craton (Tankard *et al.*, 2009, 2012).

2.2.3. Triassic climate

Several concepts simplify the understanding of global climate and climate change. The most important concept is the alternating global Hot and Ice House conditions and the existence of global climate belts parallel to lines of latitude (Scotese *et al.*, 1999; Kidder and Worsley, 2010).

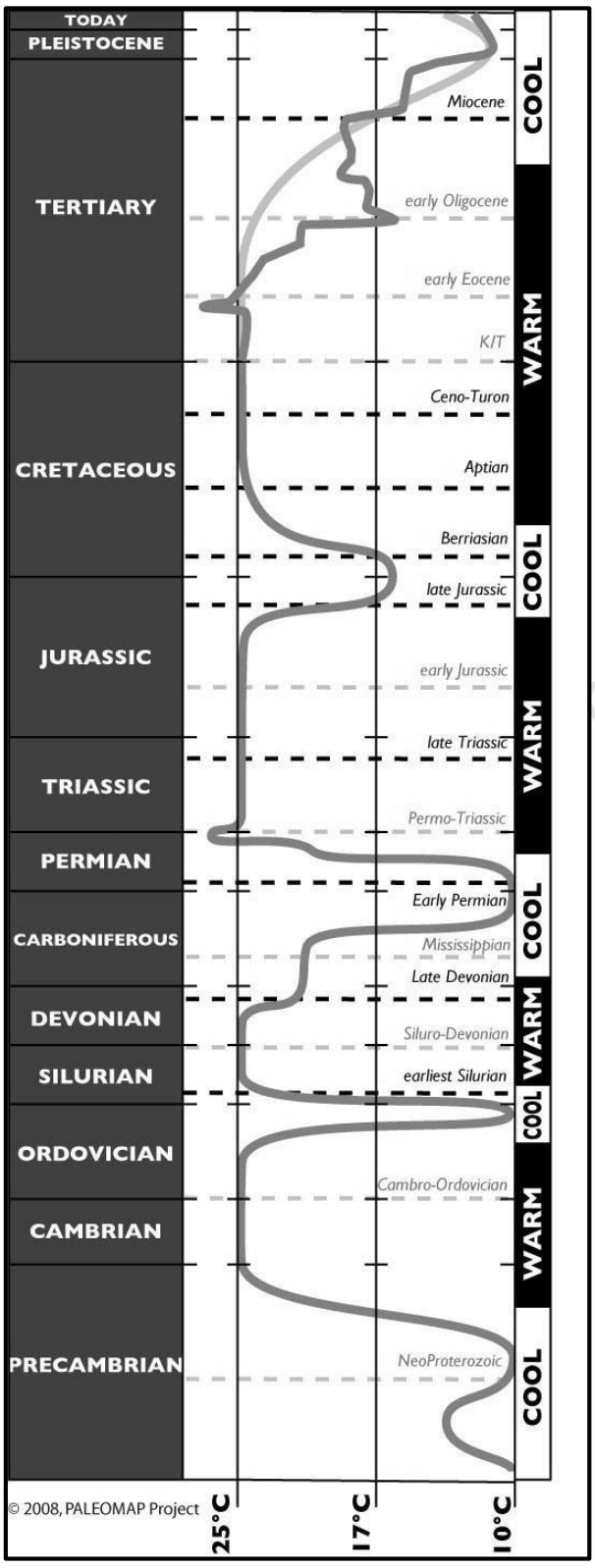

According to Scotese *et al.* (1999), the global climate has alternated between Hot and Ice House conditions over the last 600 Ma (Figure 6). During Hot House conditions, there is no polar ice and the Arctic Circle may experience warm temperate conditions; during Ice House conditions, at least the polar regions are covered by permanent ice caps (Scotese *et al.*, 1999).

There are several variations of the climate belt concept, and these generally consist of a relatively symmetrical arrangement of climate belts on either side of the equator (Figure 7). These belts could include, moving from the equator outwards, a humid equatorial zone (Tropical A), dry subtropical zone (Arid B), warm temperate zone (Temperate C), cool temperate zone (Cold D) and a polar zone (Polar E) (Scotese *et al.*, 1999; Peel *et al.*, 2007).

Figure 6. A geological timescale showing the alternating Ice House (cool) and Hot House (warm) conditions, with the temperature changes indicated as well (from Scotese, 2008).

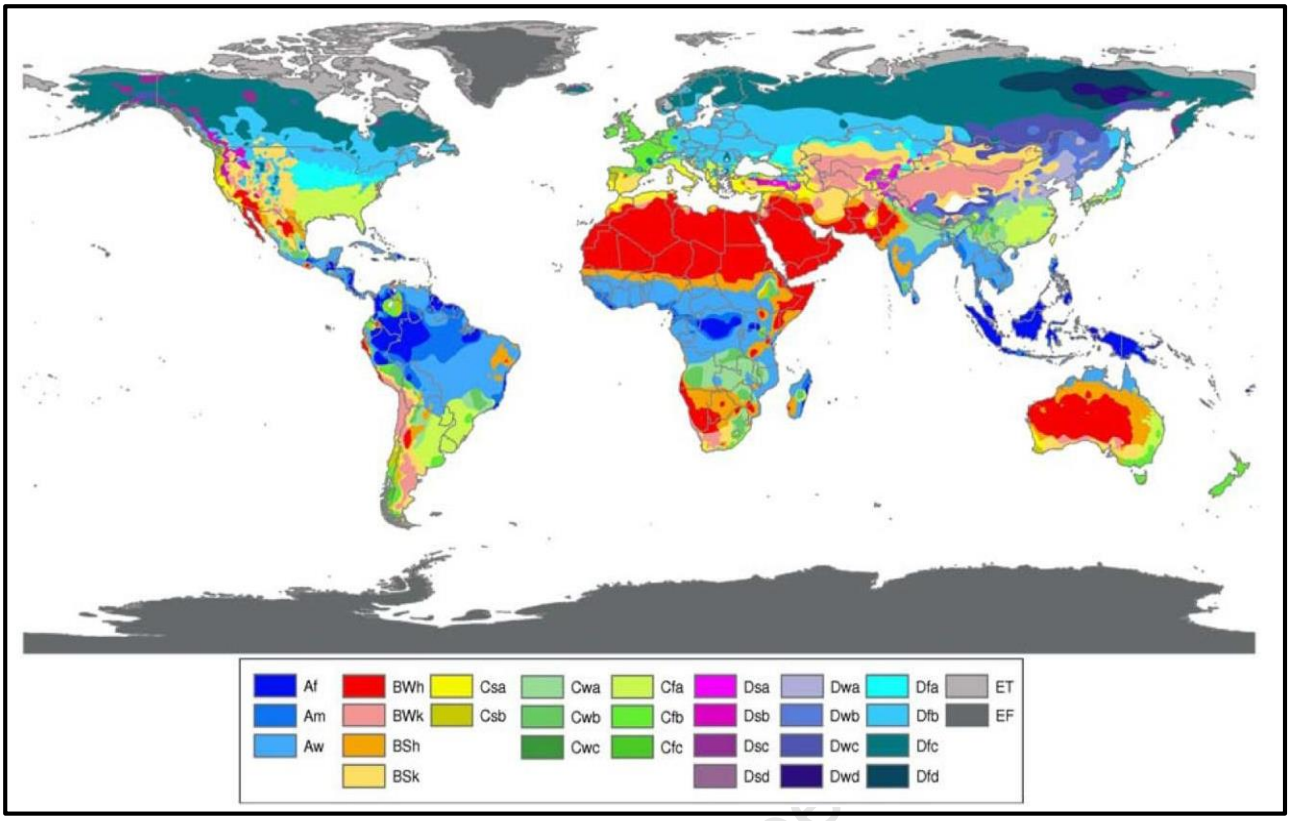

Figure 7. Koppen Geiger climate type map of the modern World with the familiar pattern of similar climates occurring at the same latitudes and the deviation from this pattern due to the influence of continental area, oceanic currents and topography (Peel et al., 2007). The major climate classes by land area are B arid (30.2%), D cold (24.6%), A tropical (19.0%), C temperate (13.4%) and E polar (12.8%) (Note the upper case prefix denotes the major climate class are represented on the map in the colours indicated in the key. The letters following the prefix indicate climate types e.g., Af = Tropical rainforest, Am = Tropical monsoon).

Pangaea was positioned mostly in the southern hemisphere in the Carboniferous, but as the supercontinent grew and moved northwards, the ice caps melted and the continental interiors experienced extreme continental conditions (Scotese and McKerrow, 1990; Chumakov and Zharkov, 2003). Continental conditions refer to a climate characteristic of continental interiors which experience extreme seasonal and diurnal changes in weather conditions, without the moderating effect of the oceans which buffer the variations in heat transfer (Stouffer *et al.*, 2006). During the Late Carboniferous, peat formations began to occur at higher latitudes and the continental regions became more arid (Parrish, 1993). During the Permian, the equatorial regions became dryer, seasonality increased, and the monsoonal climate became established (Scotese and McKerrow, 1990; Parrish, 1993). During the Late Permian, the global climate could still be considered to be in Ice House conditions, based on the occurrence of ice caps in the polar regions (Chumakov and Zharkov, 2002).

It is believed that the global climate specifically in the Triassic had a similar arrangement of latitude parallel climate zones as present today despite the vastly different continental configuration (Scotese *et al.*, 1999; Chumakov and Zharkov, 2003). However, other authors contend that the development of a "megamonsoon" and continental collision related orogenic belts would have disturbed the latitude parallel climate zonation, resulting in the formation of regional rain shadows (Dubiel *et al.*, 1991; Parrish, 1993; Preto *et al.*, 2010).

The Permo-Triassic extinction event was initially associated with one major negative excursion in carbon isotope ratios and this has been interpreted as evidence for increased greenhouse gases that may have contributed to the long term global warming (Kidder and Worsley, 2004; Payne *et al.*, 2004; Royer *et al.*, 2004; Kiehl and Shields, 2005; Preto *et al.*, 2010). The source of these greenhouse gases is controversial (Erwin, 1994; de Wit *et al.*, 2002; Kozur and Weems, 2011). Based on isotopic studies, volcanic CO_2 alone is not considered sufficient to produce the large negative anomalies observed during the Permo-Triassic mass extinction (Retallack *et al.*, 2003; Payne *et al.*, 2004). The eruption of the Siberian Traps contributed to the elevated atmospheric CO_2 levels; however, it is thought that oceanic methane hydrates exposed on continental shelf deposits were a major source of greenhouse gasses (Erwin, 1994; Krull and Retallack, 2000; de Wit *et al.*, 2002; Kozur and Weems, 2011). Siberian Traps may have contributed to an initial acute drop in global temperatures because of increased dust, nitrates and sulphates in the atmosphere, followed by a longer term increase in temperatures as a result of the increased CO_2 (Figure 8) (Wignall, 2001; Gradstein *et al.*, 2005; Preto *et al.*, 2010). Higher resolution studies on the Early Triassic have found several major carbon isotope ratio excursions both positive and negative, stabilising in the Middle Triassic (Payne *et al.*, 2004). These major excursions are attributed to the Siberian Trap volcanism and its influence on the global climate (Payne *et al.*, 2004). In addition to these factors, the intrusion of the Siberian Traps into evaporites and organic carbon resulted in the generation and release of chlorinated and brominated halocarbons (Svensen *et al.*, 2007, 2009a, 2009b; Svensen

and Jamtveit, 2010). The release of hydrocarbons and ozone depleting gases due to the eruption and intrusion of the Siberian Traps provide evidence for processes that would have resulted in extinction by global warming and excessive exposure to radiation (Beerling *et al.*, 2007; Svensen *et al.*, 2007, 2009a, 2009b; Svensen and Jamtveit, 2010).

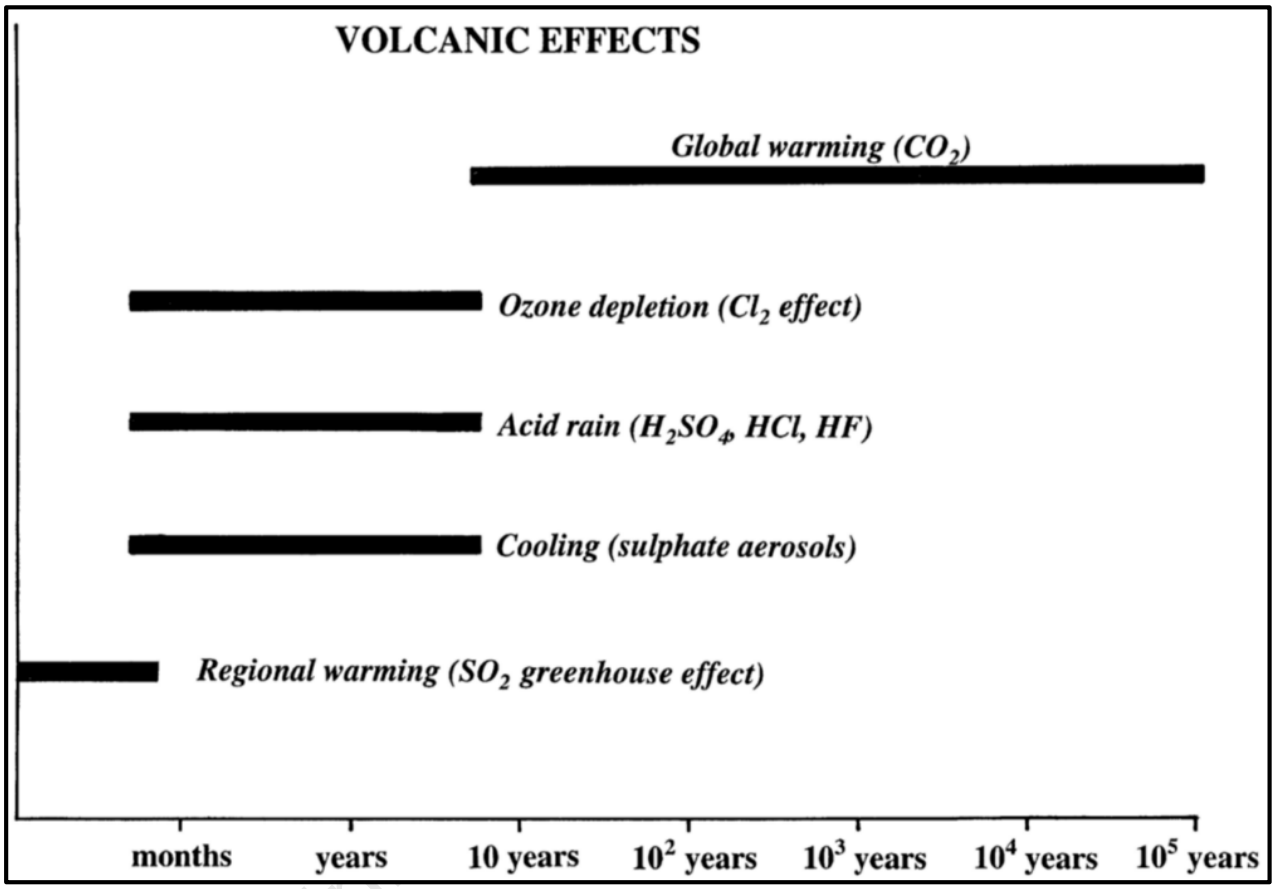

Figure 8. A schematic diagram demonstrating the effects of volcanic gasses and the different timescales they operate at (taken from Wignall, 2001).

The climate of the Triassic period is poorly documented, with much of the literature focusing on the Permo-Triassic and end-Triassic extinction events (Preto *et al.*, 2010). The Early Triassic climate was that of a Hot House with no permanent ice caps, the equatorial regions experienced arid conditions as the moisture moved towards the polar regions (Scotese and McKerrow, 1990; Parrish, 1993; Scotese *et al.*, 1999).

The concentration of exposed continents in the mid-latitudes around a warm ocean would have produced high temperatures in the interiors during summer months (Robinson, 1973 in Preto *et al.*, 2010). The concentration of landmasses into a supercontinent during the Triassic would have resulted in extreme temperature variations daily and seasonally (Figure 4). This extreme 'continentality' must be considered as a major influence on the climate of the Triassic (Robinson, 1973 in Preto *et al.*, 2010). Based on evidence from a wide variety of sciences including sedimentology, palynology, palaeobotany, palaeomagnetics and palaeontology, some reconstructions of the climate belts have been produced for the Permian and Early Triassic (Taylor *et al.*, 1992; Ziegler *et al.*, 1993; Chumakov and Zharkov, 2002; Chumakov and Zharkov, 2003).

In the Early Triassic, plants which flourish in higher temperatures (thermophilic) migrated by dispersal from the equatorial regions into the high latitudes which hosted temperate cold flora in the Late Permian (Chumakov and Zharkov, 2003). At the same time, the plant diversity across the latitudes decreased dramatically (Chumakov and Zharkov, 2003). These changes in flora, which indicate the position of climate belts in the past, suggest that the temperatures were increasing and the difference in temperature between the latitudes decreased (Ziegler *et al.*, 1993; Chumakov and Zharkov, 2003).

In the Late Permian and Early Triassic, the Transantarctic Mountains experienced at least 3 months of summer without ice in the southern coastal regions that were situated 80°-85°S (Jefferson, 1983; Ziegler *et al.*, 1993; Chumakov and Zharkov, 2003). The Early Triassic is characterized by a global lack of diversity of fauna most likely related to the low pole-to-equator temperature gradient and low levels of floral diversity (Chumakov and Zharkov, 2003; Preto *et al.*, 2010). This coupled with the failure of most communities to radiate during the Early Triassic suggest that the conditions after the mass extinction event continued to be harsh and particularly hot (Dubiel *et al.*, 1991; Preto *et al.*, 2010).

Further evidence for a warmer arid climate also include ventifacts and aeolian dunes found in Europe as well as the abrupt lack of coal deposits (coal gap) from the end of the Permian (252.28±0.08Ma) until the Middle Triassic (243Ma) that resulted from lack of moist environments suitable for peat formation (Retallack *et al.*, 1996; Shen *et al*., 2011). Palaeosols indicating a humid climate have been found in the same deposits as those indicating an arid climate, which suggests extreme seasonality (Retallack *et al.*, 1996). In addition to climate change, the possible causes for the "coal gap" include tectonic uplift or evolutionary advances in fungal decomposers and insect or tetrapod herbivores (Retallack *et al.*, 1996). The cause favoured by Retallack *et al.* (1996) is that the coal-producing fauna went extinct during the Permo-Triassic event and the gap represents the time it took for other species adapted and reclaim the ecological niche left in their wake (Retallack *et al.*, 1996).

The Triassic Megamonsoon

The Triassic represents a time when, due to the symmetrical continental configuration relative to the equator, and the position of the Tethys between the two halves of Pangaea it was possible for a theoretical "megamonsoon" climatic system to develop (Dubiel *et al.*, 1991; Parrish, 1993; Wang, 2009). Monsoon refers to a global climatic system that is considered to occur because of the seasonal migration of the intertropical convergence zone (ITCZ) (Wang, 2009). The ITCZ migrates towards the hemisphere experiencing summer, bringing with it wet tropical conditions, while the other hemisphere experiences dry conditions (Figure 9) (Wang, 2009). This global monsoon demonstrates cyclicity brought on by cycles that influence the global temperatures (Wang, 2009). The monsoon cycle is influenced by Wilson cycles (1-100 Ma), Milankovitch cycles (10-100 kiloannum (ka)), solar cycles (1ka) and shorter scale cycles (Scotese *et al.*, 1999; Wang, 2009). These cycles influence distribution and intensity of the monsoon system; for example, the amalgamation of all the continents into Pangaea resulted in a peak in monsoon intensity, demonstrating the influence of the Wilson cycle on the monsoon system. This peak in intensity is termed a "megamonsoon" (Wang, 2009). This megamonsoon may have resulted in considerably

deformed global climate belts, which varied depending on the seasons (Figure 9) (Parrish, 1993; Preto *et al.*, 2010). Models for this megamonsoon, during the Triassic, predict a seasonal reversal in wind direction, which thus meant that summers were humid and winters were dry along the eastern coastline of Pangaea (Figure 9) (Wang, 2009).

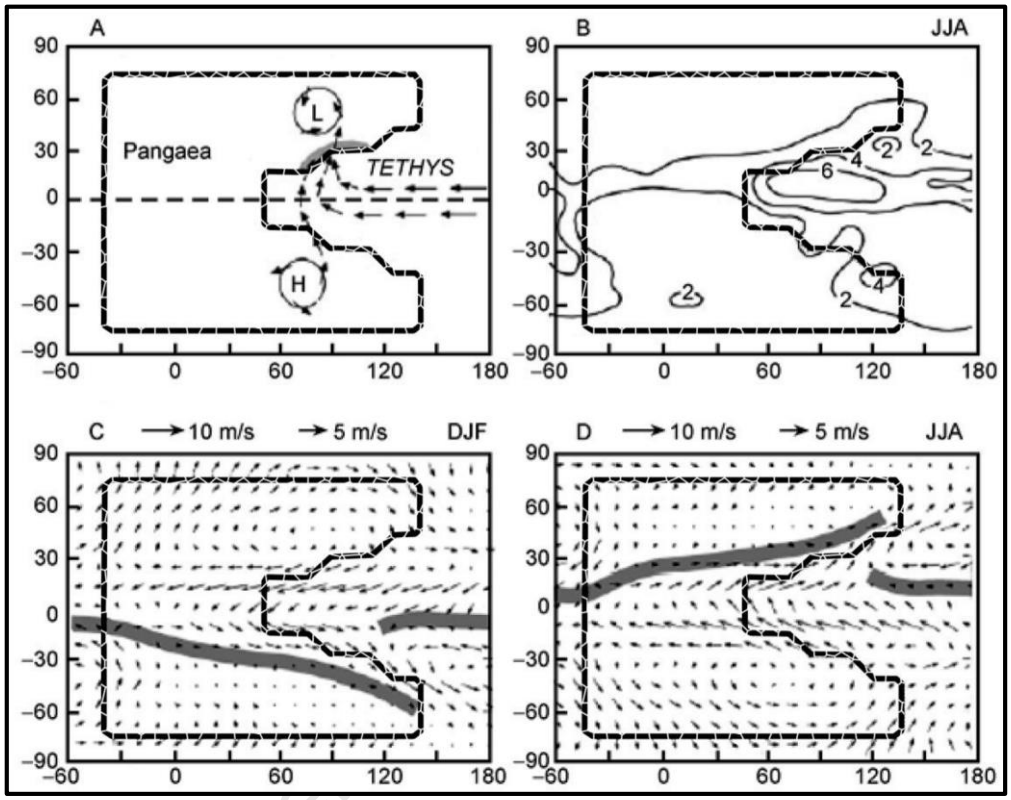

Figure 9. Climate modelling of megamonsoon of Pangaea is illustrated with in monsoonal circulation during the northern summer in A; while in B the precipitation in mm/day for the same periods is demonstrated. C and D demonstrate the seasonal change in wind direction from winter to summer respectively. Note the poleward migration of the grey bar represents the Intertropical Convergence Zone and monsoon during the summer of the respective hemispheres (taken from Wang, 2009).

2.2.4. Triassic climate of the Karoo Basin

The climate in the Late Permian and Early Triassic Karoo Basin is inferred from evidence from sedimentology and palaeontology of the Beaufort Group. The Permian-Triassic boundary is located within the Palingkloof Member of the Balfour Formation (Hiller and Stavrakis, 1984; Smith and Botha, 2005). Hiller and Stavrakis (1984) proposed that the changes between the Balfour and Katberg Formation record a change in the climate to increasingly warm and arid conditions. The

Balfour Formation is characterised by grey and green coloured sandstones and mudstones that indicate a reducing environment, commonly resulting from high water table levels and rainfall (Hiller and Stavrakis, 1984). The climate during the Late Permian is semi-arid based on the occurrence of desiccation cracks, palustrine carbonate beds, pedogenic carbonate horizons and gypsum desert-rose evaporates (Smith, 1990; Keyser, 1966 in Catuneanu *et al.,* 2005). The Katberg Formation is characterised by reddish sedimentary rocks, which result from oxidising conditions, however there is debate about whether oxidising conditions only occur because of an arid climate (Hiller and Stavrakis, 1984).

The seasonality of the Late Permian climate is suggested by the occurrence of desiccation cracks in conjunction with channel deposits, and the preferential preservation of upper flow regime beds alternating with lower flow regime ripple cross-laminations in channel sandstones (Smith, 1990; Catuneanu *et al.,* 2005). The decrease in mudstones relative to sandstones in the Katberg and the occurrence of pedogenic calcareous nodules in the Burgersdorp Formation indicate an environment with low water tables and low seasonal rainfall in the Early Triassic Karoo Basin (Hiller and Stavrakis, 1984). The Katberg Formation contain sedimentary features such as desiccation cracks, intense localised calcareous concretions and thick sandstones with scattered pebble and rip-up mud clasts and these features, together, suggest an arid climate with seasonal rainfall-induced debris flows (Johnson, 1976; Hiller and Stavrakis, 1984).

These interpretations are supported by the contrastingly rich biodiversity in the Balfour Formation juxtaposed with low biodiversity in the Katberg Formation (Smith, 1990; Hiller and Stavrakis, 1984). Based on this the climate during the Late Permian and Early Triassic was semi-arid with aridity increasing in the Karoo Basin during the Early Triassic.

While there is debate about the climatic models, interpretation of climate proxies and causes of climate change, it is generally accepted that the climate was warmer in the Triassic than the Permian and that climate change did occur. These warm conditions continued throughout the Triassic and into the Jurassic (Scotese, 2008). The climate in the Karoo Basin, as recorded in the strata of the Beaufort Group, was not atypical in this warm seasonal Triassic world.

2.2.5. Triassic stratigraphy

The Triassic period is a geological time interval, which starts at the end of the Permian with the Permo-Triassic extinction event 252.28±0.08 Ma and ends at the start of the Jurassic period 199.6 Ma (International Commission on Stratigraphy, 2009; Shen *et al*., 2011). The base of the Triassic is also the base of the Mesozoic era, a subdivision of the Phanerozoic eon (ICS and IUGS, 2012). The subdivision of the global geological record is formally defined by the lower boundary of each subdivision. The Triassic is divided chronostratigraphically into three series and seven stages (Table 1) (Lucas, 2010a; ICS and IUGS, 2012). The boundaries of the Triassic are defined by global stratotype sections and points (GSSPs, see Table 1). The subdivision of the Triassic into 15 substages is not completely defined chronostratigraphically.

There are three series and seven stages based on strata originally deposited over the Boreal and Tethyan periphery of Pangaea during the Triassic (Lucas, 2010a). The subdivision of the Triassic is based mainly on marine deposits; the non-marine subdivision is based on correlation with the marine subdivision and vertebrate biostratigraphy among other methods (Lucas, 2010a).

Subdivision of the Triassic based on marine and land correlatives					
Period	**Series**	**Stages**	**Biostratigraphic indicator species**	**Location (GSSP)**	**Tetrapod timescale**
Jurassic		Hettangian	LO *Psiloceras spelae* ammonoid	Kuhkoch, Austria	Wassonian
Triassic	Upper	Rhaetion	LO *Misikella posthernsteini* conodont	Seinbergkogel, Austria	Apachean
		Norian	Conodont event at the base of the *Stikinoceras kerri* ammonoid zone	Black Bear Ridge, Canada or Pizzo Mondelo, Sicily	Revueltian
		Carnian	LO *Daxatina canadensis* ammonoid	Stuores Wiesen, Italy	Adamanian
					Otischalkian
					Berdyankian
	Middle	Landinian	LO *Eoprotrachyceras curioni* ammonoid	Bagolino, Italy	
					Perovkan
		Anisian	LO *Chiosella timoresis* conodont	Desli Cairia, Romania	
	Lower	Olenekian	LO *Neospathodus waageni* conodont	Spiti, India	Nonesian
		Induan	*LO Hindeodu parvus* conodont	Meishan	Lootsbergian
Permian		Changxingian			Platbergian

Table 1. Triassic chronostratigraphic scale based on GSSP and land vertebrate correlatives (LO = Last Occurrence, GSSP = global stratotype sections and points) (Lucas, 2010a, 2010b).

Tetrapod biostratigraphy and biochronology allows the non-marine Triassic timescale to be divided into eight land-vertebrate faunachrons (LVF), with boundaries defined by first appearance datums (FADs) of tetrapod genera or species (Table 1 and Figure 10) (Lucas, 2010b). LVFs are biochronological units, which begin with a FAD of an index tetrapod taxon and ends with the beginning of the next LVF (Lucas, 2010b). LVFs are defined by distinctive assemblages of vertebrate fossils, and are named after the geographical location where the characteristic vertebrate fossil assemblage was collected (Lucas, 2010b). The tetrapod-based Triassic timescale is independent but is correlated with the Standard Global Chronostratigraphic Scale (SGCS), the timescale based on GSSPs from marine deposits (Lucas, 2010b). A global correlation of LVFs independent from the SGCS is possible because of the arrangement of the continents into the supercontinent of Pangaea (Scotese and McKerrow, 1990; Scotese *et al.*, 1999; Lucas, 2010b). The fact that the continents were connected allowed for some land vertebrate to spread across most of the world's land area (Lucas, 2010b; Preto *et al.*, 2010).

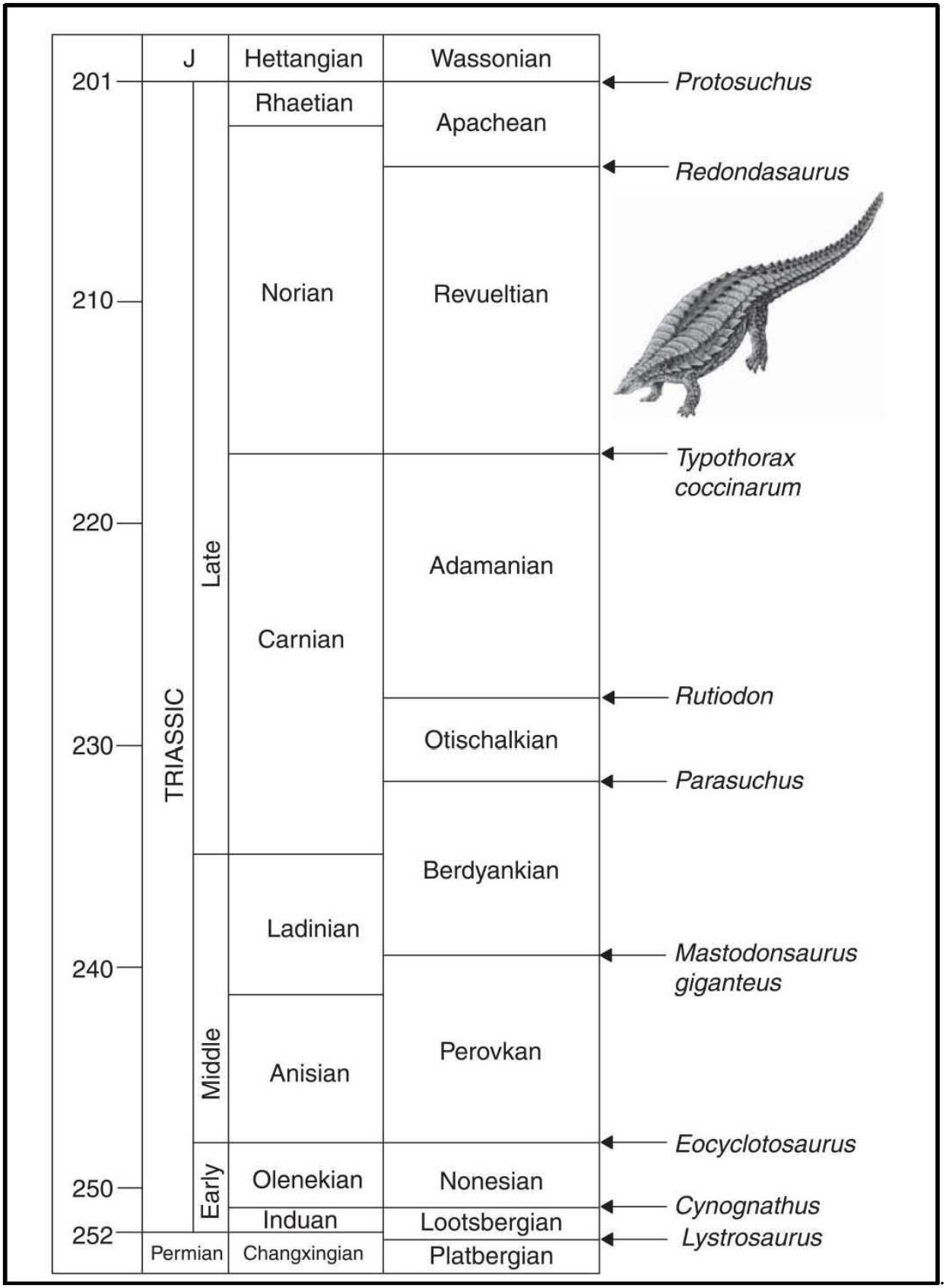

Figure 10. The Triassic timescale based on tetrapod biostratigraphy and biochronology (taken from Lucas, 2010b).

The Triassic tetrapod timescale is based on fossil assemblages and index fossils from the main Karoo Basin in South Africa, the Ural Basin in Russia and the Chinle Basin in Western USA (Lucas, 2010b) (Figures 4 and 10). The index fossils refer to fossils that are temporally restricted, but widespread, common and easily identified. The biostratigraphic correlation and radiometric dating of ash beds has allowed for the subdivision of the Karoo Supergroup in South Africa (Broom, 1909 and Kitching, 1970 in Tankard *et al.*, 1982). The main Karoo Basin contains the *Lystrosaurus* Assemblage Zone, which represents the Lootsbergian LVF, and the *Cynognathus* Assemblage Zone which characterizes the Nonesian LVF (Tables 2 and 9) (Lucas, 1998, 2010b; Botha and Smith, 2007). The tetrapod assemblage is representative of the Lower Triassic; however, there is a hiatus after the *Cynognathus* Assemblage Zone in main Karoo Basin (Lucas, 1998). Fortunately, there is a temporal overlap between the upper parts of the Triassic Karoo stratigraphy and the lower parts of Triassic Urals Basin in Russia (Shishkin, 1995 in Lucas, 1998; Hancox and Rubidge, 2001). The Middle Triassic biochronology is based on tetrapod assemblages from the Ural Basin in Russia, which characterize the Perovkan and Berdyankian LVFs (Lucas, 2010b). The Chinle Basin in the USA contains tetrapod assemblages of the Otischalkian, Adamanian, Revueltian and Apachean LVFs of the Upper Triassic (Figures 4 and 10, Table 1) (Lucas, 2010b).

TRIASSIC	Nonesian 	B	*Cynognathus* with *Kannemeyeria*
		A	*Cynognathus* without *Kannemeyeria*
	Lootsbergian 	C	*Lystrosaurus* with *Procolophon*
		B	*Lystrosaurus* without *Dicynodon* and *Procolophon*
P		A	*Lystrosaurus* with *Dicynodon*

Table 2. Subdivision of the Lootsbergian and Nonesian LVFs based on the biostratigraphy of the Karoo Basin (modified after Lucas, 2010b) (artistic representation of *Dicynodon* Matt Celeskey and the *Cynognathus* by Tamura 2007).

2.2.6. *Lystrosaurus* Assemblage Zone

The *Lystrosaurus* Assemblage Zone (Early Triassic) has low levels of biodiversity (a global trend for this time), dominated by the dicynodont *Lystrosaurus* (95% of vertebrates), however the procolophonoid *Procolophon* is found in isolated (yet highly concentrated) occurrences (Groenewald and Kitching, 1995; Neveling, 2004; Cisneros, 2008). Fossil abundances decrease towards the top of the biozone and as an arid, hot climates favour a reduction in organism size (Lilliput effect), the fauna in Karoo Basin became smaller (Neveling, 2004; Rubidge, 2005; Twitchett, 2007; Harries and Knorr, 2009; Sun *et al.*, 2012).

The Hobbs Hill locality (Figures 1, 2 and 12) exposes the middle-upper Katberg Formation, of the late Early Triassic (Olenekian, 249.5-245.9 Ma), latest *Lystrosaurus* Assemblage Zone (Groenewald and Kitching, 1995; Neveling, 2004; Cisneros, 2008). The stratigraphic position of the Hobbs Hill locality is based on the occurrence of the index genus *Procolophon*, which only occurs between the middle part of the Katberg Formation and lowermost Burgersdorp Formation (Groenewald and Kitching, 1995; Neveling, 2004; Cisneros, 2008). It is also the type locality for the holotype of the parareptile *Kitchingnathus untabeni*; BP1/1187, originally considered a juvenile specimen of *Procolophon trigoniceps*, now considered a new taxon (Cisneros, 2008). This is based on the difference in dentition (bicuspid and more conical), small specimen size with well-ossified skeletal elements (therefore not likely a juvenile) and at least five anatomical features which are in contrast to adult and juvenile *Procolophon* (Cisneros, 2008). *Kitchingnathus untabeni* is considered to have been an insectivore based on its dentition (comparable to modern hedgehog) and small size (Cisneros, 2008).

Other fauna that occur in the Karoo Basin are mentioned in Chapter 7 in reference to the burrows they may have produced. They include *Trirachodon* (therapsid), *Galesaurus* and *Progalesaurus* (cynodont), *Thrinaxodon liorhinus* and the akidnognathid *Olivierosuchus* or *Moschorhinus* (therocephalian) (Groenewald *et al.*, 2001; Miller *et al*., 2001; Damiani *et al.*, 2003; Retallack *et al.*, 2003; Sidor et al., 2008; Modesto and Botha-Brink, 2010a; Bordy et al., 2011).

2.3. 3D digital burrows

Burrows and other trace fossils are three-dimensional (3D) objects have to be described in two-dimensional (2D) terms (e.g. on paper). This has been done in previous studies by describing the length, height, width, cross-sectional shape, by using sketches and photographs of different views of the object (Bromley and Frey, 1974; Smith, 1987; Dubiel *et al.*, 1987; Groenewald, 1991; Hasiotis and Mitchell, 1993; Kinlaw, 1999; Groenewald *et al.*, 2001; Miller *et al.*, 2001; Damiani *et al.*, 2003; Sidor *et al.*, 2008; Modesto and Botha-Brink, 2010a). This allows the reader to create a 3D mental picture of the burrow. When dealing with more complex structures these methods become less effective. This method often results in a great deal of data being lost. For example, in case of a burrow with variable diameters, the range of diameters or a single measurement does not provide an accurate representation of the burrow's dimensions.

Identification of the producer of a burrow involves an accurate account of burrow characteristics (Miller *et al.*, 2001; Remondino *et al.*, 2010). The great variation in specific properties of described (i.e., lack of standardized descriptors) and the lack of details on the specifics of the measurements in previous studies make comparisons difficult. To overcome this problem, in some cases it is necessary to make measurements from figures, because diagnostic measurements were poorly and inconsistently reported (e.g., Groenewald, 1991). Moulds of type specimens can provide the desired measureable 3D properties. Creating moulds is a tedious task and transporting them is relatively inefficient considering the possible digital alternative (Remondino *et al.*, 2010).

Digital 3D copies of burrows and fossils can be sent virtually anywhere in the world via the internet and are a much more efficient method of information transfer (Platt *et al.*, 2010; Remondino *et al.*, 2010; Bordy *et al.*, 2011; Moulon and Bezzi, 2011). One of the major benefits of 3D scanning is the high speed at which the physical measurements of nearly any object can be captured (Falkingham, 2012). The 3D copies of burrows can be analysed using software or converted to hardcopy, via 3D

printing, for physical measurement. 3D printing is already increasingly affordable and most major cities have companies that provide 3D printing services (e.g., rapid prototyping). It is likely that in the near future 3D printing will become as commonplace as 2D printing.

Current 3D scanning techniques and devices include: 3D laser scanning, white light scanning, photogrammetry, machine vision, co-ordinate measuring machines, destructive slicing, 3D CT or magnetic resonance imaging (MRI) scanning, theodolite and tracking devices (Platt *et al.*, 2010; Remondino *et al.*, 2010; Falkingham, 2012; Newby, 2012). Many of these techniques are prohibitively costly, specialised and not necessarily more accurate than photogrammetry (Gruen, 2012).

Platt *et al.* (2010) proposed the use of 3D scanning technology citing numerous benefits for the study of large burrow casts. However, they used multistripe laser triangulation (MLT), which although a lot less expensive than MRI, is a highly specialised 3D scanning technique, requiring a relatively bulky and expensive ($2995.00 USD at time of writing 10/12/2012) equipment. Researchers with a limited budget studying complex 3D objects are unlikely to have access to specialised and costly 3D scanning equipment. Therefore, 3D scanning techniques need to be affordable, effective and user-friendly.

Stereoscopy is an affordable technique used to produce 3D representation of traces fossils (Figure 11) (Groenewald *et al.*, 2001; Bown, 1982 in Platt *et al.*, 2010). It only requires 2 photographs of the same object taken from slightly different perspectives to create a the illusion of 3 dimensions when viewed side by side through a stereoscope, similar to the analysis of stereoscopic aerial photographs (Evitt, 1949; Groenewald *et al.*, 2001; Bown, 1982 in Platt *et al.*, 2010). While stereoscopy produces the illusion of three dimensions, it has limited use for making measurements of 3D features (Figure 11) (Evitt, 1949).

Figure 11. Stereoscopic images of a complex burrows system that produces and illusion of 3D, but it is generally impossible to measure in the vertical plane (taken from Groenewald *et al.*, 2001).

To obtain accurate measurements from a 3D copy, a digital version is needed so that the object can be rotated and looked at from all possible perspectives. A more practical alternative to stereoscopy is photogrammetry, which is the process of acquiring geometrical properties of 3D objects using photography and has been around since the early stages of photography (Yilmaz *et al.*, 2008). According to the International Society for Photogrammetry and Remote Sensing (ISPRS) "Photogrammetry and Remote Sensing is the art, science, and technology of obtaining reliable information from non-contact imaging and other sensor systems about the Earth and its environment, and other physical objects and processes through recording, measuring, analysing and representation." (ISPRS, 2008, p.1). Recently the proliferation of photogrammetry software and associated cloud processing has made photogrammetry more accessible (Mathews, 2008).

3. Methodology

3.1. Introduction

To answer the research questions, evidence was gathered from three primary fields of geology namely sedimentology, ichnology and paleontology. The approach was essentially descriptive (qualitative), at multiple scales and within a multidisciplinary framework. To give the ichnology and palaeontology observations context, the data collection employed sedimentology first. Applying detailed sedimentary facies analysis on the field descriptions, photographic and laboratory (petrographic anaylsis and acid test) evidence.

3.2. The study area

The study sites were selected from localities previously observed (by the author and Dr Emese Bordy) and described in literature; based on the occurrence of good outcrops of the Katberg Formation with large penetrative burrows (~10 cm diameter). The most productive location, the Hobbs Hill farm (Table 3, Figures 2 and 12) was identified in 2010 during an ichnological recognisance trip in the Eastern Cape. The Hobbs Hill site (Figure 12) exposes several good outcrops of the Lower Triassic Katberg Formation and contains some of the best-preserved large burrows and a bone bed. This site was documented in more detail because it showed potential. The study area also included sites from the south-eastern exposures of the Katberg Formation in South Africa (Figure 1), as mentioned in Groenewald (1996).

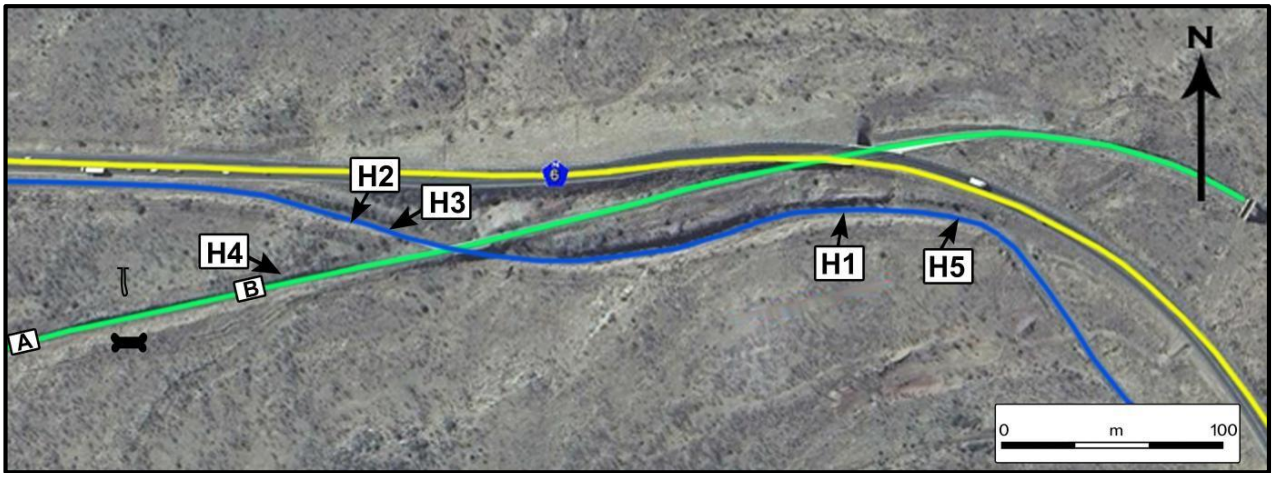

Figure 12. Aerial photograph of the Hobbs Hill study site showing the location of the detailed sedimentological sections. Location of bone bed marked with a black bone symbol. Logs H1, H2, H3 and H5 were recorded along a disused road cutting (in blue); log H4 and the bone bed are located along a railway cutting (in green). The majority of the burrows were found between A and B (burrow symbol) along the railway (green) The N6 national highway is marked in yellow (image taken from Google Earth 2011).

Site	GPS Co-ordinates	Proximity to nearest town	Province	Burrow Occurrence
Hobbs Hill	32° 15.892′ S 27° 8.586′ E	2km north west of Cathcart	Eastern Cape	Observed
Holmsgrove (Boesmansberg 86)*	30° 34.789′ S 26° 00.966′ E	8km south south east of Bethulie	Eastern Cape	Observed
Keerom (55)*	30° 49.229′ S 25° 36.98′ E	17km west south west of Venterstad	Eastern Cape	Reported by Groenewald (1991) p. 19
Rooiwal (129)*	30° 51.607' S 25° 34.960' E	25km south west of the Venterstad	Eastern Cape	Reported by Groenewald (1991) p. 17
Kapteinskraal	30° 23.097′S 26° 1.802′ E	14 km north north east of Bethulie	Free State	Reported by Groenewald (1991) p. 19
Speelmanskop (113)*	30° 19.500' S 26° 7.000' E	24 km north north east of Bethulie	Free State	Reported by Groenewald (1991) p. 19
Jakkalsfontein (169)*	31° 09,748′ S 25° 10.595′ E	21 km east of Noupoort	Northern Cape	Reported by Groenewald (1996)

Table 3. The locality details of the sites visited are summarised, and indicated on the map in Figure 1 and 12, (*indicates the municipal farm number). The "burrow occurrence" refers to whether the site was reported in literature to contain possible burrows or was observed by the author and Dr Emese Bordy during fieldwork.

3.3. Sedimentology

3.3.1. Observations

The following was recorded at each locality: GPS coordinates of the site (or outcrop), the geographical location (relative to landmarks or towns), height and length of the outcrop; the thickness, lateral extent, continuity and shape of the beds; the type of sedimentary structures in the beds (e.g., massive, horizontally laminated, cross-bedded); bed-top and bed-bottom sedimentary features; grain size variations (with in beds and within successions); post-depositional features such as bioturbation, desiccation cracks and soft-sediment deformation features. Grain sizes were assessed using a comparison chart and fluvial lithofacies types were assigned a code following Miall's lithofacies system (Miall, 1985, 1996, 2000). The Munsell Rock Colour Chart (2009) was used to determine the colours of the rocks.

These sedimentary features provided evidence of the energy and the direction of the sedimentary processes that transported the sediments. They were observed vertically and laterally, recorded in the form of sedimentary logs and photographic panoramas respectively (with annotated sketches and notes). Representative samples were taken of the beds and labelled according to the sites and logs (all logged beds except from log H1). All of the samples were tested with dilute HCl (10%) for carbonate content and the dominant facies types were thin-sectioned for petrographic analysis. The latter was undertaken to determine the composition of the rocks, and for comparison with the burrow fill material.

The photographs were taken with a Canon PowerShot S5 IS and a Panasonic (Lumix) DMCTZ2 digital camera in the field and in the lab. The thin sections were analysed using a Nikon Optiphot PoL Mplan petrographic microscope with an Olympus CS20 camera and Olympus Soft Imaging Solutions software. The sedimentary logs were digitized using SedLog and illustration software. The photomosaics were produced manually using photographic imaging software such as Gimp, Photoshop and Illustrator.

3.3.2. Facies Analysis

To interpret what depositional environment is represented by a particular set of sedimentary features, analysis of the sedimentary facies, architectural elements and depositional elements is necessary. In sedimentology, the term facies refers to a unit of rock that is distinct from other rock units based on its observable attributes (Miall, 2000; Boggs, 2006). While the term lithofacies is slightly more specific in that those attributes, which include composition, grain size, bedding characteristics and internal structures, may represent a discrete depositional event (Miall, 2000; Boggs, 2006).

Facies associations are groups of facies that are repeatedly found in association with one other. Walter's Law states that facies that occur on top of each other in a conformable sedimentary sequence represent depositional environments that occurred next to each other at the time of deposition (Boggs, 2006). Considering Walter's Law, specific sets of facies associations can characterise specific depositional environments. Facies models represent the "norm" which can be used as a comparison by distilling away the local variabilities of each type of depositional environment. Facies models simplify the process of facies analysis by summarising the common attributes of ancient and modern depositional environments.

The sedimentary rocks in this study are subdivided into lithofacies types according to Miall's (1996) classification system (Table 4). These include sandstone lithofacies (Sm, Sh and Sl), gravelly lithofacies (Gmm and Gh) and fine-grained lithofacies (Fm and Fl). The ssd lithofacies here refers to all those mudstone beds that show soft sediment deformation. These lithofacies are summarised into sedimentary logs that record the vertical relationships between the lithofacies (Figures 18-20).

Code	Lithofacies type
Gmm	Matrix-supported massive gravel
Gh	Horizontally bedded gravel
Gt	Trough cross stratified gravel
Gp	Planar cross-stratified gravel
Sm	Massive or faintly laminated sand
Sh	Horizontally laminated sand
Sl	Low-angle cross bedded sand
Sr	Ripple cross-laminated sand
Fm	Massive mud or clay
Fl	Laminated sand, silt and clay
ssd	Soft-sediment deformation

Table 4. Lithofacies types and corresponding facies codes used in this study (modified from Miall 1985 and 1996; Colombera *et al.*, 2012).

3.3.3. Architectural element analysis

To constrain the depositional environment, the lateral variation of lithofacies and the three-dimensional architecture of the beds must be described and analysed as well. This is achieved by the vertical profiling of sedimentary features and lithofacies by identifying:

(1) bed geometries, delineated by the bounding surfaces between them,

(2) internal structures and

(3) palaeo-current directions.

These three attributes define architectural elements as described by Miall (1985, 1996). Architectural elements are grouped into channel elements (CH) and flood plain elements (FF), which can be referred to as depositional elements (Colombera *et al.*, 2012). The channel elements (CH) can be further subdivided into smaller scale elements that are more specific to particular subenvironments. For example, downstream accretion macroform (DA), lateral accretion macroform (LA) and scour-hollow fills (HO) (Miall, 1985, 1996; Colombera *et al.*, 2012).

The specific method applied for this purpose was the analysis of the photomosaics using logs, sketches and notes made in the field to delineate bounding surfaces. The bed geometries and palaeo-current directions (determined from scour marks and foreset dip directions) were then utilized to classify the type of elements observed. These elements were then used to identify the type of depositional environments and the subsenvironments that would have produced them.

3.4. Ichnology

3.4.1. Inorganic Origin

The accurate identification of trace fossil requires a good knowledge of sedimentary structures to avoid confusion between the two. First observing the sedimentary features and then the trace fossil that they contain is an ideal approach. Trace fossil are generally identified based on their resemblance to modern traces, for example, trace fossil tracks are sometime identical to modern tracks. The filling of burrows, lithification, compaction, bioturbation and weathering of sedimentary rocks often obscure and distort the original form of the trace fossil. It is for this reason that a good knowledge of sedimentology and the appearance of sedimentary features are required to distinguish trace fossils from features purely sedimentary or diagenetic in origin. The trace fossils in this study are large penetrative burrows and are relatively easy to identify, due to their large size, crosscutting relationship with the bedding, positive relief due to resistance to weathering and generally contrasting composition between the host rock and burrow fill (mudstone and sandstone, respectively).

3.4.2. Field Techniques

The burrow characteristics that were analysed include those used in previous studies of relatively large continental trace fossils (Frey and Pemberton, 1985; Smith, 1987; Hasiotis and Mitchell, 1993; Groenewald *et al.*, 2001; Hembree and Hasiotis, 2007; Martin *et al.*, 2008; Ekdale and De

Gibert, 2010). These features include the overall geometry of the burrow (referred to as architectural morphology); the features preserved on the surface of the burrow cast (surficial morphology or bioglyphs); and the features preserved inside the burrow (sediment fill). The same tools and techniques used for the sedimentary descriptions and analysis were used for the trace fossils (e.g., descriptions and photographs of burrows in outcrops, sampling for further analysis). The burrow characteristics described in this study primarily based on the observable attributes, recording the observation in the form of text, numbers and photographs.

Architectural morphology

Architectural morphology refers to the geometrical measurable attributes of burrows (Hasiotis and Mitchell, 1993; Hasiotis *et al.*, 2007). The attributes should include the general dimensions such as the width (or diameter) and preserved length. The overall outline and cross-sectional shape (circle, oval, lobate, medial groove), size range (minimum, maximum and average diameters), the orientation and inclination of the burrows in outcrop, should be measured and recorded. All attributes that describe the complexity of the burrows should also be recorded. They include but are not limited to the presence/absence of spiralling; tightness of spiral shafts, angle of ramp; the type of branching (true vs. apparent resulting from crosscutting); branching angles; the degree of interconnectedness of the burrow elements (shafts and tunnels); presence/absence of chambers (enlargements); presence/absence of original entrances, their number and shape (Hasiotis and Mitchell, 1993; Hasiotis *et al.*, 2007). The architectural morphology of burrows may indicate the purpose of the burrow, the behaviour and often the identity of the burrow maker (Hasiotis *et al.*, 2007). Large penetrative terrestrial burrows generally have multiple purposes, however there are specific cases were the burrow are for one use only (e.g., lungfish aestivation burrows) (Carlson, 1968; Dubiel *et al.*, 1987). The size and complexity of the burrows relate to the organism that produced it and may be used to determine whether one or many organisms produced/used the burrows (Kinlaw, 1999; Hasiotis, 2003; Riese *et al.*, 2011).

Surficial morphology

Surficial morphology or bioglyphs describe the occurrence of ornamental structures on the burrow surfaces which result from the bioturbation and bioerosion activities of the burrow makers (Ekdale and De Gibert, 2010). Such ornaments include scratch marks, scrape marks, striation, traces of appendages and other distinctive (ir)regularities (ridges, bumps, knobs, furrows, nodes, blisters, indentations, etc.) (Hasiotis and Mitchell, 1993; Hasiotis *et al.*, 1993; Ekdale and De Gibert, 2010). Bioglyphs are used to identify an organism that used or produced a burrow in a way similar to using a fingerprint to identify a person (De Gibert and Ekdale, 2010). For instance, the impression that a crayfish claw produces is very different to that of a vertebrate paw. The orientation of ornaments relative to each other and with respect to the architecture of the burrow is an important diagnostic feature.

Other diagnostic features that are preserved in the surficial morphology include linings such as mud lags, faecal matter or other biogenic material, and these can indicate how the burrow was created, maintained or used, as well as provide important clues on the identity of the trace maker (Hasiotis and Mitchell, 1993; Hasiotis *et al.*, 1993, 2007; Ekdale and Gibert, 2010).

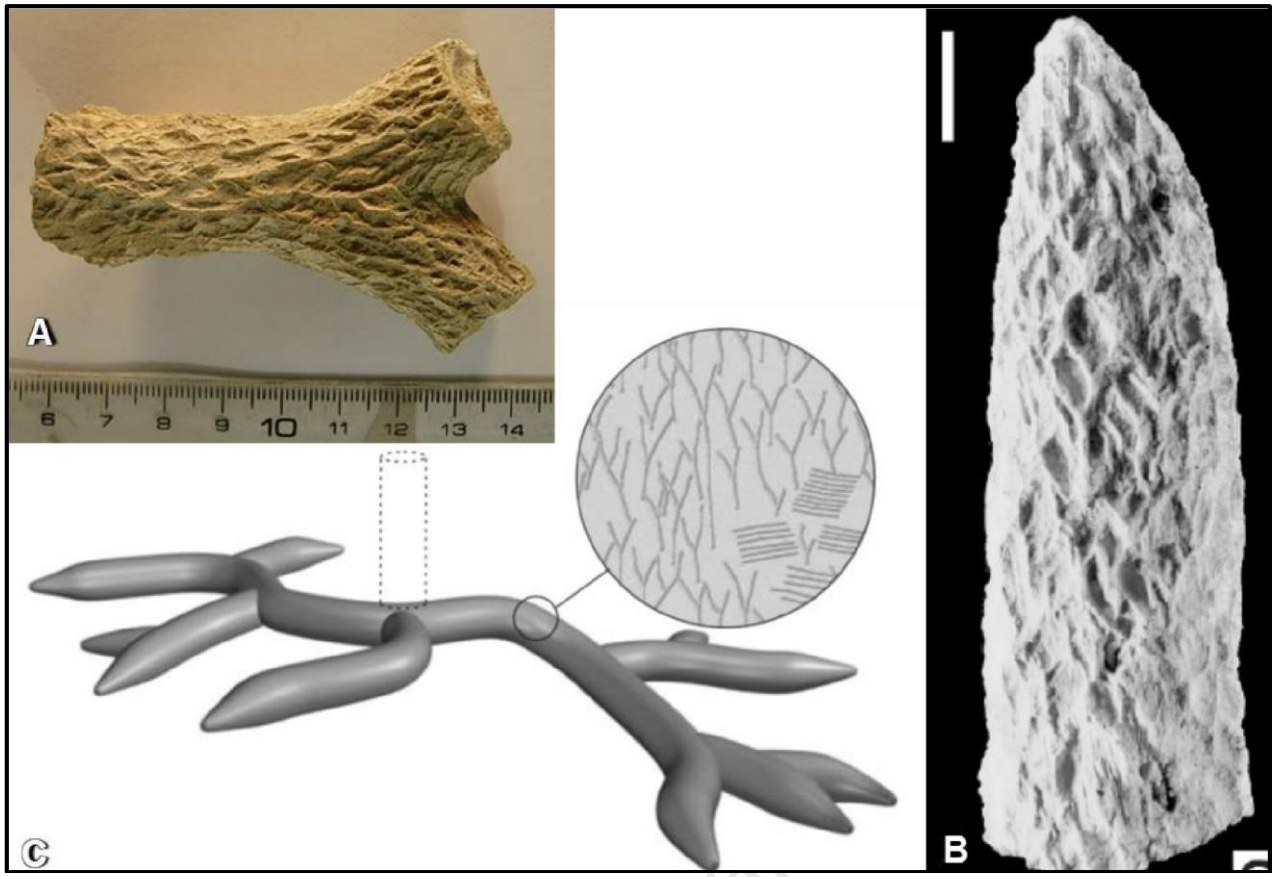

Figure 13. Very well-preserved Y-shaped bioglyphs (A and B) and surficial morphology (A and B) of a burrow that has been confidently attributed to a crustacean producer. A reconstruction of the burrow *spongeliomorpha* (C) with an inset indicating the Y-shaped bioglyphs position (taken from De Gibert and Ekdale, 2010).

In the study of marine trace fossils, various terms have been developed to describe reoccurring morphologically similar trace fossils which can and have been used in the study of large terrestrial burrows (Smith, 1987; Groenewald, 1991). *Daimonelix* refers to very large scale *Gyrolithes*, a spiralling burrow, while *Spongeliomorpha* refers to burrows which can be confidently attributed to crustaceans, and have a characteristic surficial morphology consisting of Y-shaped bioglyphs (Figure 13) (Bromley and Frey, 1974; Smith, 1987; Groenewald, 1991; Saporta, 1887 in De Gibert and Ekdale, 2010). This characteristic surficial morphology has been used to describe certain large terrestrial burrows (Groenewald, 1991). However since it is possible to measure and describe the large surficial morphological features on burrows (vertebrate and invertebrate) such terms should be accompanied with detailed measurements and descriptions of the surficial morphology (Miller *et al.*, 2001; De Gibert and Ekdale, 2010).

Burrow fill

The preservation of a burrow requires the filling of those structures by a material that can become lithified. A burrow can be filled: (1) actively when the burrow maker fills it the by some behaviour, such as feeding, or (2) passively when filling of burrows occurred by physical processes (Pemberton *et al.*, 2001). The burrow fill material gives an indication of the processes occurring in the environment around the burrows and may contain clues to what organism could have produced the burrow. Some of the features that have been described by authors pertaining to burrow fill include: presence of pellets and their accumulation, evidence of incremental or chaotic sediment infill, and presence/absence of mud chips in the burrow (Hasiotis *et al.*, 1993; Groenewald *et al.*, 2001). Other features of burrow fill include the properties of the infilling sediments such as sorting, grain size, colour, staining, cement and its relationship with host sediments (Hasiotis *et al.*, 1993; Groenewald *et al.*, 2001; Martin *et al.*, 2008). Some of these features are very useful in determining the possible burrow maker or user, while others are more indirect in that they provide evidence that can assist in the interpretation of the palaeo-environment and process that occur during and after filling.

3.4.3. Sample processing

The above characteristics were described and noted in the field, photographs and samples were taken for further analysis. The samples were cleaned and described in more detail, especially the surficial morphology and burrow fill. The burrow fill was described with the aid of petrographic thin sections, for a compositional comparison with the host rock, to look for pellets and other features that might help identify the burrow maker. The samples were also tested for carbonate content with dilute HCl (10%); testing the burrow fill, burrow surface and host rock that was still attached to the burrow. The test for carbonate was done to aid in the petrographic analysis to determine the type of cement (e.g., silica vs. carbonate).

Burrow analysis

A list of organisms that could have produced burrows with the features described above was created and each one was assessed separately. Smith (1987) and later Miller *et al.* (2001) developed some criteria to identify the producers of terrestrial burrows; based on the confidence with which a particular burrow can be assigned to a particular organism (Figure 14). These criteria were used in conjunction with comparisons of modern and ancient burrowing organism to assess the most likely trace maker candidates. The characteristics were compared with those that were extant during the Early Triassic and later those organisms identified in the bone beds.

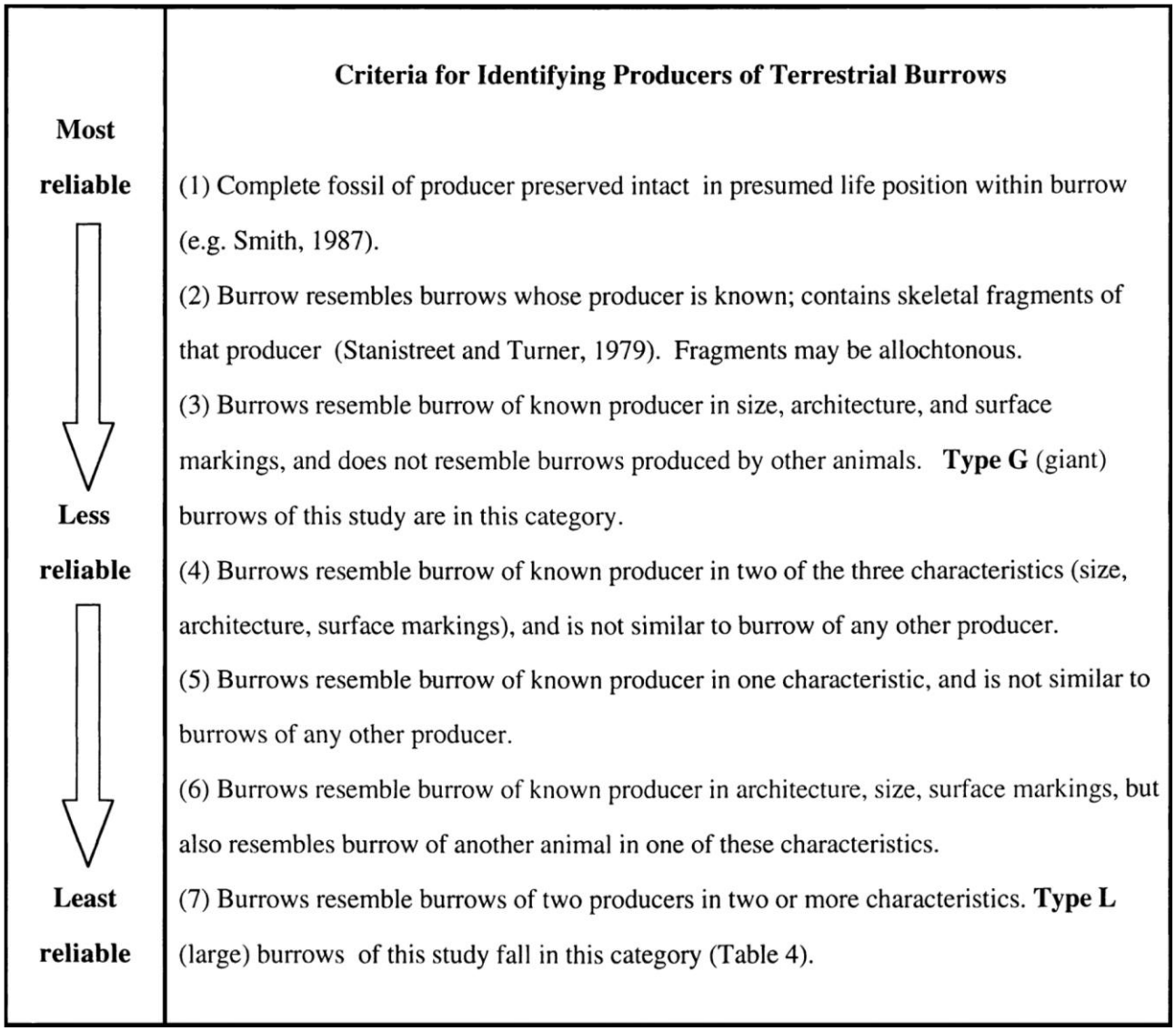

Figure 14. Flow chart of criteria for identifying producers of terrestrial burrows with relative confidence (modified from Miller et al., 2001)

3.5. Photogrammetry

3.5.1. Introduction

Photogrammetry was used in an attempt to create 3D digital copies of the Hobbs Hill type burrows because of the low cost, unspecialised and ubiquitous nature of the hardware required (digital camera and computer). In addition to the hardware benefits, photogrammetry can be done using free and user-friendly software. The primary software utilized for the photogrammetry included 123D applications (Autodesk) and the Python Photogrammetry Toolbox (Moulon and Bezzi, 2011).

3.5.2. Definitions

Photogrammetry is the process of acquiring measurable data from multiple overlapping photographs using metrology, in this context, is the process of producing 3D coordinates from 2D photographs (Veldhuis and Vosselman, 1998; ISPRS, 2008; Newby, 2012; G.S.I., 2013). To produce accurate data using photogrammetry, both the photography and metrology need to be done correctly (Yilmaz *et al.*, 2008; G.S.I., 2013). High quality photographs require the consideration of three properties: (a) field of view, (b) exposure and (c) focus (Mathews, 2008; Thomson, 2010). The amount of data available for metrology is dependent on the quality of these three properties of photography (G.S.I., 2013).

A ray is a line from a point in a photograph to the camera (or perspective centre); a single ray can only give directional information about an observed object (Veldhuis and Vosselman, 1998; Kalloniatis and Luu, 2007). This is why depth perception is lost when one eye is closed (Kalloniatis and Luu, 2007). With two cameras (eyes), two rays can intercept and the object's distance from the cameras can be calculated (at the correct focus) (Kalloniatis and Luu, 2007). This is a greatly simplified explanation, however additional calculations involve co-planarity and least squares methods, a thorough explanation is beyond the scope of this project (Veldhuis and Vosselman, 1998; Smith, 2006; Yilmaz *et al.*, 2008; Merry and Held, 2011; Falkingham, 2012; Gruen, 2012; Newby, 2012).

For photogrammetry, a single camera can be used when looking at stationary objects by taking photographs from at least two slightly different angles (Moulon and Bezzi, 2011; Falkingham, 2012). However to increase accuracy, more than two viewpoints are necessary, and this distinguishes 3D photogrammetry from stereophotogrammetry (Yilmaz *et al.*, 2008; Moulon and Bezzi, 2011; Falkingham, 2012; G.S.I., 2013). The human brain knows the position of the eyes and can therefore calculate the position of the object using intercepting rays reflected from a single point at the correct focal length (Kalloniatis and Luu, 2007).

To create a 3D object using photogrammetry, specialized software is used to determine the position of the camera when each photograph was taken (Veldhuis and Vosselman, 1998; Yilmaz *et al.*, 2008; Merry and Held, 2011; Falkingham, 2012; Gruen, 2012; Newby, 2012). The position of the camera in 3D space is defined by X, Y and Z co-ordinates, calculated from multiple common points in different photographs (Figure 16) (Veldhuis and Vosselman, 1998; Yilmaz *et al.*, 2008; Merry and Held, 2011; Falkingham, 2012; Gruen, 2012; Newby, 2012). The software must therefore be able to identify common points in different photographs for triangulation calculations to solve for the distances and angles between the camera and points on the object (Veldhuis and Vosselman, 1998; Yilmaz *et al.*, 2008; Merry and Held, 2011; Falkingham, 2012; Gruen, 2012; Newby, 2012).

This is where the three properties of good quality photographs become important, if the objects are not in focus or are poorly exposed, the number of matching points between photographs will decrease and therefore the accuracy of the calculations will decrease (Scheidegger *et al.*, 2005).
In short, good photogrammetry software should produce sets of 3D co-ordinates of the camera position related to specific photographs (where the camera was relative to the object when it took each photograph) and the 3D positions of points of the object photographed (Moulon and Bezzi, 2011).

Photogrammetry reproduces the surface of the study object by capturing thousands (to millions) of points on the surface, and these are referred to as "point clouds" (Falkingham, 2012; Newby, 2012). A point cloud is a set of vertices defined by X, Y and Z co-ordinates in a 3D co-ordinate system. However, a medium sized data set can have over 9 million points which may be impractical to use on most computers (ALOOPINICON, 2009). A mesh or meshing is derived from the German "Masche" or "maschen" which refer to tessellation (i.e., building of a mosaic from the repetition of a geometric shape without overlaps or gaps; also see Delaunay triangulation) processes which are required for producing triangulated irregular networks (Newby, 2012).

Point clouds are often converted to meshes, because more applications are able to processes objects in this format (Scheidegger *et al.*, 2005; Moraes, 2012a). Printing a 3D object requires the conversion of cloud points into an STL (STereoLithographic or Standard Tessellations Language) file format. However, the point clouds need to be converted into a mesh first (Newby, 2012). The STL file communicates to the 3D printing machine the dimensions of the object in slices that are printed or cut out and assembled to produce the 3D hardcopy (Ennex Corporation, 2013). The STL file describes the position of triangles in a space using the 3D Cartesian co-ordinate system. Various software can be used to measure and manipulate the variety of file formats available; often more than one program is needed to produce a printable 3D copy of an object (Moraes, 2012a; Noursalehi, 2012; ProtoCAM, 2012; G.S.I., 2013)

Several choices are available for producing a digital 3D copy of a burrow using photogrammetry. Since the goal was to determine the ease and adoptability of photogrammetry in the study of large trace fossils, free software was the preferred option. Two suites were tested including 123D by Autodesk and the Python Photogrammetry Toolbox (Moulon and Bezzi, 2011; Noursalehi, 2012).

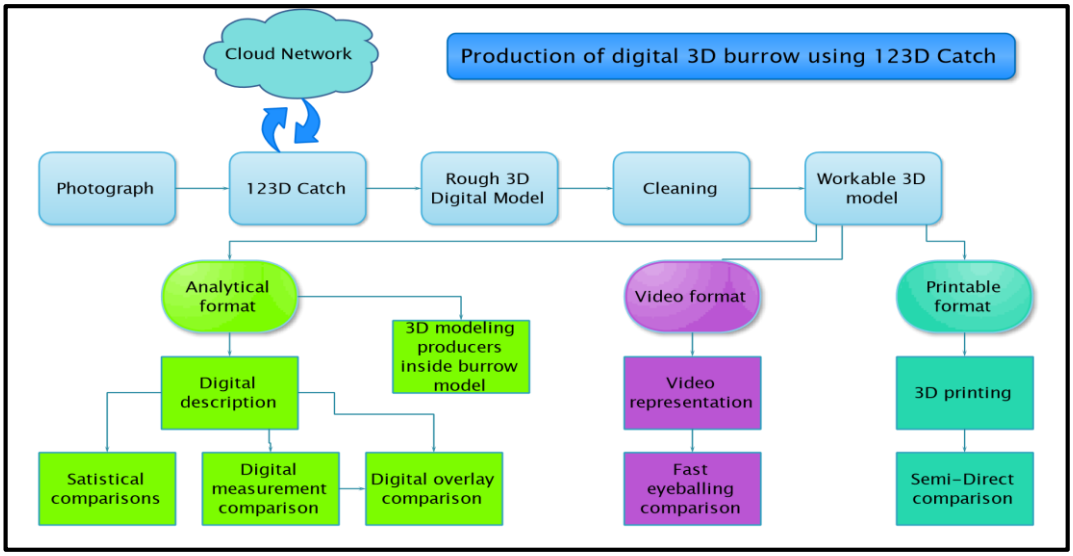

Figure 15. Schematic flow diagram illustrating the workflow of 123D Catch, using photogrammetry, 123D software and cloud processing (Autodesk) (Flow chart produced using Edraw Max)

3.5.3. Photogrammetry workflow

The first step was to photograph a burrow sample using procedures outlined on the 123D Autodesk website and in a YouTube video made by Ehsan Noursalehi (Noursalehi, 2012). The burrow section was placed on a non-repetitive surface (newspaper) for increased number of unique stitching points in the photographs (Figure 17). The burrow was photographed about its circumference with at least ~50% overlap between consecutive photographs. The sample was photographed in the initial spiral ensuring multiple points of reference were captured in the photographs. Thereafter the sample was photographed from slightly higher up (in a spiral). Close-up photographs were then taken at different angles to focus on smaller details.

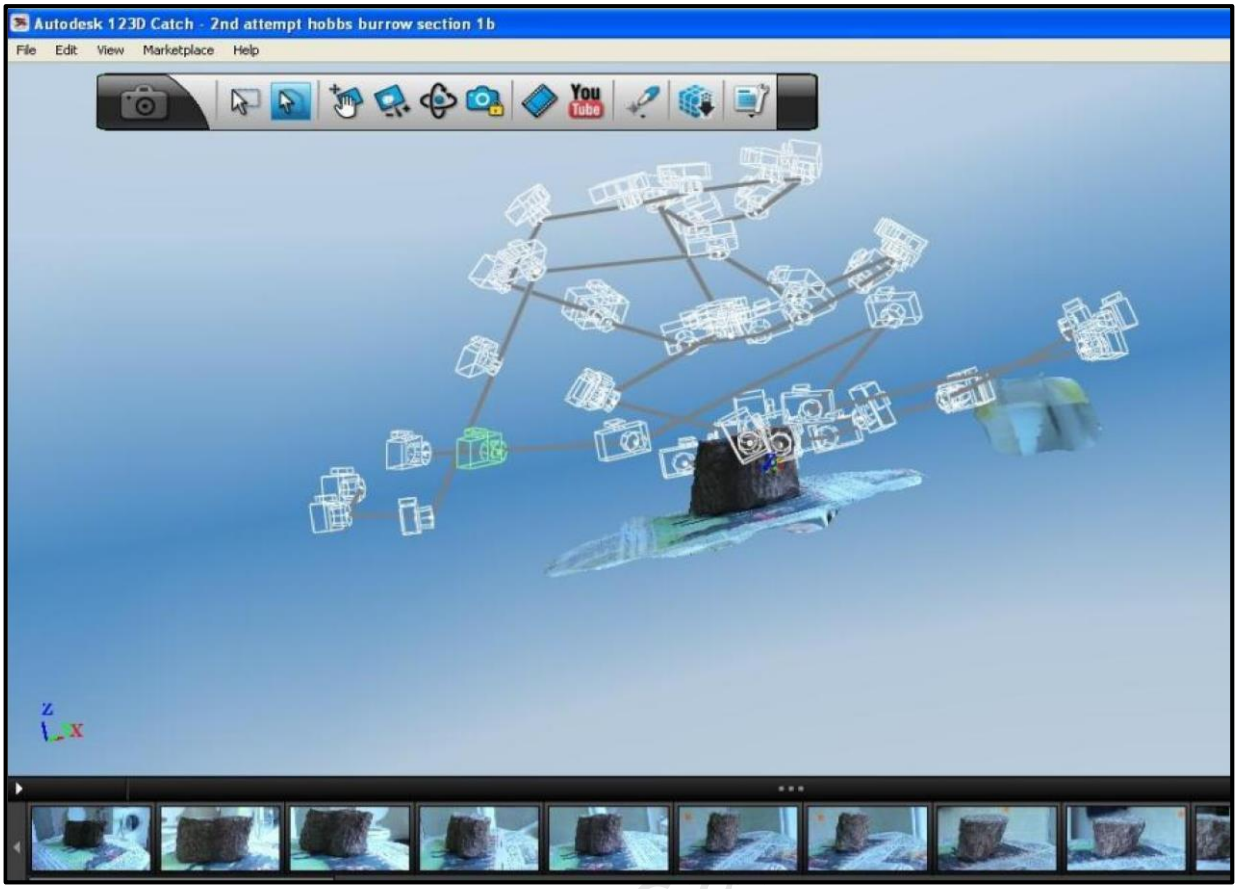

Figure 16. The camera position of the each photograph is graphically presented in Autodesk 123D Catch, software that calculates the position of the camera relative to the object during any given shot. The line between the cameras indicates the spiral pattern used to ensure that the sample was photographed from all angles for maximum coverage, ideal overlap and detail.

Figure 17. A burrow sample on a non-repeating surface (newspaper) with relatively good non-background (the edge of the door is unique); where the background was monotonous different coloured pieces of paper were pasted to serve as unique points of overlap.

The photographs were uploaded onto 123D Catch and processed in their cloud servers (Figure 15). The processed 3D object was then downloaded and when needed photographs were manually stitched and re-uploaded for processing. The corrected 3D object was then cleaned of artefacts. An appropriate format of the burrow section was then opened up in 123D Make; it was then sliced up into cross-sections ideal for 3D printing or cutting out of 2D printed stencils. In addition to the printable format, the 123D Catch outputs were converted to video format and other 3D formats that are compatible with 3D measuring and manipulating software.

Essentially the same methods were used to test the potential of Python Photogrammetry Toolbox (PPT) produced by Moulon and Bezzi (2011). The photographs taken for the 123D Catch software were used for the PPT software. PPT was run on a personal computer (1.8 GHz, on board graphics card) which although not suited for the application produced several meshes. The meshes were then imported into MeshLab to produce a 3D object (Figure 64). The workflow of PPT was not completed, since it requires several more steps that are beyond the scope of this project. A more detailed workflow for PPT is outlined in a post on the ATOR blog; members of the ATOR and PPT projects are willing to help (Moraes, 2012b).

3.6. Palaeontology descriptions and analysis

Fossils were photographed and locations were recorded. Only fossils near the burrows and in danger of being lost due to weathering were collected. They were taken were from the scree material at the base of the railway cutting below the bone bed at Hobbs Hill. The fossils were shown to palaeontologists (Drs JC Cisneros, F. Abdala) to ascertain the need for preparation and further investigation. Upon their advice, specific bones in the samples are planned to be prepared at the Iziko Museum and identified based on cranial features and dentition.

4. Sedimentological Results

4.1. Introduction

The observations and descriptions are summarised here in the large photomosaic in Figure 18 and the composite sedimentary log for Hobbs Hill (Figure 22). The details of the features, structures, facies and their distributions are described in following text.

4.2. Facies Descriptions and Assemblages

In this study, there are two facies assemblages recognised: (1) sandstone assemblage and (2) fine-grained assemblage. Both vary with respect to sedimentary properties and relative thickness between the southeastern and northwestern exposures. At Hobbs Hill (Figure 18), the facies assemblage dominated by laterally extensive stacked sandstone beds is ubiquitous; the sites towards the north (specifically Holmsgrove – see Figure 19) contain more of the fine-grained facies assemblage. This fine-grained facies assemblage is also present to some extent in the western outcrops at Hobbs Hill, which contain the bone beds and burrows.

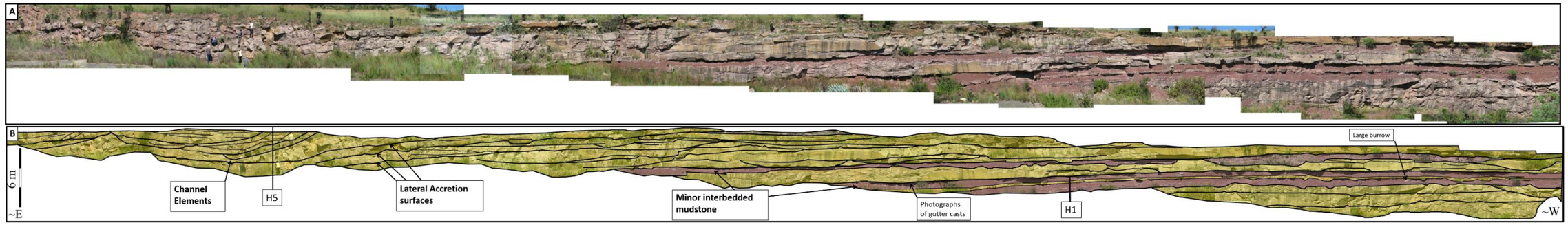

Figure 18. Bed geometries in the Katberg Formation at Hobbs Hill (see Figure 12, H5 to H1). The multi-storey and laterally extensive sandstone packages contain channel elements, lateral accretion surfaces and minor interbedded mudstone beds (outlined and indicate in B, described in section 4.3.). In B the black lines indicate contacts between beds, the yellow areas indicate sandstone facies assemblage and the brown areas indicate fine-grained facies assemblage. The palaeo-current direction is to ~NW (towards the reader) in this ~E-W orientated outcrop (this outcrop is partially visible on google Earth street view).

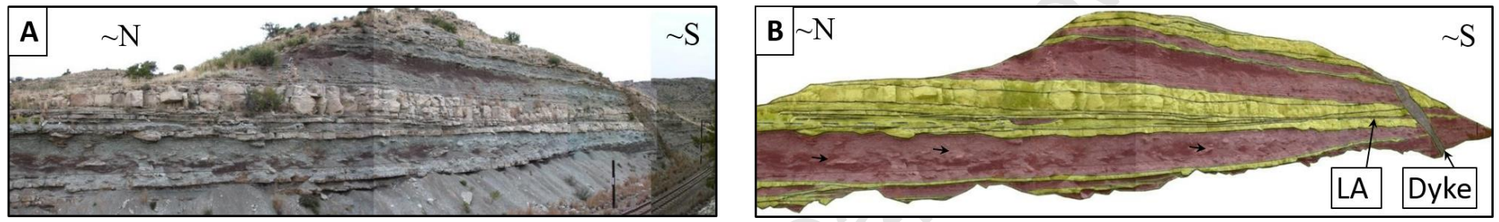

Figure 19. Photomosaic of fine-grained facies dominated outcrops at Holmesgrove (perspective view), the sandstone bodies are thinner than at Hobbs Hill (Figure 18) and isolated sandbodies (~50 – 100 cm) in fine-grained beds are more common. The geometries of the beds are illustrated in B by the same convention used in Figure 18, however the isolated sandbodies are not yellow but are indicated by the arrow in B. LA referes to low angle lateral accretion surfaces and note the dyke has cause some displacement (illustrated in B).

Figure 20. Thick fine-grained facies association (Hobbs Hill, Figure 12 between A and B),with irregular bone beds, “horizontally laminated” ghosts and water escape structures (position indicated by arrows, more detailed photograph in Figures 38 - 42) in a genereally massive unit. Note the fossil material was found below the the arrows.

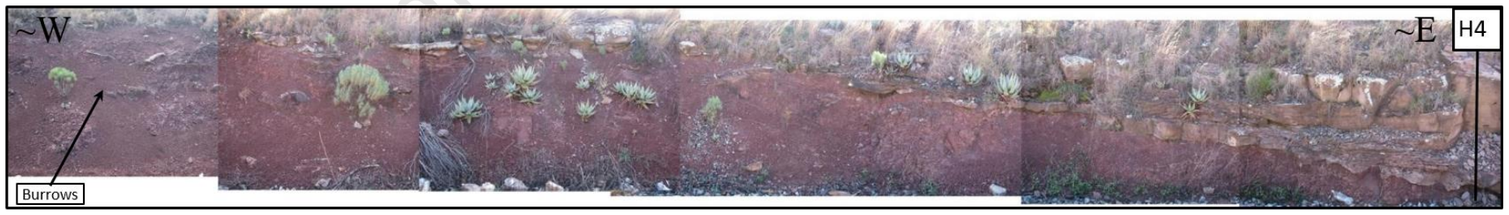

Figure 21. Thick fine-grained facies association (Hobbs Hill, Figure 12 from burrow symbol to H4, opposite side of the railway relative to Figure 20), position of log H4 is indicated (see more detailed illustration in Figure 33) and the area with highest concentration of burrows is indicated (close up in Figure 52).

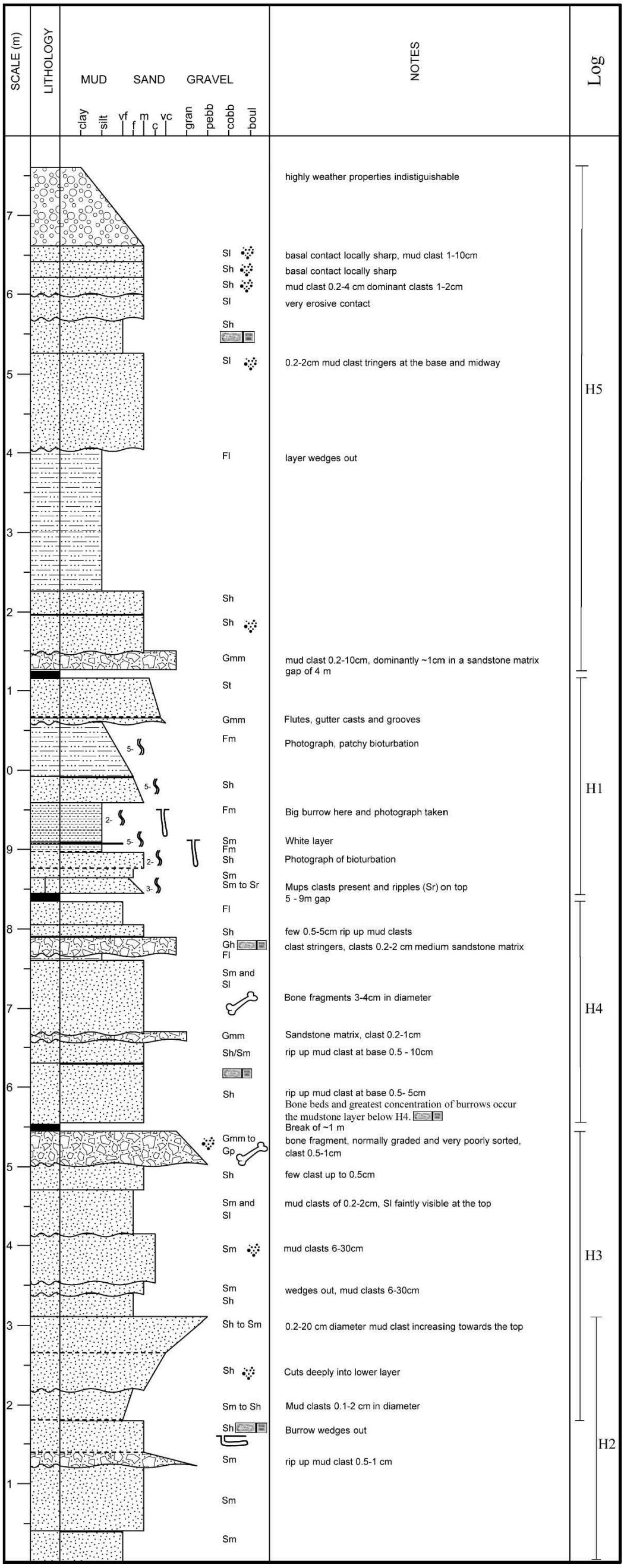

Figure.22. Composite log of Hobbs Hill outcrops made up of logs H5, H1, H4, H3 and H2 (See Figure 12, 18 and 22). The dominant grain size and lithology is indicated for each bed, with facies codes, symbols and notes summarising their physical properties (see legend below). Hand specimen samples were taken from all the beds except from log H1 and reactivity to dilute HCl is indicated (see legend). Representative samples were thin sectioned and the beds are indicated with a thin section symbol (Produced using SedLog).

LEGEND

Code	Lithofacies type
Gmm	Matrix-supported massive gravel
Gh	Horizontally bedded gravel
Gt	Trough cross stratified gravel
Gp	Planar cross-stratified gravel
Sm	Massive or faintly laminated sand
Sh	Horizontally laminated sand
Sl	Low-angle cross bedded sand
Sr	Ripple cross-laminated sand
Fm	Massive mud or clay
Fl	Laminated sand, silt and clay
ssd	Soft-sediment deformation

Symbols

- Large burrow
- Carbonate content
- Fossils
- Thin sections
- 5 Bioturbation intensity (1-5)

Contacts

- Sharp
- Gradational
- Erosive

Lithology

- Gravelly
- Sand
- Mud

4.2.1. Sandstone facies assemblage

This assemblage is most common in the outcrops in the south eastern exposures of the Katberg Formation and the outcrops at Hobbs Hill are good representatives of the region (Figures 18, 19 and 21) (Hiller and Stavrakis, 1984). They consist of laterally extensive, ~50 cm thick tabular sandstone to gravelly beds, stacked on top of each other into package up to 6 meters thick, with minor interbedded mudstone (and siltstone) beds. At Hobbs Hill, the sandy lithofacies dominates (76%), followed by gravelly lithofacies (12%) and fine-grained lithofacies (12%) (Figures 22 and 24).

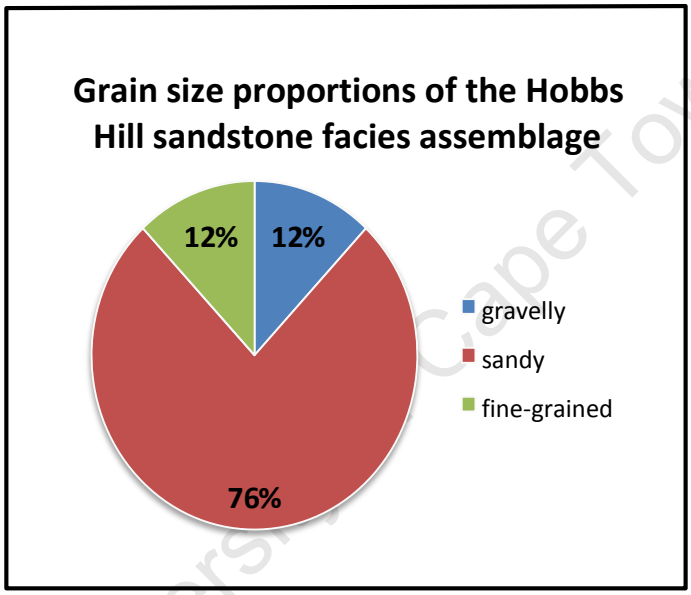

Figure 23. The dominance of sandstones is illustrated as a percentage of the sandy facies assemblage logged at Hobbs Hill.

Sandy lithofacies (Sm, Sh and Sl)

The sandy lithofacies are pale yellowish brown (code 10YR 6/2 in the Munsell rock colour chart, 2009) to pale red (5R 6/2) in colour. The sandstones vary in thickness from 1-90 cm, are very fine to coarse-grained, with minor intraformational clasts ranging from 0.2 mm to 30 cm in diameter. The majority of the beds are composed of medium-grained sand (Figure 24). The two most common lithofacies at Hobbs Hill are the horizontally laminated (Sh, 47%), massive (Sm, 32%) and low-angle cross-bedded sandstones (Sl, 15%) (Figure 25). Unidentified bone fragments (3-4 cm in diameter) were also noted in several beds (Figure 22).

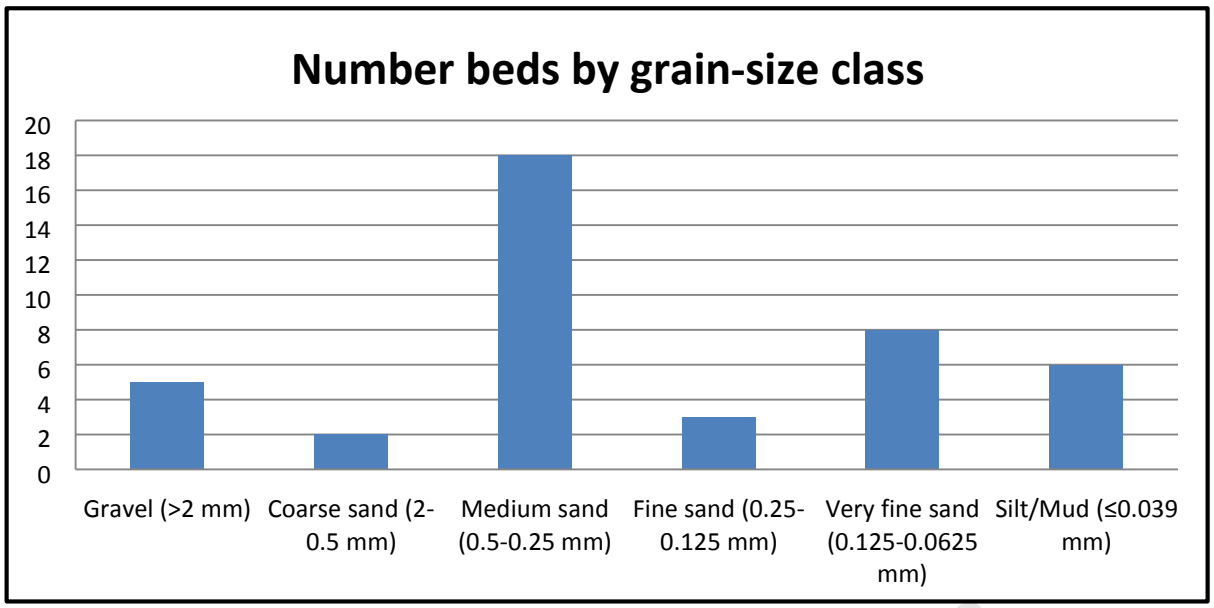

Figure 24. Number of beds by grain-size classes, with medium-grained sandstones dominating the Hobbs Hill outcrops with 18 out of 42 logged beds.

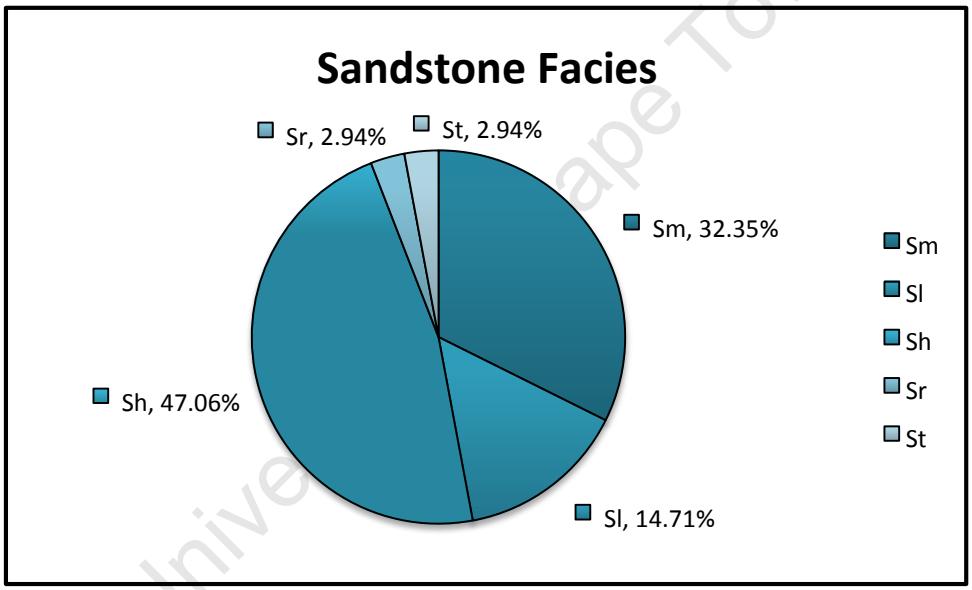

Figure 25. The horizontally laminated, massive and low-angle cross-bedded lithofacies make up the majority of the sandstone beds. This indicates that high-energy conditions dominated during deposition (cf. Miall, 1996).

Petrography

The sandstones are composed of rounded to subangular, poorly sorted, very fine to coarse-grained sand (0.1 to 0.5 mm average 0.3 mm). The particles are predominantly quartz (65%); feldspar (20%) is less common, but more numerous than lithic fragments (15%).

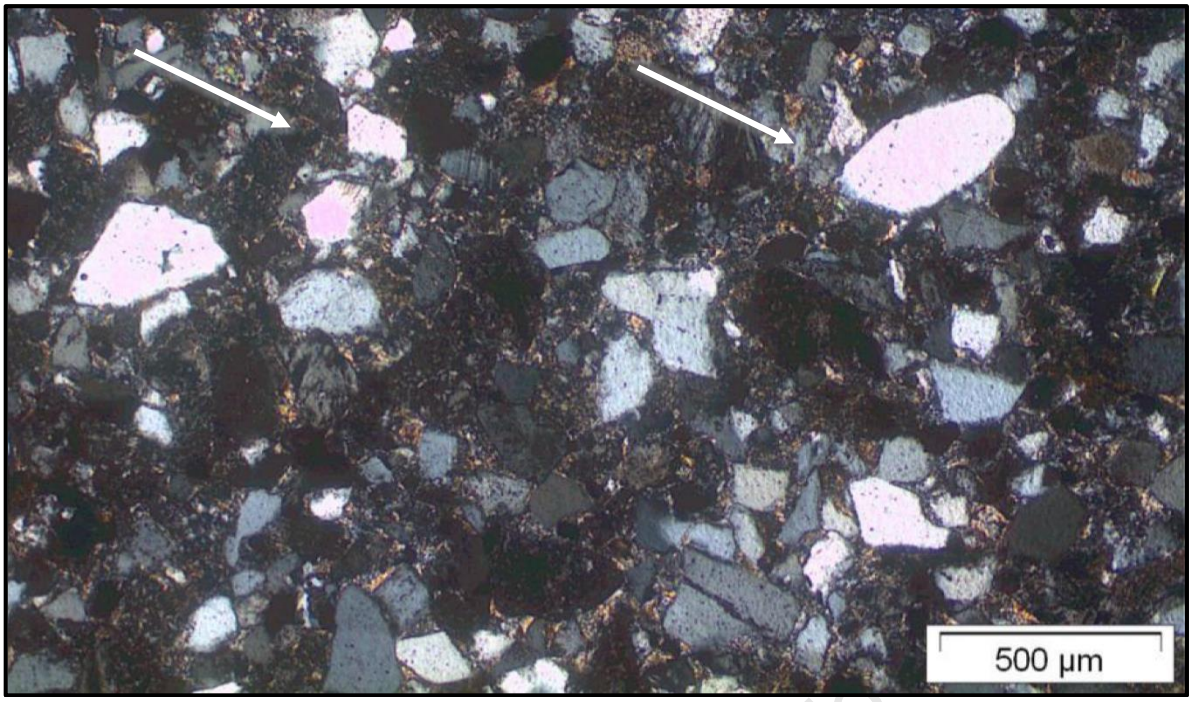

Figure 26. The large variation in size and roundness of the quartz grains (indicated by the white arrows) in a relatively poorly sorted medium-grained sandstone sample taken from Hobbs Hill (Figure 22, log H4 bed 1) (the dominant lithology see Figure 24).

The matrix is mostly made up minerals (presumably clay) too small to see in thin-section using standard petrographic methods, however some mica and poorly recrystallized quartz (opal or chert) were identified (Figure 28). The cement is not visible, but the presence of quartz overgrowths and poorly recrystallized quartz in the matrix would suggest that quartz is a component in the cement (Figure 27). Dilute HCl testing indicated that although not seen in thin-sectioned samples, carbonate is a component in some sandstones (Figure 26). Quartz grains tend to be monocrystalline, with a wide range of grain sizes (0.1-1 mm) and levels of roundness (well rounded to angular) (Figures 26, 27 and 28). Feldspar is often more angular than quartz and generally altered giving it a dusty appearance in plain polarized light and obscuring the twining, however albite and cross-hatch twinning can be observed (Figure 28). The lithic fragments include chert, igneous (possibly volcanic), metamorphosed mudstones (fragments composed of "foliated" grains), mudstones, heavy minerals and opaques (Figure 27 and 28).

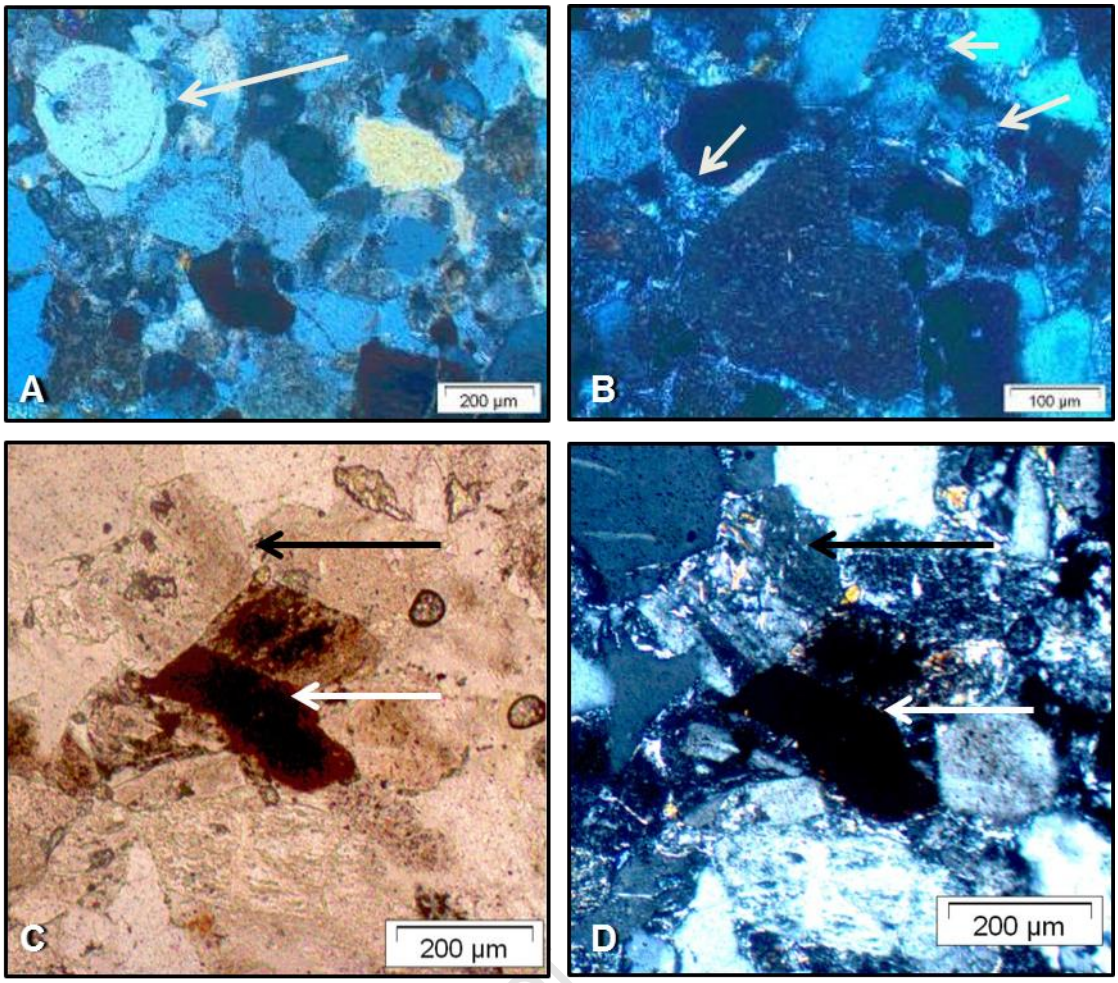

Figure 27. Quartz overgrowths on a rounded quartz grain (A, white arrow) and poorly recrystallized quartz (B, white arrows) (x10 and x20 magnification respectively). The dusty appearance of an altered feldspar grain (black arrow) in plain polarised light (C) and the obscured twinning of the same grain in cross-polarised light (D). The dark grain (white arrow) in the centre of C and D is a mudstone fragment (Samples from Hobbs Hill, log H2 bed 4, Figure 22).

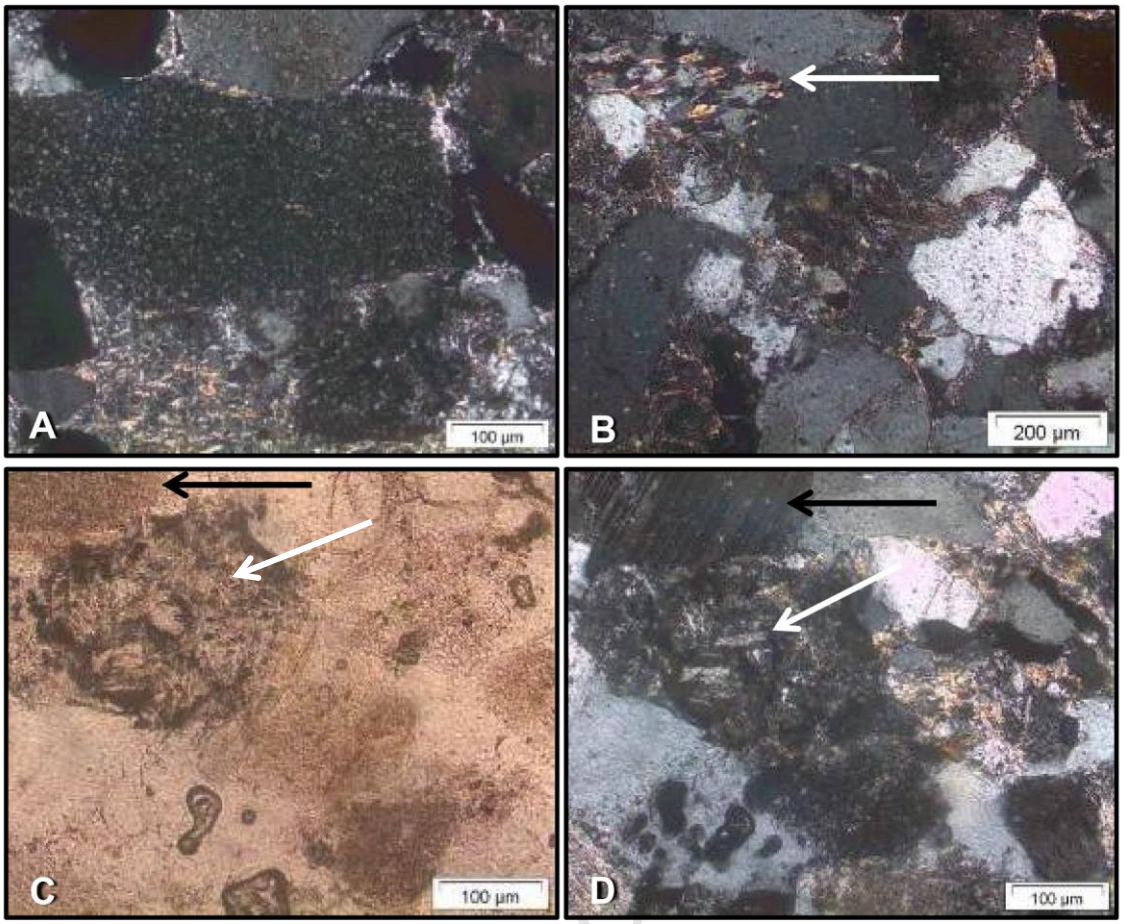

Figure 28. Lithic fragments in the sandstones from Hobbs Hill: Chert (centre of A), possible metamorphosed sedimentary fragment (B, white arrow) and a possible volcanic grain (white arrow in C and D) consisting of several needle shaped grains. Note the dusty appearance of the feldspar grain in plain polarised light (C, black arrow), showing twining in crossed polarised light (D). All photomicrographs are at 20x magnification except B which is in 10x magnification (Samples from Hobbs Hill, log H5 bed 6, Figure 22).

The heavy minerals and opaques such as zircon and metal oxides respectively tend to be smaller than the other minerals, more in the 0.05 – 0.1 mm range than around 0.3 mm. These minerals occur in trace amounts distributed throughout the thin sections but sometimes concentrated in lamina (Figures 29 and 18). The heavy mineral stringers are visible in outcrop scale as dark lines in horizontally laminated sandstones and in thin section as concentrated lamina (Figure 29).

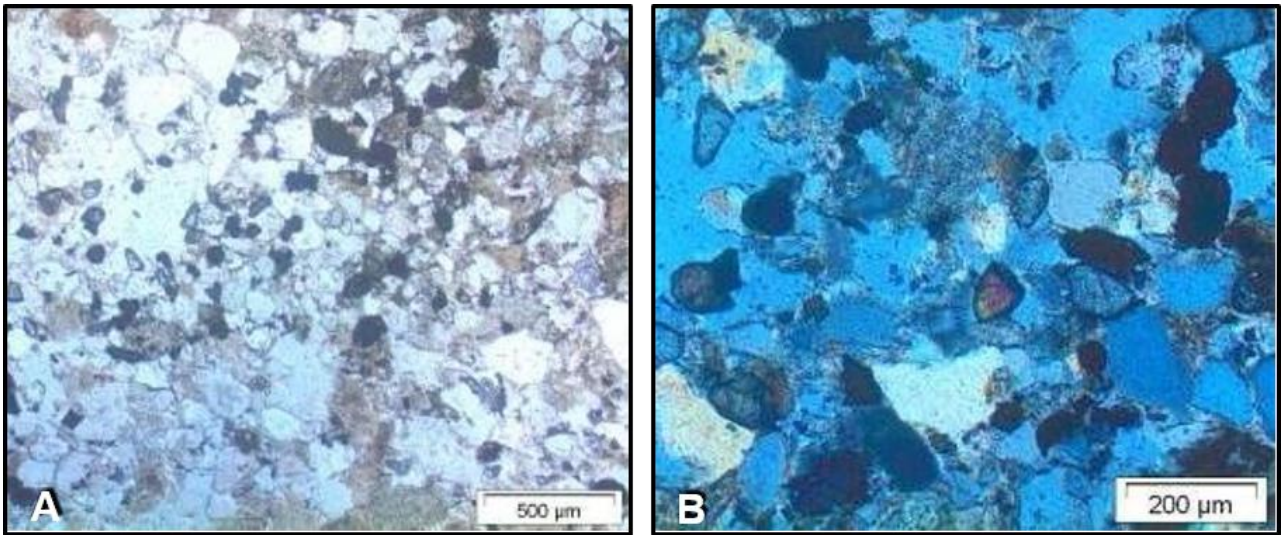

Figure 29. Heavy mineral stringer from an Sh facies sandstone (Figure 22) composed of opaque and high refractive index minerals in A (concentrated diagonally across A, plain polarized light and 5x magnification), these mineral are identified as zircons and oxide minerals based on their appearance in cross polarised light at 10x magnification (B) (Samples from Hobbs Hill, log H2 bed 4, Figure 22).

Lithofacies variations

The Sm lithofacies, show gradational changes in terms of both grain size and internal structures. For instance, some beds show grading from medium-grained massive sand (Sm) at the base to very fine-grained sand with ripple marks (Sr) at the top of the bed. Changes from horizontally laminated sandstone (Sh) with rip-up mudstone clasts at the base to massive sandstone (Sm) at the top are also noted. The horizontally laminated sandstones (Sh) are generally medium-grained, less commonly very fine to fine-grained sand and have minor components of rip-up mudstone clasts ranging in diameter from 0.5 to 5 cm.

The beds are 15 to 90 cm thick and have generally uniform grain size, however rip-up mudstone clasts up to 2-3 cm in diameter tend to occur at the lower parts of the beds (Figures 34, 35 and 50). The low-angle cross-bedded sandstone lithofacies (Sl) is relatively uncommon at Hobbs Hill. They are 20-120 cm thick, predominantly medium-grained and locally fine-grained. In some beds, there are intraformational clast stringers in the middle and at the base, with clasts of 0.2-2 cm in diameter. The lower contacts of the sandstone beds are often sharp or erosive with rip-up mudstone clasts

generally 1-2 cm in diameter (Figures 18, 30 and 32), scour marks, gutter and flute casts (Figure 32). The contacts between some sandstone and fine-grained beds preserve desiccation cracks in the northern parts of the study area (Figure 32).

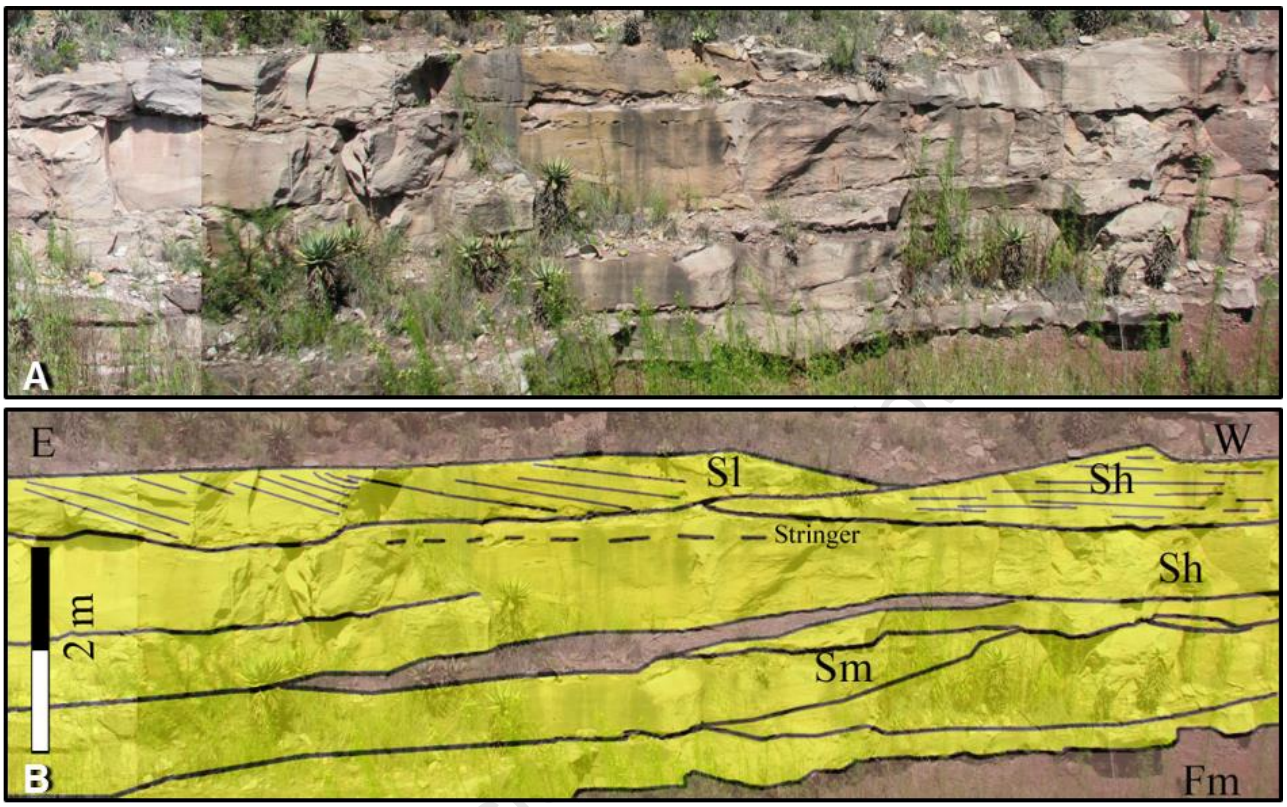

Figure 30. Stacked tabular and wedge shaped sandstone beds separated by sharp and erosional contacts (outlined in B). Lithofacies visible in A and indicated in B include low angle cross-bedded (Sl), horizontal laminated (Sh), massive sandstone (Sm) and massive fine-grained mudstones (Fm). Note the cross-beds are dipping roughly west, while the erosional surfaces tend to dip towards the east. The thick solid lines indicate strong erosion surfaces; the dashed line indicates a mudclast stringer and the thinner lines highlight the internal structures (Hobbs Hill outcrop at log H5 in Figure 12, see lateral accretion surfaces).

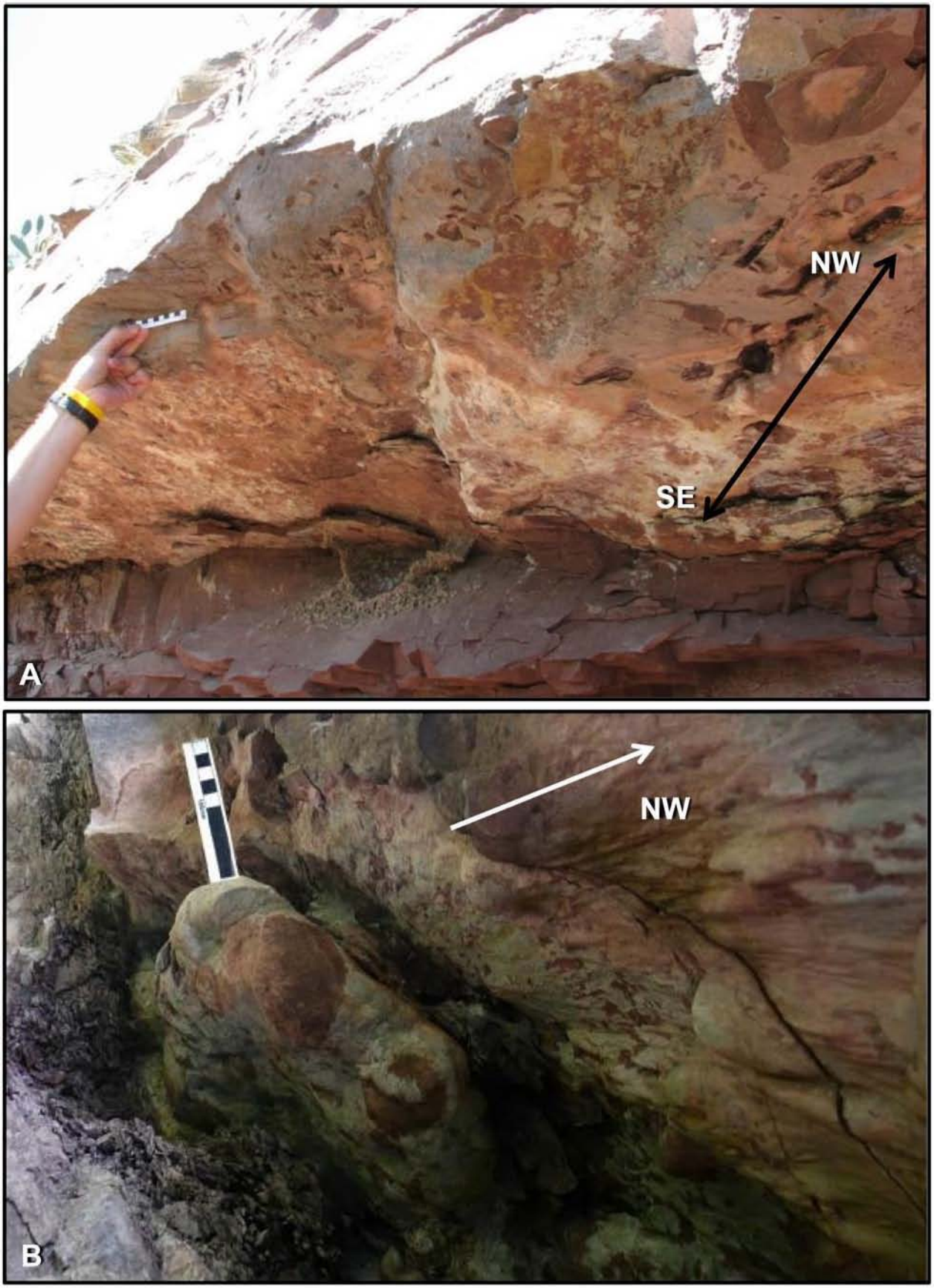

Figure 31. Some examples of scour marks and flute casts that often occur at the erosional contacts between sandstone and fine-grained (mudstone) beds. The black arrow indicates the SE/NW trend of the scour marks in A (Scale bar = 5 cm). In B, the flute cast indicate a northwesterly flow direction (white arrow) (Scale bar = 10 cm). The large sandstone structure below the scale bar in B is best explained as a very large and unusual rip-up clast or a gutter cast (Photograph taken at Hobbs Hill, between H5 and H1).

Figure 32. Sand-filled desiccation cracks in massive mudstone (Fm) near Holmsgrove (A) (near Figure 19) and at Kapteinskraal (B Scale bar = 10 cm).

Gravelly lithofacies (Gmm, Gh and Gp)

The beds containing Gmm, Gh and Gp, are those that contain 30% or more grains larger than 2 mm. The beds range in thickness from <5 cm up to 40 cm, containing clasts composed of almost exclusively mudstone chips, ranging in size from 0.2 cm to 10 cm in a matrix of fine- to coarse-grained sand (Figure 21 and 33). These beds are generally massive, however in some cases the mudclasts are aligned as stringers (Gh and Gt) or grade from massive (Gmm) at the base to stratified at the top (Gp). The gravelly lithofacies at the sites near Bethulie contain bone fragments and reworked pedogenic nodules. This type of conglomerate was not observed at Hobbs Hill. The majority of gravelly samples at Hobbs Hill did not react with dilute HCl (10%) indicating the absence of carbonates.

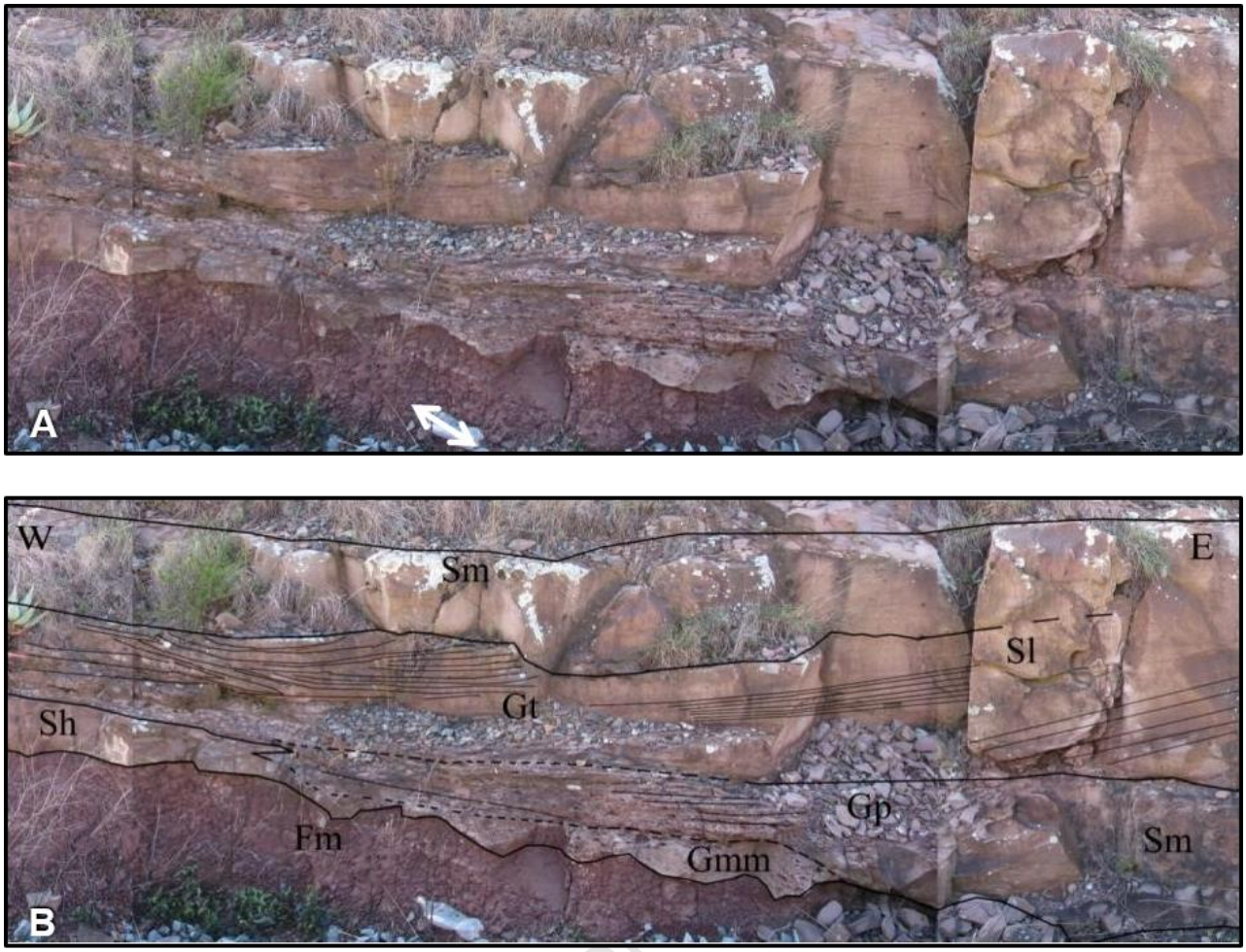

Figure 33. A channel filled by the sandstone facies assemblage consisting of a gravely lithofacies at the base that cuts into the mudstones of the fine-grained facies assemblage (Fm). The sedimentary structures outlined in B include trough cross-bedding (Gt), low-angle crossbedding (Sl) and a general upward fining cycle from Gmm, Gp, Gt, Sl and Sm. The mudstones (fine-grained assemblage) contain burrows and several discontinuous bone beds at Hobbs Hill (Figure 21) (Scale = 30 cm bottle).

Petrography

The particles in the conglomerate thin section are all mudstone clasts, ranging in size from sand to gravel (0.2-2 cm) (Figure 33). The clasts are plate like, sometimes with curved edges (Figures 33, 34 and 35). The size, composition and appearance in hand specimen and outcrop indicate that these particles are rip-up mudstone clasts. The matrix is the same as the sandstones (Figures 34 and 35). No other diagnostic features (such as concretions, fossil fragments, rhizocretions, coprolites), which could have shed light on the palaeo-environment, were identified in the samples studied.

Figure 34. Scanned thin section of a sample from Hobbs Hill (in Figure 22, log H4 unit 6, and thin section symbol) of the Gh lithofacies. Note that the overall fabric is highlighted by the orientation of the rip-up mudstone clasts (black double arrow is 2.7 cm for scale).

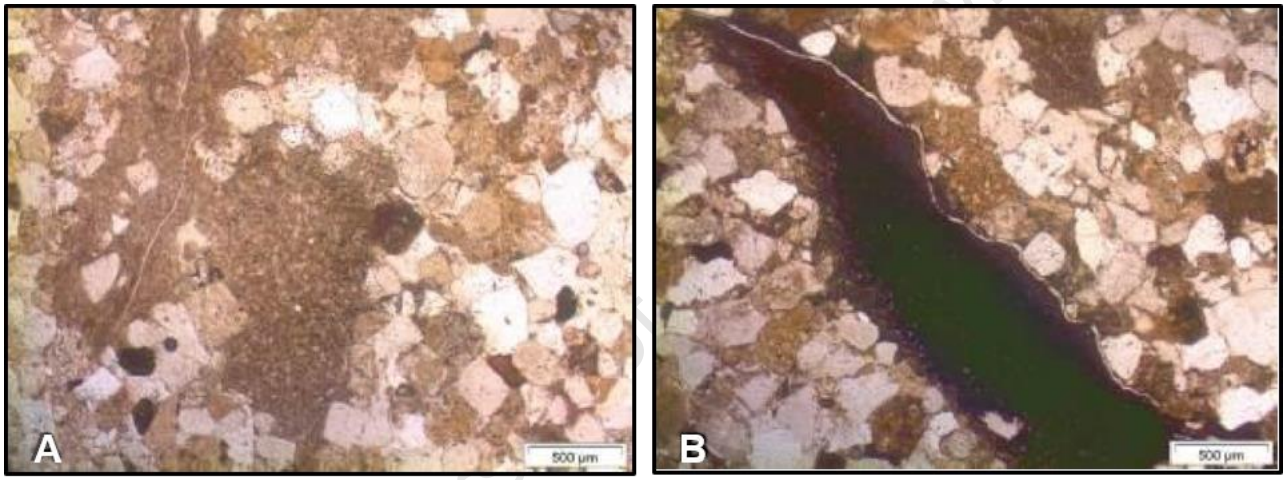

Figure 35. The large rip-up mudstone clast in Figure 34 (above) at 5x magnification in plain polarised light. Note that the clast in A has appears to have "mixed" with the matrix material (suggesting a soft and unconsolidated nature of the clast during deposition) while in B the mudstone clast has more discreet boundaries; the latter is much more common.

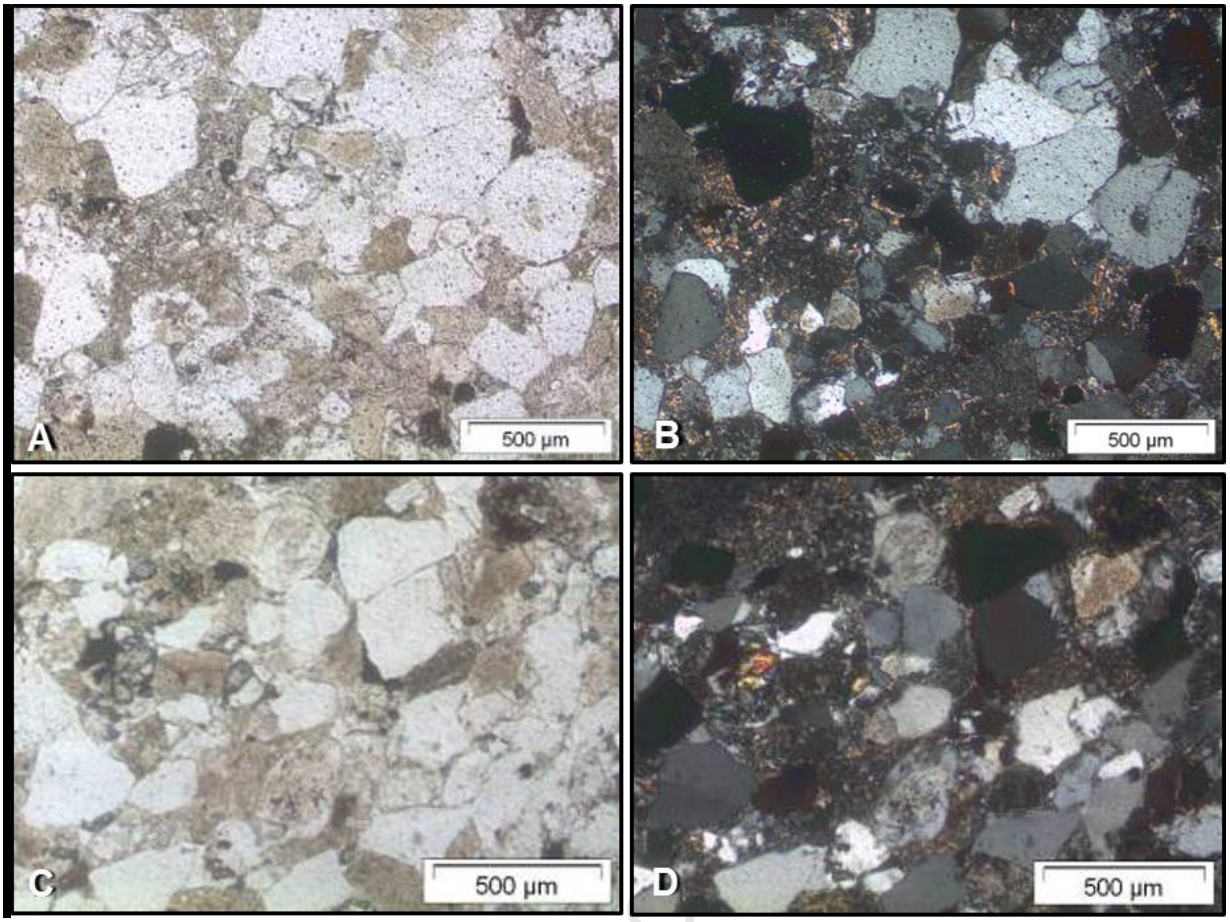

Figure 36. The matrix of the conglomerates (A and B) (in Figure 22, log H4 unit 6, thin section symbol) consist of the same material as the sandstones (C and D) (in Figure 22, log H5 unit 6, thin section symbol) in plain polarised light (A and C) and cross polarised light (B and D) at 5x magnification.

4.2.2. Fine-grained facies assemblage

The fine-grained facies assemblages occur as relatively thick successions of mudstone to siltstone beds (>1.8m) with minor sandstone beds (Figures 19, 20 and 21). When interbedded with the sandstone facies assemblage, they generally occur as isolates drapes or lenses but also as laterally extensive (up to 30m) interbeds, ranging in thickness from 0.1-1.8 m (Figures 18 and 37). The sandstone facies that occur in the thick fine-grained packages were not studied in detail, but the majority occur as isolated irregular lenses 50 cm thick and up to 4 m in lateral extent (Figure 19). The contacts of the beds are mostly erosional at the base and the top when occurring between sandstone beds; only one mudstone bed was found with a gradational contact (Figures 18, 19, 31, 32 and 33). Contacts between fine-grained beds in the thick fine-grained package were not common

and when visible they are irregular and diffuse (Figures 39, 40 and 41). The lack of visible contacts in the thick fine-grained packages is most likely because of multiple processes including bioturbation, blocky weathering and possibly pedogenesis. At Hobbs Hill, the mudstones of this assemblage are blackish red (5R 2/2) to greyish red (10R 4/2), while towards the north they are more varied with some greenish grey (5GY 6/1 to 5G 6/1) mudstones (Figures 20 and 19 respectively). The beds are generally massive (Fm) with minor occurrences of horizontal lamination (Fl) observed, several of the mudstone beds showed evidence of soft sediment deformation (ssd) (Figure 37). These features occur in isolated lenses of mudstone between laterally extensive sandstone beds and in the thick fine-grained packages. The deformed parts of the mudstones contain irregular lobe or raindrop shaped mudstone and sometimes sandstone (Figure 37). In addition to soft sediment deformation, the thick mudstone beds at Hobbs Hill contain horizons and pockets of bone fragments ranging from over 10 cm to a few mm (Figures 12, 21, 40, 41 and 42). None of the fine-grained samples reacted when exposed to dilute HCl; however, it must be noted that the samples tested did not contain bone fragments or nodules.

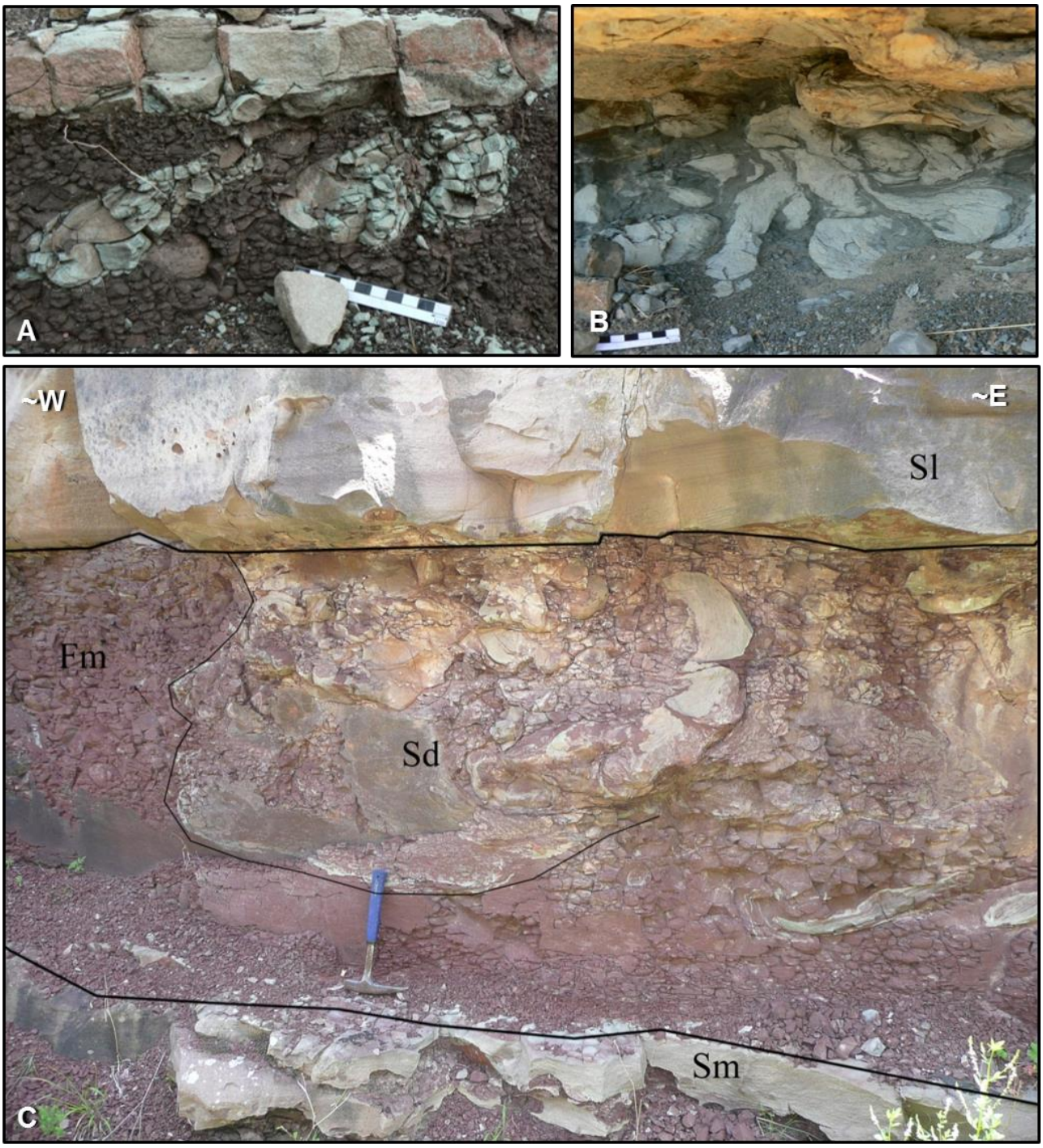

Figure 37. Soft-sediment deformation features including teardrop-shaped lobes of mudstone (A, Rooiwal), irregular lobes (B, Jakkalsfontein), a mix of mudstone and sandstone (C, Hobbs Hill, ~5m below H1 in outcrop opposite the one illustrated in Figure 18 and 22). Note C show a mudstone lens between sandstone beds, the thinner black line outline the interface between the massive mudstone (Fm) and the mixed zone (scale bar 10 cm in A, 6 cm in B and ~30 cm geopick in C).

Figure 38. Water escape structure in a mudstone bed of the fine-grained facies assemblage (Figures 40 and 20) (Scale = 2 cm).

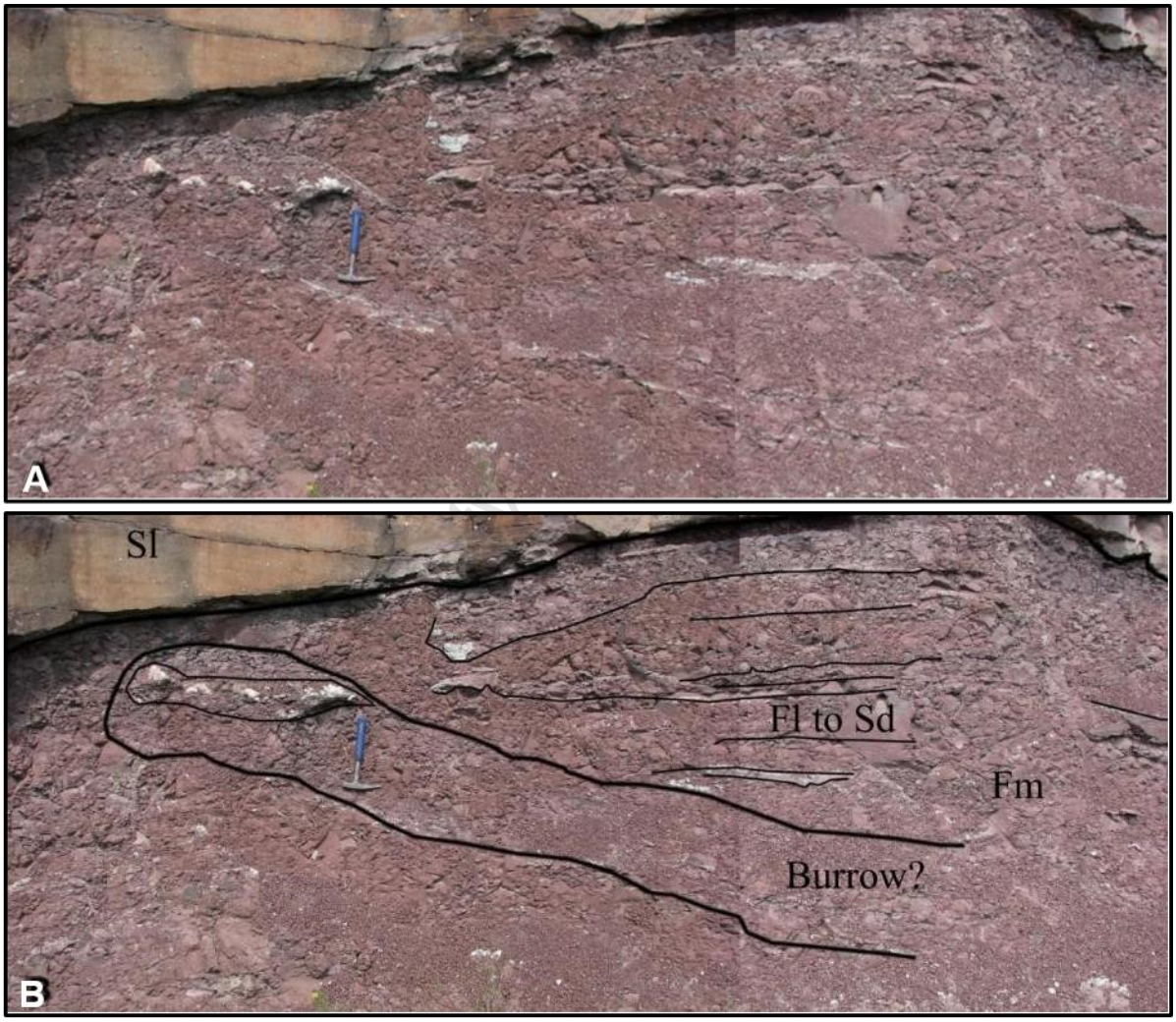

Figure 39. The vague outline of a possible very large burrow (outlined in B, from Hobbs Hill see Figure 20) containing a pocket of fossil fragments (above geopick), in a generally massive mudstone bed (Fm), with some faintly laminated parts (Fl) (indicated by finer lines in B) which have been disturbed by soft sediment deformation or bioturbation (Figures 41 and 47). The contact with the low angle cross-bedded sandstone above is erosional. Note the geopick is ~30 cm for scale.

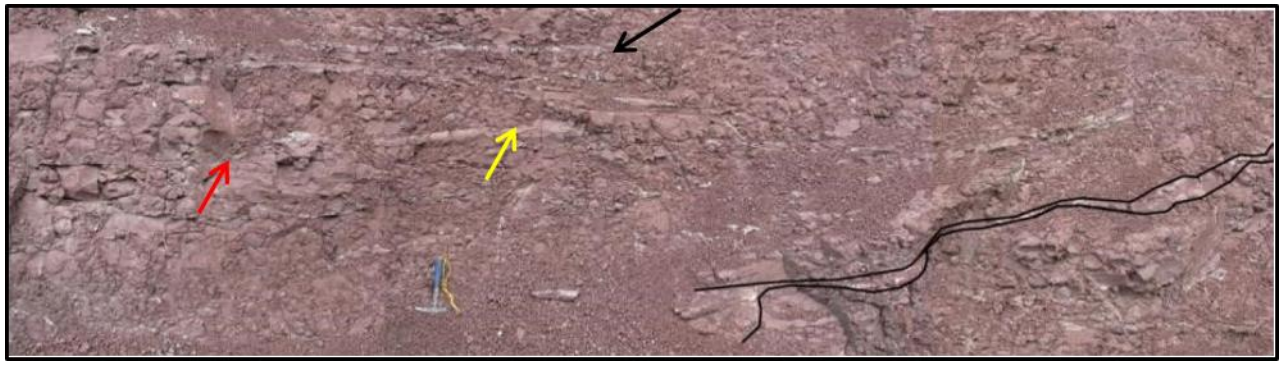

Figure 40. Bone bed (black outline) in the thick mudstone bed (Figure 20) that is mostly massive, but contains some faint horizontal lamination, water escape structures (yellow arrow and in Figure 38) and pockets of bone fragments (Red arrow and in Figure 41).

Figure 41. A close up of the bone horizon (Figure 40), note the size range (~0.1 cm to 9 cm) and fragmented nature of the fossil. Soft sediment deformation features (white arrow) are also visible below the bones. The black arrow indicates an area containing several millimetre scale bone fragments (white spots).

Figure 42. Bone fragments at the base of the mudstone unit directly below the bone horizon indicated in Figure 40, the arrow indicates a tusk and part of a skull (Scale bar = 10 cm).

4.3. Architectural Element Analysis

There are four architectural elements (AE) identified in this study based on the lithofacies, sedimentary structures, palaeo-current directions, geometries of the beds, erosional contacts and the spatial relationships of the beds (Miall, 1985, 1996; Colombera *et al.*, 2012). The architectural elements occur at different scales with (1) large-scale channel elements (CH) containing (2) lateral accretion macroforms (LA) and (3) sandy bedforms (SB), eroding into (4) floodplain fines (FF) (Figure 43).

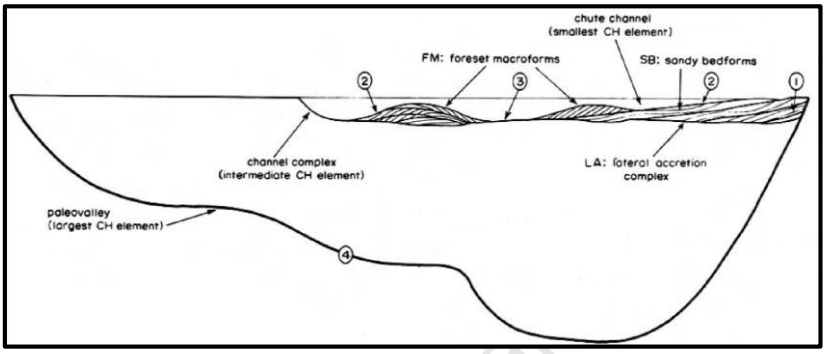

Figure 43. A schematic diagram of the possible architectural elements which can occur in a channel (taken from Miall, 1985).

4.3.1. Channel elements (CH)

The channel element refers to the large or intermediate scale structure with a concave-up erosional base, filled up with channel fill deposits (indicating fluvial processes) (Figure 43) (Miall, 1985). In the study, palaeovalley channel element is not confined (Figure 18), however locally margins are preserved of intermediate channel elements (Figure 33). The margins are identified where thick mudstone beds are truncated by irregular, concave-up erosional bases overlain by gravelly to sandy facies (Figures 18, 21 and 33).

The channel fill consist of fining upward sequences of gravelly beds locally (Gmm to Gp to Gt) to sandy beds (Sm, Sl and Sh) with minor interbedded fine grain beds (Fm and Fl). Figure 33 gives a good overview of the features of the channel margin and base, with most of the outcrops preserving the central parts of the CH and the FF elements (Figure 18-22). Within the CH several macroforms such as Lateral Accretion (LA) and Sandy Bedforms (SB) occur.

4.3.2. Sandy Bedforms (SB)

Sandstone units occur as laterally extensive sheets (Figure 18) and stacks of tabular, lens and wedge shaped beds (Figure 30). The top of these stacks of are often irregular and erosional, some are draped or capped by finer grained beds (Figure 18).

The SB element can be divided into different elements based on more detailed investigations of the geometries of the beds and the macroforms. Those that have gently dipping bounding surfaces indicate possible Lateral or Downstream Accretion elements (see below).Within the stacks of sandstones there occur laterally extensive tabular bodies made up of lens and wedge shape beds. These multi-element tabular bodies fit well with the description of the Foreset Macroforms (FM) element of Miall (1985). The Foreset Macroform elements (FM) refer to sequences of beds that are interbedded and cut into each other to produce convex up erosional contacts that suggest that they were deposited at the same time. The nature of the bounding surfaces allow their distinction from the Lateral Accretion (LA) elements described below (4.2.3). Therefore, the SB elements referred to here are only those elements consisting of the larger scale tabular bodies that are made up of fewer, but thicker and more extensive beds that do not have bounding surfaces that dip sufficiently enough to be considered LA or DA.

.

4.3.3. Lateral Accretion elements (LA)

Lateral and downstream accretion elements (LA and DA) refer to sequences of beds that were deposited simultaneously and interbedded over wide areas with dipping bounding surfaces (Miall, 1996). The main difference between LA and DA is the relationship between the dipping accretion surface and the current direction. Downstream accretion refers to beds, which dip downstream within 60° of the palaeo-current direction (dips “parallel” to current direction).

Lateral accretion (LA) refers to units with almost the exact same architecture as DA but with beds dipping roughly perpendicular to the palaeo-current direction. At Hobbs Hill, palaeo-current indicators included: gutter casts (SE/NW trend, Figure 31), flute casts (NW direction, Figure 31), cross-bedding (~W flow direction, Figure 30) and trough crossbedding (~NW/SE trend, Figure 33). All together, these features suggest a general northwest flowing palaeo-current (for Hobbs Hill). This palaeo-current direction is consistent with the general palaeo-current for the Katberg Formation in the south-eastern parts of the main Karoo Basin (Johnson, 1976; Hiller and Stavrakis, 1984; Groenewald, 1996; Bordy *et al*., 2010). The bounding surface between the beds, which conform to accretion type geometries tend to dip towards the west.

The palaeo-current direction is thus roughly perpendicular to the dip of the accretion surfaces (Figure 18). The accretion elements observed in the sandstone facies assemblage of the outcrops at Hobbs Hill and Holmsgrove are therefore Lateral Accretion Elements.

4.3.4. Floodplain Fines Element (FF)

The fine-grained assemblages that occur as thick successions in the western part of the Hobbs Hill outcrop are considered Floodplain Fines (FF) elements. Their lateral extent and thickness distinguish them from the fine-grained assemblages, which are part of the CH, SB and FM elements. The geometries of the fine-grained beds that make up this element were not visible; the coarse-grained beds that occur within are irregular and diffuse but do suggest floodplain channels may have existed (Figures 22 and 40). The contacts between FF and other elements are sharp and erosional (Figures 21 and 22).

4.4. Sedimentology of the burrow fill

Burrows contain features and structures that provide further evidence for the processes and conditions that occurred between deposition and lithification. This information together with conventional sedimentary structures can be used for the reconstruction of the depositional environment.

The burrows in this study all have carbonate content, based on the reaction with dilute HCl, while the host rocks do not. In thin sections, the burrow casts show grains that appear to "float" in a carbonate cement, with carbonate replacement of feldspar occasionally observed (Figure 44).

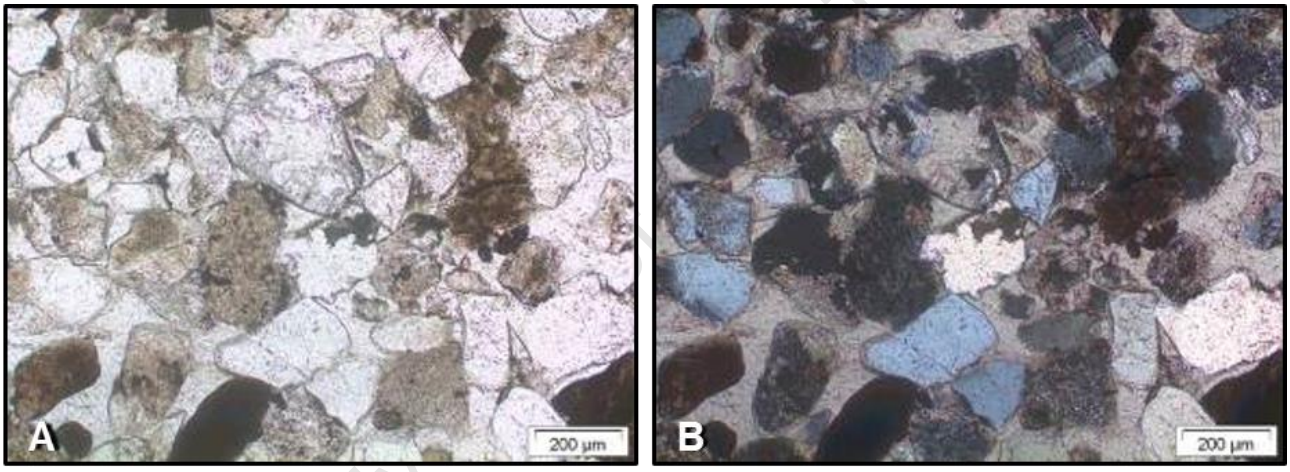

Figure 44. Burrow fill matrix in plain polarised light and in cross-polarised light at 10x magnification, note how the grains appear to be floating in calcite and how feldspar has altered to calcite in the larger grain (top centre) and in several smaller grains (Hobbs Hill burrow sample, see Figure 52).

The texture in Figure 44 could at first glance be considered ether floating grains or poikilotopic carbonate (Quast *et al.*, 2006). Both terms describe clasts that are not or are in limited contact with each other and surrounded by carbonate minerals (Friedman, 1965 and Goudie, 1983 in Quast *et al.*, 2006). The major difference being that floating grains occur in a fine (cryptocrystalline) carbonate matrix, while the poikilotopic carbonate is coarse-grained (<40 µm) (Quast *et al.*, 2006).

This difference in grain size is important for their origin as floating grains are precipitated in the vadose zone (shallow depths, above the water table) and poikilotopic carbonates are thought to form in the phreatic zone or during deep burial, without a change in volume (no displacement) (Quast *et al.*, 2006). This gives an indication of depth of carbonate precipitation relative to the water table.

4.4.1. Displacive carbonate

Displacive carbonate or displacive calcite refers to the growth of carbonates in sediments near the surface (vadose zone), during diagenesis while simultaneously dispersing and expanding the clast (Saigal and Walton, 1988). Evidence for this includes exploding grains, floating grains, granular cracks and floating grains (Klappa, 1979; Saigal and Walton, 1988; Quast *et al.*, 2006). Exploding grains were not seen in any of the thin sections, some burrows showed features that indicate displacive carbonate growth. In thin sections, some of the burrows show carbonate that appears to have torn the matrix apart near and at the interface between the burrow fill and the host rock (Figure 45).

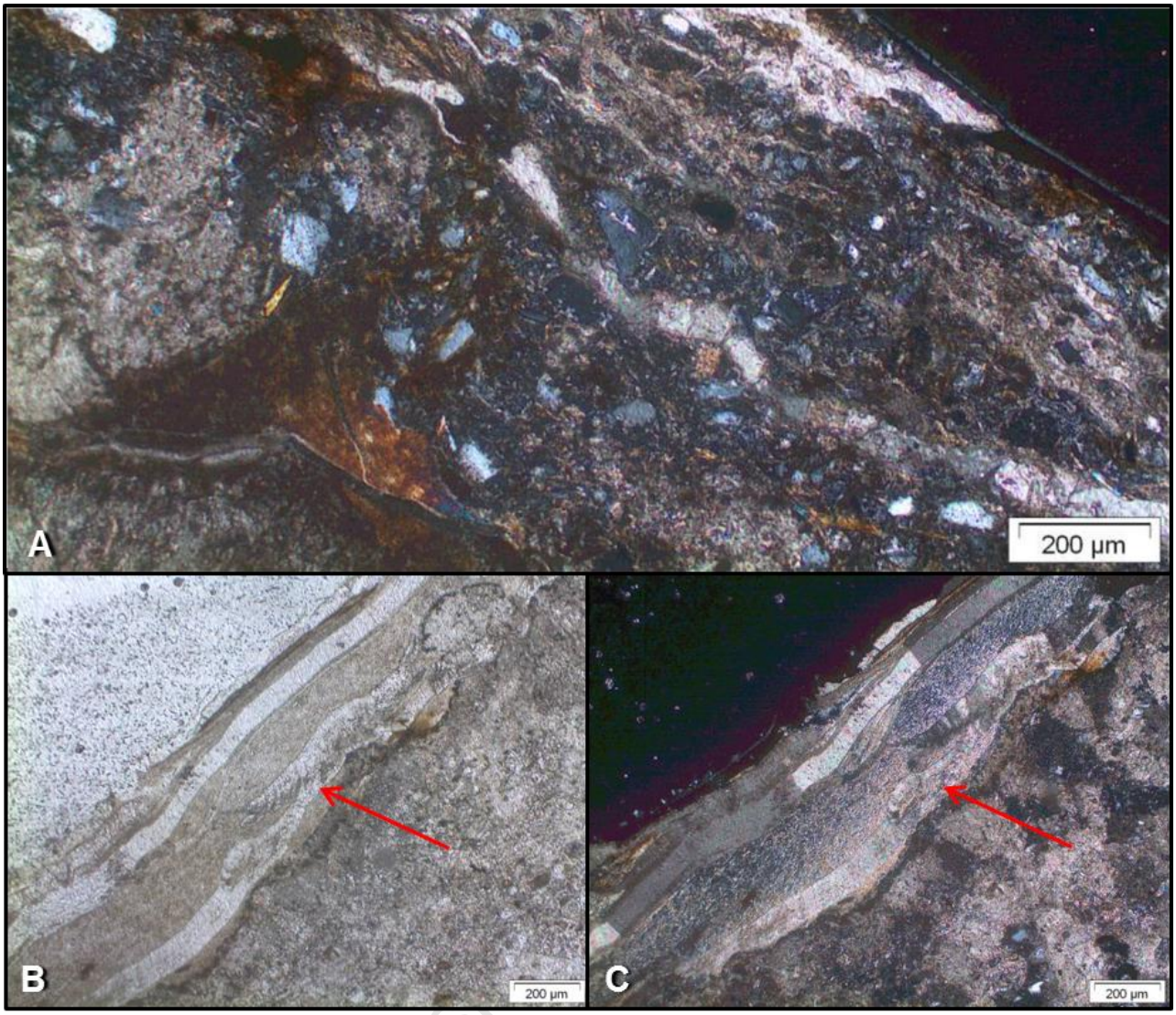

Figure 45. Calcite layer (not a burrow lining) that occurs at the interface between the host rock and burrow fill in the Holmsgrove sample. Note that the two calcite layers and the material in between make up a layer about 0.5 mm thick. Displacive growth of carbonate is clearly visible as the carbonate tore the matrix apart most dramatically (indicated by red arrows). The feathering of the matrix into fibrous structures between more consolidated matrix separated by carbonate could not have formed in a void filling process. This structure requires simultaneous precipitation of carbonate minerals and expansion of host material (by the force of the carbonate under low pressure or other mechanisms at greater depth).Plain polarised light (B) and cross polarised light (A and C) at 10x magnification in all.

Large concretions are visible inside a burrow (Kapteinskraal) and appear to have deformed the original morphology of the burrow (Figure 46). Thin sections of the burrow show radial fibro carbonate minerals (Figure 46 A), feathery micritic carbonate (Figure 46 B), carbonate vein or fracture filling and carbonate cement (Alonso-Zarza and Wright, 2010).

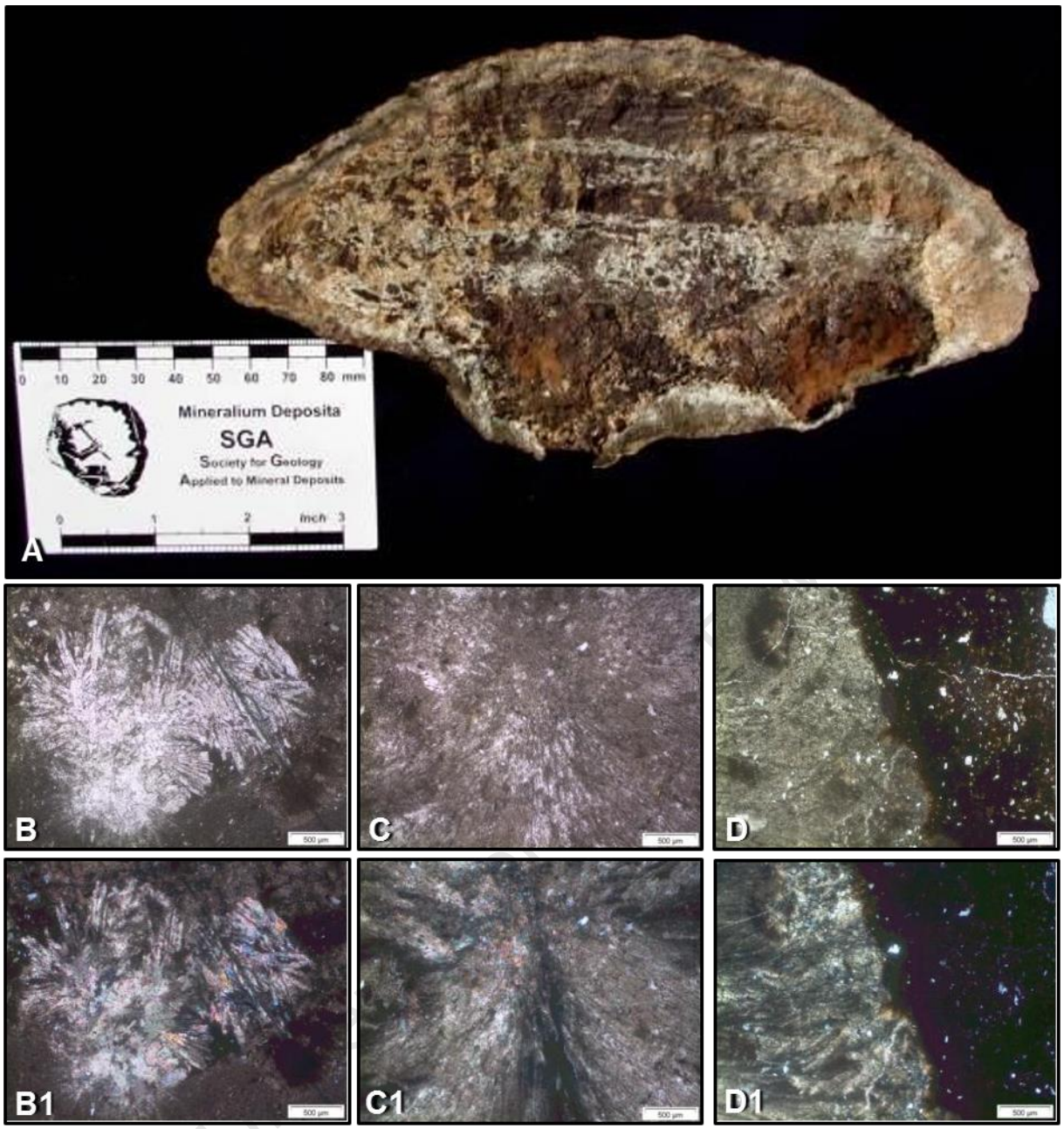

Figure 46. Possible terminal chamber form Kapteinskraal viewed in cross-section (A) (see Figure 54). Note the mushroom shape and the associated two dark, round shapes at the base are diagenetic nodules (Scale = 9 cm). Carbonate concretions in hand specimen and the associated coarse-grained radial acicular calcite (B), finer grained more feathery acicular needle-fibre calcite (C, D), in thin section at 5x magnification in plain polarized (B, C and D) and cross polarized light (B1, C1 and D1).

5. Ichnological Results

5.1. Bioturbation

In order to avoid confusion, trace fossils or burrows with diameter less than 3 cm are referred here as bioturbation. Bioturbation was observed in a variety of forms at all the sites. The most common form of bioturbation is identifiable by millimetre scale disruptions of the sedimentary structures (Figure 47). This type of bioturbation was observed at all the sites and has undoubtedly rendered the beds in fine-grained assemblages massive; especially when occurring in combination with blocky weathering (Figure 47). Another fairly common type of bioturbation includes *Katbergia isp.* that was observed at the sites near Bethulie, but not at Hobbs Hill (Figure 48). *Katbergia isp.* consist of long (5 to >40 cm), 1-2 cm diameter cylindrical burrows with a ramp of 15°-38°, terminating in a slightly enlarged terminal chamber (Gastaldo and Rolerson, 2008). While all the other features described by Gastaldo and Rolerson (2008) were present in the *Katbergia isp.* no enlarged terminal chambers were observed in this study. They are interpreted to have been produced by a decapod crustacean that produced the burrow above the water table in inceptisols and were abandoned before aggradation and a rise in water table (Gastaldo and Rolerson, 2008).

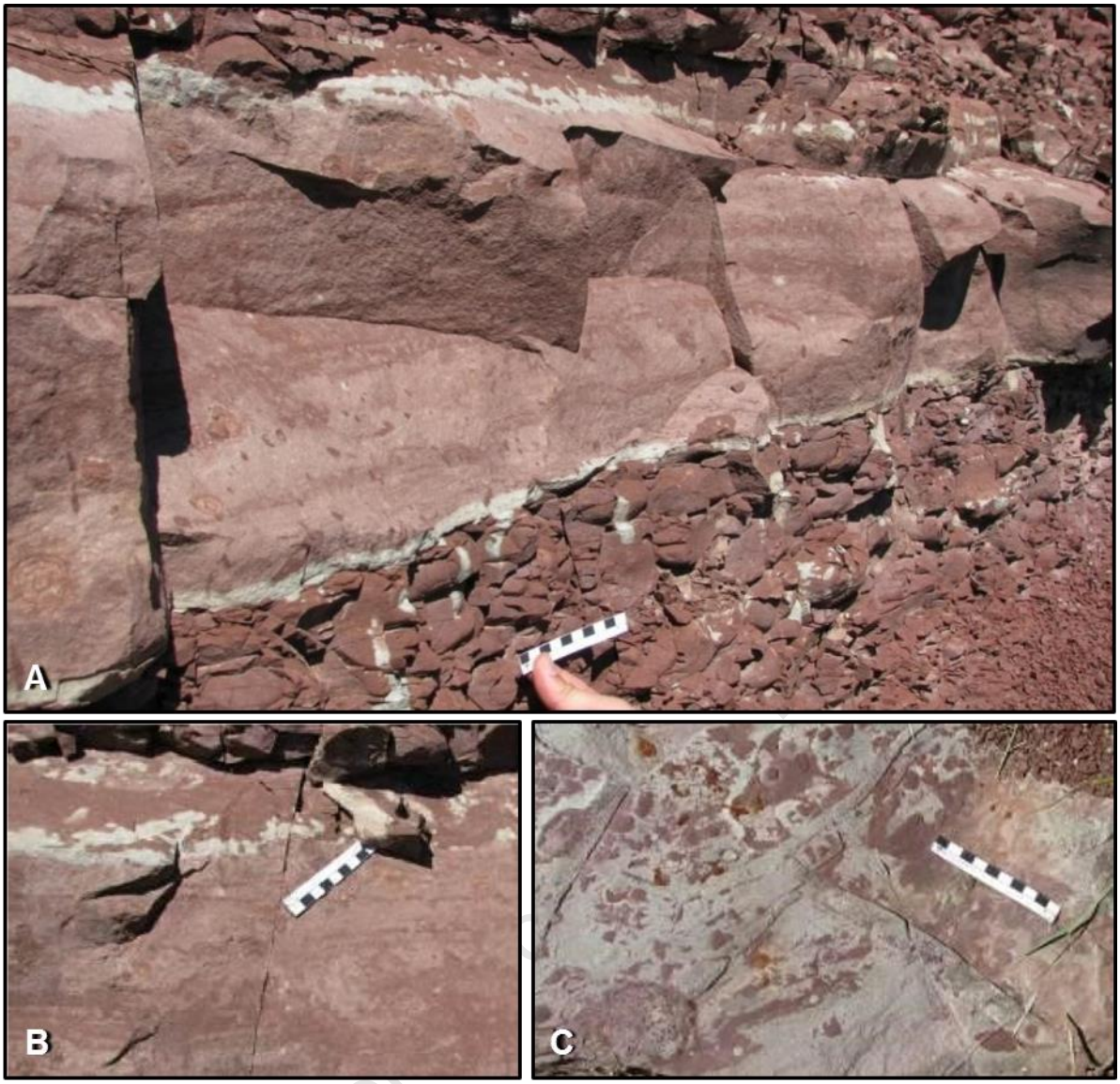

Figure 47. Bioturbation in cross-sectional view in medium- to fine-grained sandstones and into underling mudstone bed (A and B) and on the bedding surface of a sandstone slab (C). Also note the blocky weathering in the mudstone (A) (all from Hobbs Hill, log H1, bed 3, see Figure 22, Scale bar = 10 cm).

Figure 48. *Katbergia isp.* in mudstones at Holmsgrove (A, B) and at Kapteinskraal (C), no enlarge terminal chambers were observed (Scale bar = 10 cm).

5.2. Architectural morphology

Those burrows that were most similar to the type found at Hobbs Hill are considered to have been produced by the same organism. The general dimensions of the studied burrows are summarised in Table 5. Representative samples were taken at Hobbs Hill (Table 5 and Figure 21), Holmsgrove (Figure 49) and at Kapteinskraal (Figure 54) for detailed measurements, photographing and thin sectioning.

Study Site and burrow number	Horizontal Diameter (cm)	Vertical Diameter (cm)	Aspect ratio	Length (cm)	Ramp	Cross-sectional shape
Hobbs Hill 2	10	10	1	35	45°	Circle
Hobbs Hill 3	10	6	1.67	36	32°	Bilobate
Hobbs Hill 4	14	6.5	2.15	102	30°	Bilobate
Hobbs Hill 5	9.5	9.5	1	56	35°	Circle
Jakkalsfontein	15	5	3		20°	Oval
Holmsgrove	10	5	2	30	20°	Varied
Kapteinskraal 1	11.5	5.7	2.02	80	12°	Bilobate
Kapteinskraal 2	12	N/A	N/A	170	8°	N/A

Table 5. A summary of the general dimensions of burrows observed in the field. N/A refers to details that were not visible in the field, because they were obscured by country rock.

The burrows are generally horizontal to sub-horizontal with an average horizontal diameter of ~10 cm. The horizontal diameters range from 9.5 to 15 cm and the vertical diameter range from 5 to 10 cm resulting in a an aspect ratio ranging from 1 to 3 and a variety of cross-sectional shapes (Table 5). The cross-sectional shape ranges from circular to flattened oval. Bilobate burrows were also noted at Hobbs Hill and Kapteinskraal (Figures 49-53). The cross-sectional shape is consistent along the length of the burrow, except for those at Holmsgrove and Kapteinskraal. The Holmsgrove sample varies in cross-sectional view from circular, to tear drop shaped to flattened oval shaped.

One of the Kapteinskraal burrows has horizontal diameters that gradually change from 12 to 20 cm. This "loose" (detached) burrow segment resembles a terminal chamber and was located ~1 m from two burrows that were *in situ* (Figure 54). The cross sectional shape of this possible terminal chamber changes from blocky oval at the narrow end (12 cm) to mushroom shaped at the broader end (20 cm). The presence of concretions at the base of the possible chamber appear to have deformed the cross sectional shape (Figure 46). The variability of the vertical diameters could be a result of compaction.

The ramp (angle of inclination) ranges from 8° to 35°; the burrow from Hobbs Hill log H2 has a ramp of 45°. The burrow from Hobbs Hill log H2 is different from the other burrows in that it has a 45° ramp, occurs in a sandstone bed, is void of surface features (smooth surface) and has a nearly perfectly round cross-sectional shape (Figures 49-53). The exposed length of the burrows ranges from 35 to 170 cm. No entrances or terminal chambers were found attached to the burrows and therefore the true extents of burrows are unknown (Figures 49, 51, 52, 53 and 54). None of the burrows showed any evidence for tight curling or coiling. The burrows vary from relatively sub-linear, broadly curving (Kapteinskraal) to sub-linear with smaller scale curves in alternating direction (Hobbs Hill) forming a repeating gentle s-pattern (Figure 49, 51, 52, 53 and 54).

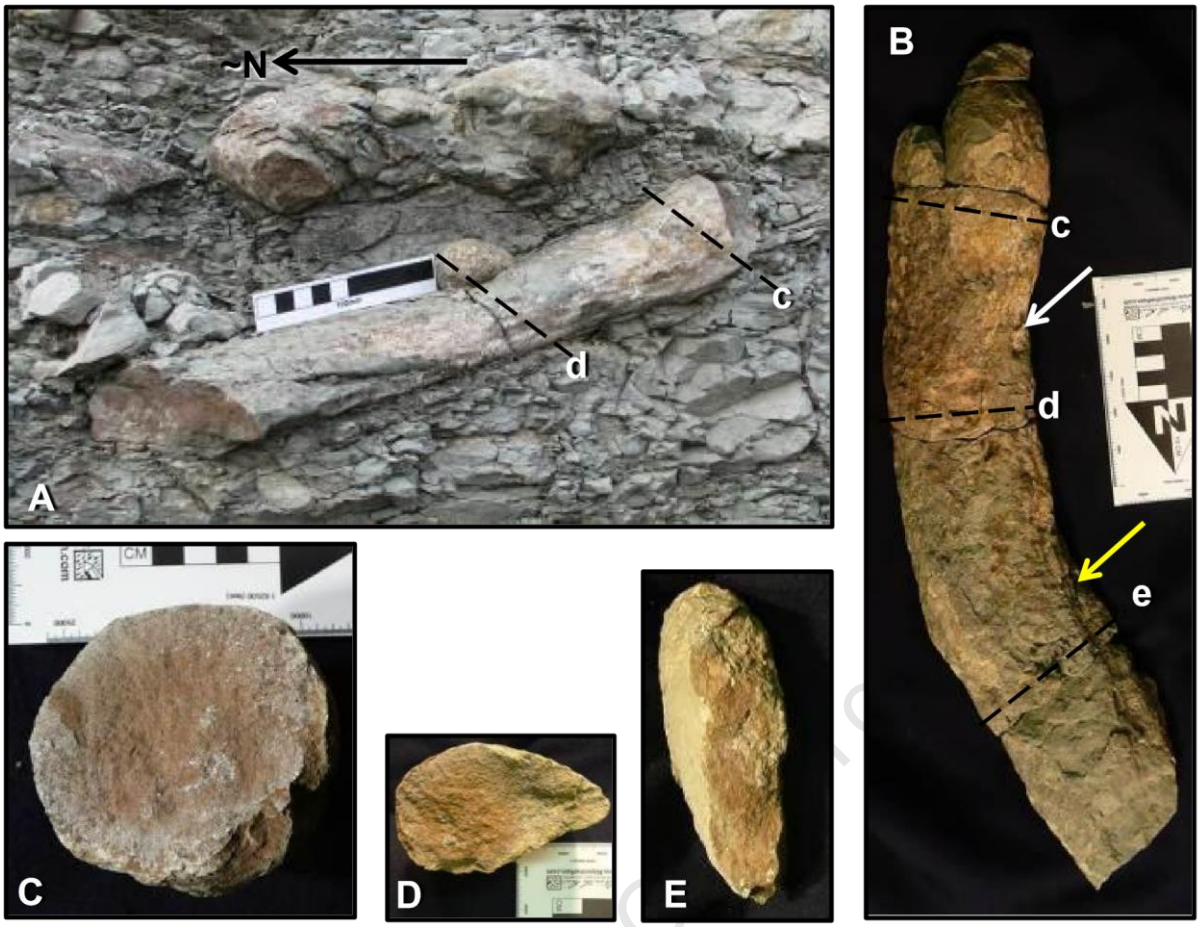

Figure 49. Holmsgrove burrow sample in situ in A (scale = 10 cm) and cleaned in B (scale = 5 cm) cleaned in plain view demonstrating the loose or open nature of the curvature of the burrow as well as some features of surface morphology (dimples and grooves, indicated by the white and yellow arrow respectively). C, D and E (at the same scale) show the three different types of cross-sectional shapes where the burrow broke indicated in A and B by c, d and e (breaks highlighted with dashed lines, this section was not logged and the outcrop is not illustrated).

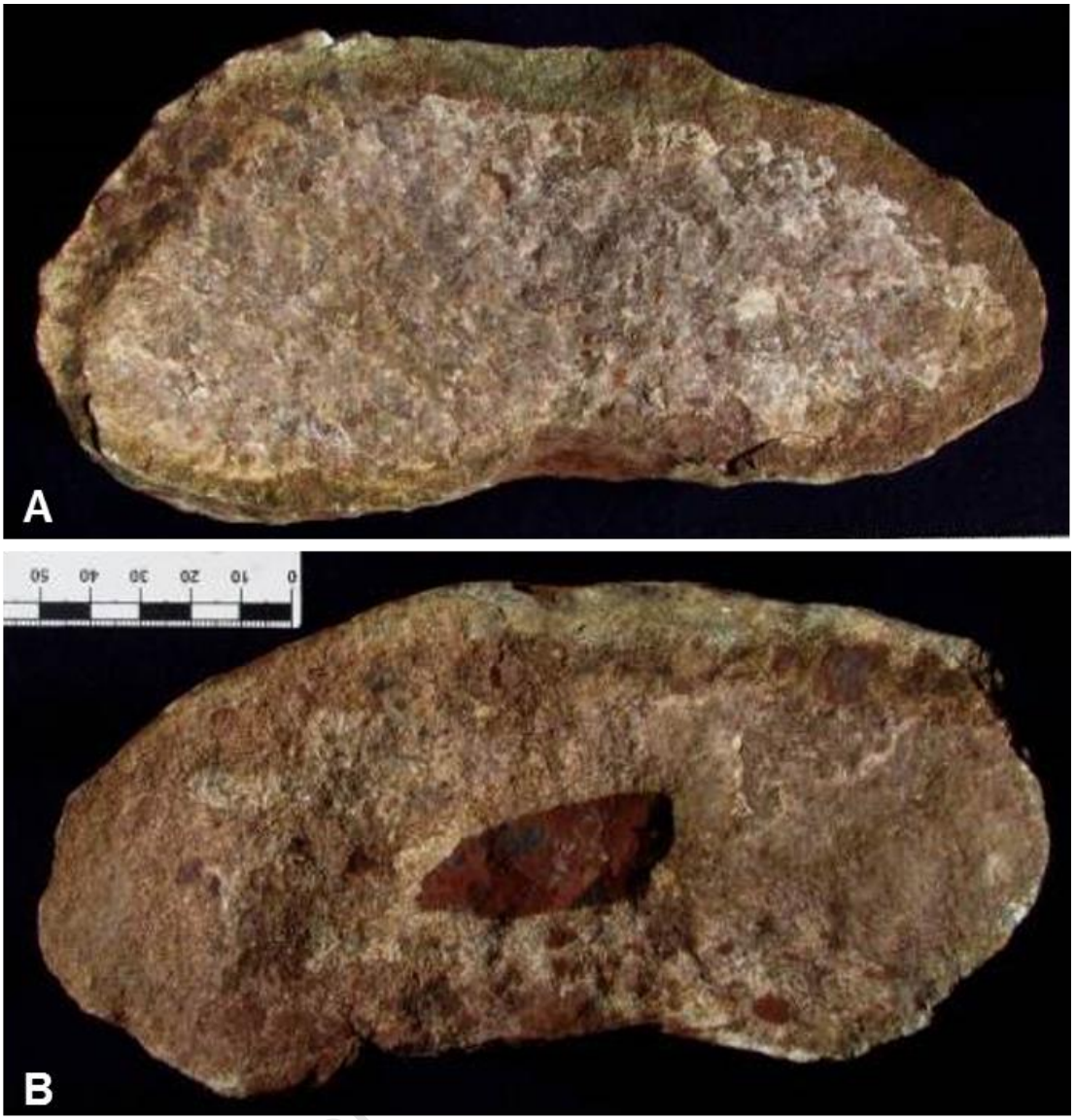

Figure 50. Bilobate cross-sectional view of the samples taken from Hobbs Hill. Note the poor sorting of the burrow fill material and the large rip-up mudstone clasts in the middle of B; the whiter interior in A is a superficial calcite lining not a lithological variation (Scale = 5 cm for both figures, see Figure 52).

Figure 51. Cross-sectional view of a semi-oval shaped burrow in situ at Hobbs Hill (see Figure 52); the top is curved and the base is slightly flatter. The host rock is massive siltstone and the burrow fill is medium-grained sandstone (Scale = 10 cm).

Figure 52. *In situ* Hobbs Hill burrows, the burrow in transverse view has a ramp of 30°, the removable portions of this burrow were sampled (parts above the scale bar) and are referred to in the figures below. The yellow arrow indicates another burrow that only protrudes out of the outcrop for <10 cm and no accurate ramp could be measured. Note the gently curving architecture of the larger burrow and the lateral extent (>10 cm) of the millimetre scale ridges (on the side of the large burrow) (Scale = 10 cm).

Figure 53. *In situ* burrow at Kapteinskraal demonstrating a slight curve and a low ramp of 12°. The white double arrow is horizontal. Note the bilobate cross-sectional shape and the poorly preserved surficial morphology, which is similar to that observed for the burrows at Hobbs Hill. The host rock is massive siltstone and the burrow fill is medium-grained sandstone. The blocky (3-5 cm) sandstone fragments have weathered from a thin sandstone layer situated less than 50 cm above the burrow (Scale = 10 cm).

Figure 54. A possible terminal chamber (circled in red) and relatively straight burrow (tunnel, yellow arrow) seen at Kapteinskraal 150 m from where Groenewald (1991) reported similar but larger diameter burrows. Note the burrow (yellow) was not connected to the possible terminal chamber (circled in red) (Scale = 10 cm).

5.3. The burrow fill

The burrow fill material is similar to the horizontally laminated conglomerate and sandstones described above, with respect to composition and grain size distribution. The most prominent petrographic difference between the burrow fill material and the surrounding rock types is the composition and the habit of the cement. It is primarily carbonate (most likely calcite) and shows a displacive texture where the grains appear to float in the calcite (Figure 44). The feldspar grains in the burrow-fill show calcite alteration (Figure 46). In the sections made from Kapteinskraal, the calcite has radial patterns which are probably related to the diagenetic nodules in the borrow fill also visible in hand specimen (Figures 64).

Hobbs Hill burrows have coarser grained matrix than the burrow fill material from the Holmsgrove and the Kapteinskraal sites. There are two types of rip-up mudstone clasts: (1) pure claystones that are identical to those observed in the conglomerate (see section 4.2.1, Sandstone Petrography), (2) are mainly mudstones consisting of clay to coarse silt to fine sand sized particles of quartz, feldspar and minor lithic fragments (Figures 34, 35, 50, 55 and 56).

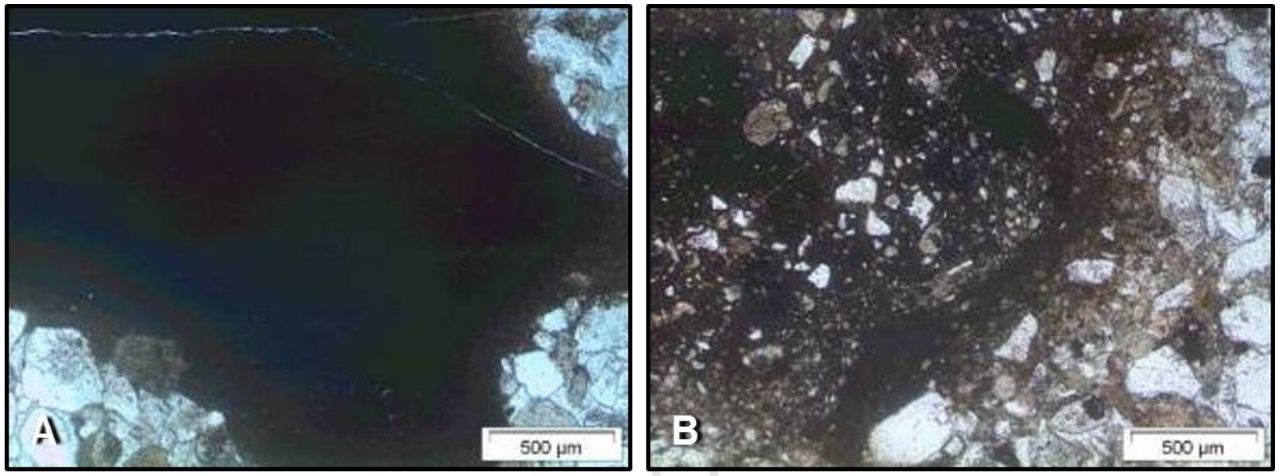

Figure 55. Photomicrograph of the two types of rip-up mudstone clasts observed in the burrows (Hobbs Hill sample, see Figure 52). The first type (A) is clean, claystone. Similar to those observed in the conglomerate (Gh), the second (B) contains some fine-grained clastic (silt and sand) material similar to the matrix inside the burrow.

The rip-up mudstone clasts also vary depending on where they are in the burrow. The thin sectioned burrow sample from Hobbs Hill has rounded rip-up mudstone clasts at the base and more tabular clasts at the top while the central part has less clasts (Figure 56). The mudstone clasts at the base contain particles similar to that of the matrix in the burrow (Figure 55B). This variation in shape of rip-up mudstone clasts, their distribution and type is accompanied by a variation in matrix grain-size from coarse silt to fine sand (0.05 -0.160 mm) at the base, with very fine to coarse sand (0.1-0.5 mm) in the middle and at the top. The distribution, variations in clast size and horizontal lamination in several burrows suggest multigenerational filling. Some burrows are massive with no apparent variation in composition or grain size. The mushroom shape in Figure 46 is most likely because of a larger scale growth of concretions seen in Figure 46.

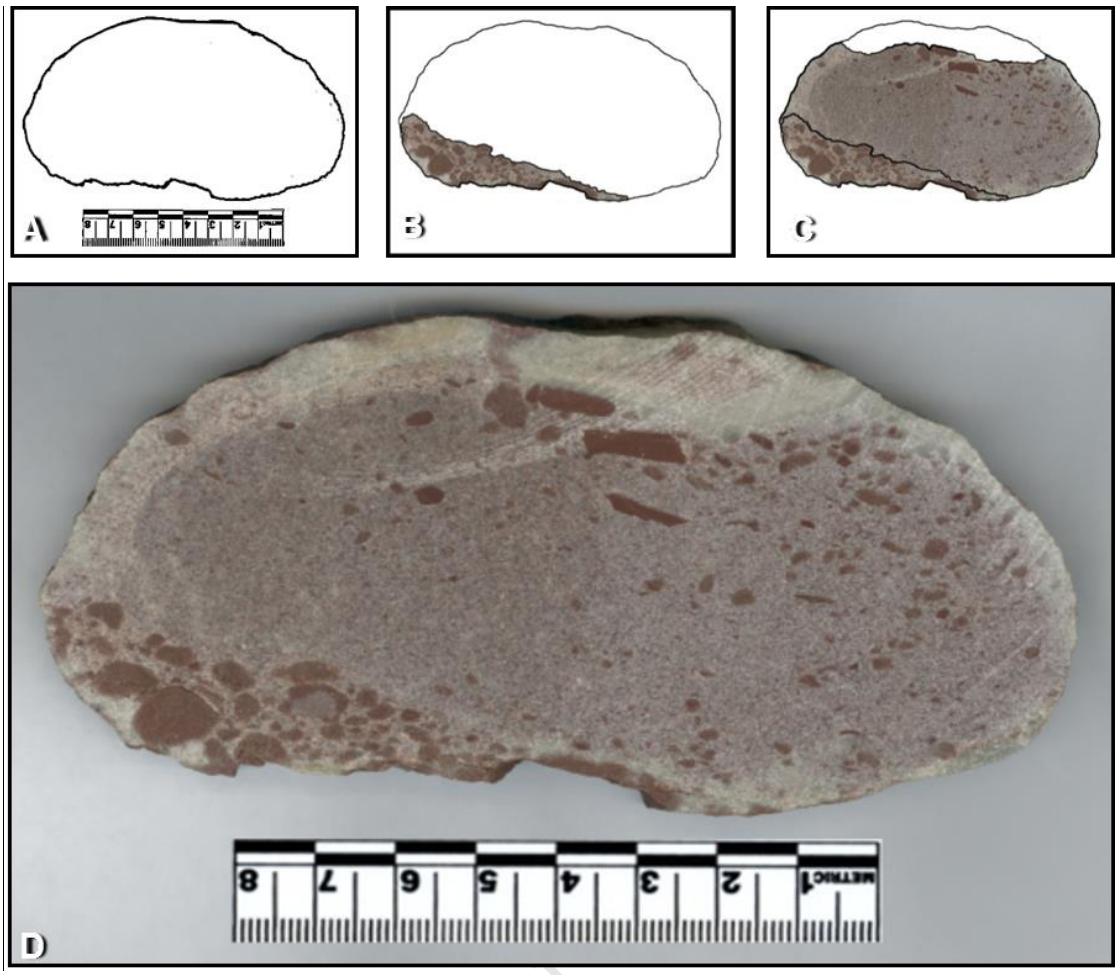

Figure 56. Cross-sectional shape (A) of a burrow cast and its incremental filling illustrated in A, B, C and D (Hobbs Hill). In D, the variation in concentration and size of clasts indicating the incremental filling can be seen (Scale = 8 cm).

5.4. Surficial Morphology

The surface morphology of the burrows is best preserved in burrows found at Hobbs Hill. Similar features are preserved on the burrows at Holmsgrove and Kapteinskraal, but the terminal chamber at Kapteinskraal does not show any features that are regular enough to be considered bioglyphs. The most prominent aspects of the surface morphology are the ridges and associated depressions that are along the axis of the burrows (Figures 49A, 49B, 52 and 57). They are best preserved on the sides and base, but tend to fade out along tops of the burrows. The ridges are up to 3 mm in height, the spaces between some semi-parallel ridges range from 5 to 20 mm and the length ranges from less than 1 cm to 15 cm with the average length being about 3 cm (Figure 57). They have two main orientations relative to each other, crosscut each other at a low-angle and as a result produce diamond-shaped depressions (Figure 58).

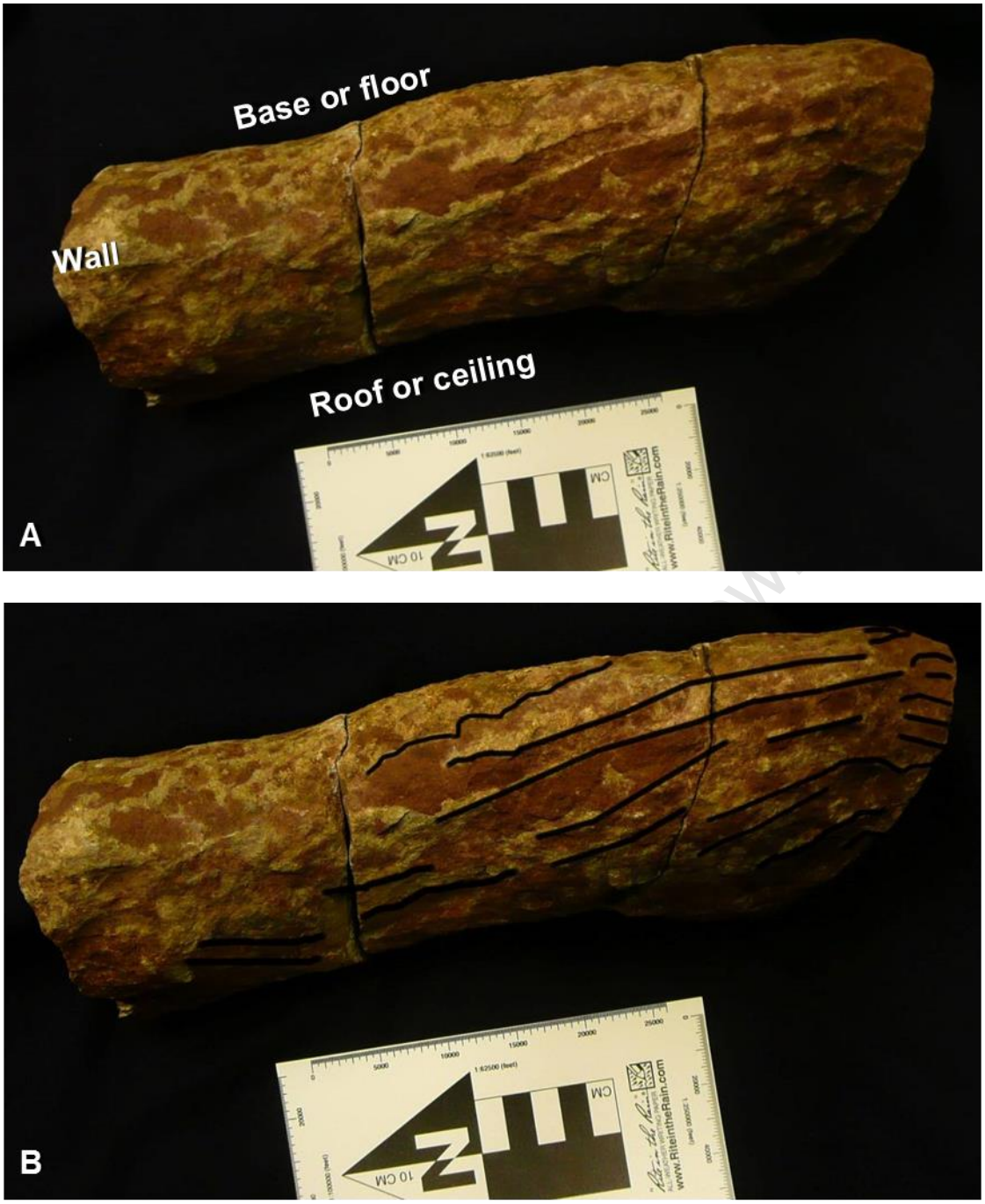

Figure 57. Parallel ridges and alternating depressions running tangentially along the length of the burrow wall (side view) and onto the roof (of a sample from Hobbs Hill) visible in A and outlined in B (Scale = 5 cm).

Figure 58. Close up of segment 1 of the Hobbs Hill sample. Note that the base and sides display the diamond-shaped (indicated by the white arrows in A and dashed lines in B) depressions that result from cross-cutting ridges. The ridges run along the axis of the burrow. The host rock is purple and is preserved in depressions, while the burrow fill is light pink/yellow sandstone, more exposed in the relatively raised parts such as the ridges (Scale = 9 cm).

The tentative terminal chamber from Kapteinskraal has a possible burrow lining visible in hand specimen. There is a ~7 mm layer that appears to line the surface of the burrow, which truncates the horizontal lamination visible further from the burrow edge (Figure 46). Microscopic investigation of this layer showed that it is an interface between the finer grained mudstone host rock and the coarser grained burrow fill material and not a burrow lining (Figure 59). The only other possibility for a burrow lining was in the thin section of the Holmsgrove sample (Figure 45).

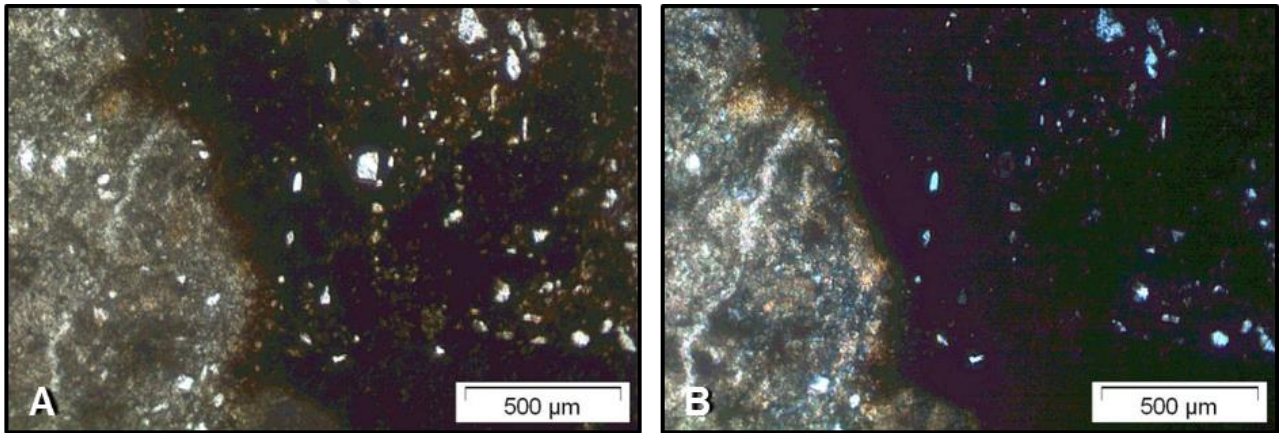

Figure 59. The irregular interface between the burrow fill and the host rock (indicated by the white arrow) is visible in a thin section of a Hobbs hill type burrow from Kapteinskraal. There does not appear to be any clear burrow lining and the burrow fill (coarser grained, with calcite cement) has incorporated some of the host rock (mudstone, dark material) and vice versa. Plain polarised light (A) and cross-polarised light (B) at 5x magnification.

Calcite occurs on the surface of burrows visible in thin-sections (Figure 45), in hand specimen on the surface (Figure 60) as well as in crack between the burrow sections (Figure 61). The occurrences of the calcite in between the burrow fill and host rock suggests it was precipitated during diagenesis. However, the occurrence of the calcite in between cracks suggests that it may have been precipitated much later when the burrow fill had already been lithified.

Figure 60. Hand specimen sampled from Holmsgrove (see Figure 49) with a relatively thick calcite layer preserved in the less exposed areas on the burrow surface such as in the depressions between ridges and dimples indicated by the arrows (from left to right respectively) (Scale bar = 9 cm).

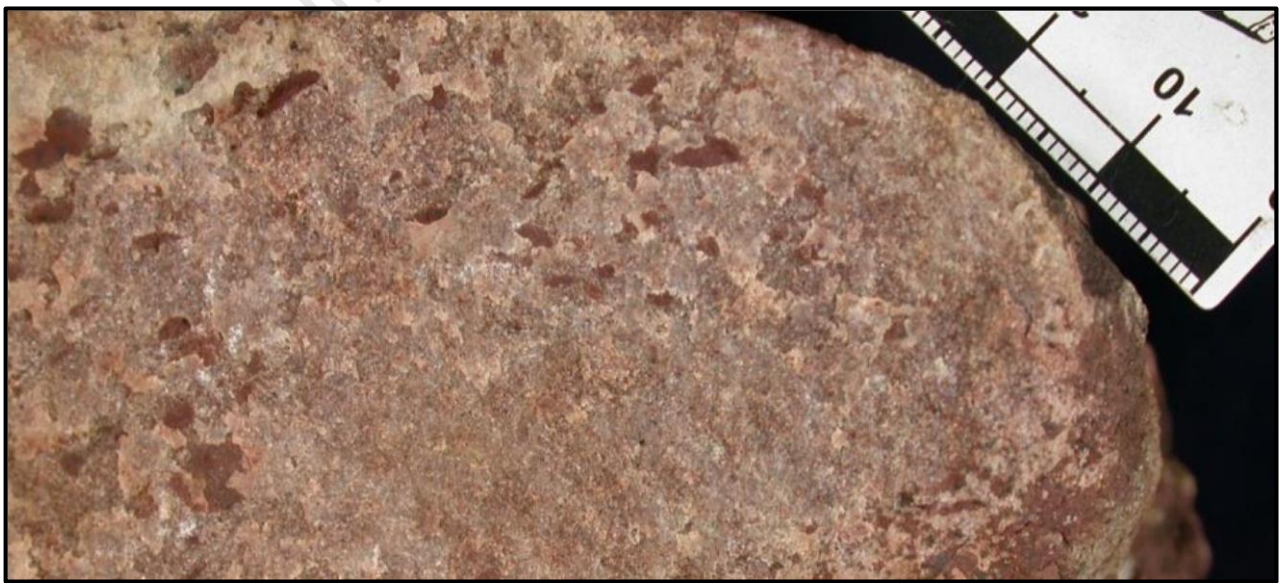

Figure 61. Close-up cross-sectional view of a burrow from Hobbs Hill (see Figure 52) where the white flaky calcite material is visible on the surface of a crack (Scale bar = 2.5 cm).

5.5. Digital 3D burrow sample

The 3D nature of the digital 3D burrows produced using 123D and PPT limit their presentation in hard copy to screen captures, and therefore the digital 3D copy of a burrow section is saved on a CD (see Appendix 1) and can be accessed in YouTube via this link: http://youtube/j0x3gAp8qV0 . The material is available in several formats including a video (.avi), object file (.obj), stereolithographic files (.stl) and encapsulating postscript files (.eps). The digital 3D copy of the burrow recorded the architectural morphology of in relatively high detail giving a reasonable representation in 3D, enough to distinguish it from other burrows and even other sections of the same burrow (Figure 62). The accuracy of the dimensions have not yet been determined in this study, however studies on the accuracy of photogrammetry indicate it is possible to produce levels of accuracy equal to or greater than 3D laser scanning (Falkingham, 2012; Gruen, 2012). A physical model has not yet been produce from the 3D digital copy, however the processing needed to do this has been done as well (Figure 63). The parts are in Figure 63B and the whole assemble product is in Figure 63A, the parts are in encapsulating postscript files (eps) in Dropbox link provided above.

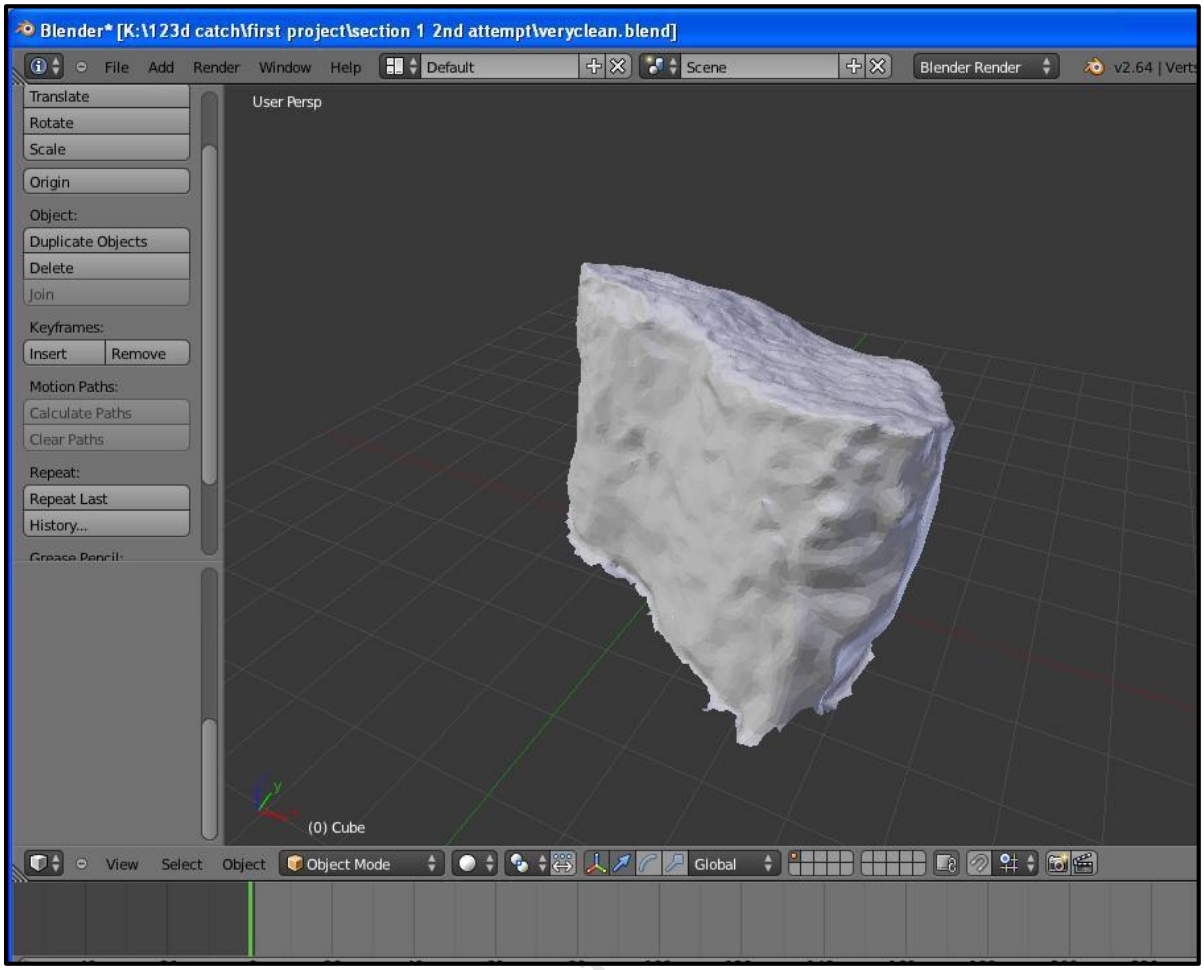

Figure 62. The digital 3D burrow sample without texture (colour) in the free 3D manipulating software Blender imported in the object format. It must be emphasised the texture (colour) was disabled to emphasize the morphology and can easily be re-enabled (image is a screen capture).

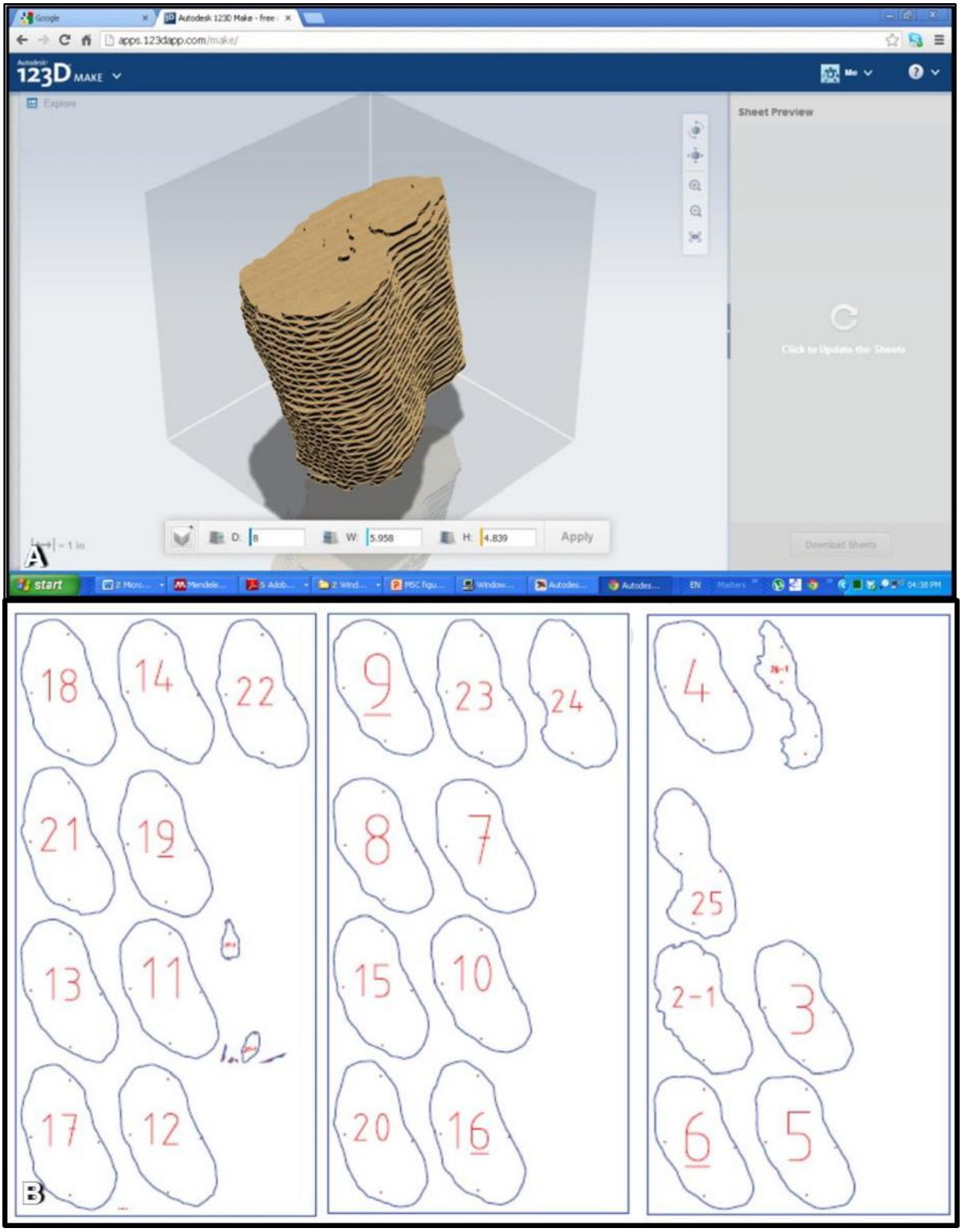

Figure 63. The cut-out preview in the Google Chrome plug-in for Autodesk 123D Make (A) and the print and cut-out format (B) produced by 123D Make which sliced up the 3D burrow into 0.443 mm (0.1772 inch) thick cross-sections(the numbers are used to order the slices during assembly, this is not to scale).

The results produced using PPT appear to be of lower quality than for 123D, however this is a not function the software (Figure 64). The laptop used (Acer Extensa 5220) to create the 3D objects was released in 2009, the hardware is outdated and performance sub-standard. 123D uses cloud

servers, which allows for the pooling of processing power of multiple systems at levels much higher than possible on a single computer. It is possible to use cloud processing to run PPT and similar result would therefore be attainable. In addition to the processing limitation the 3D output from PPT has not been cleaned, which also would require more processing power.

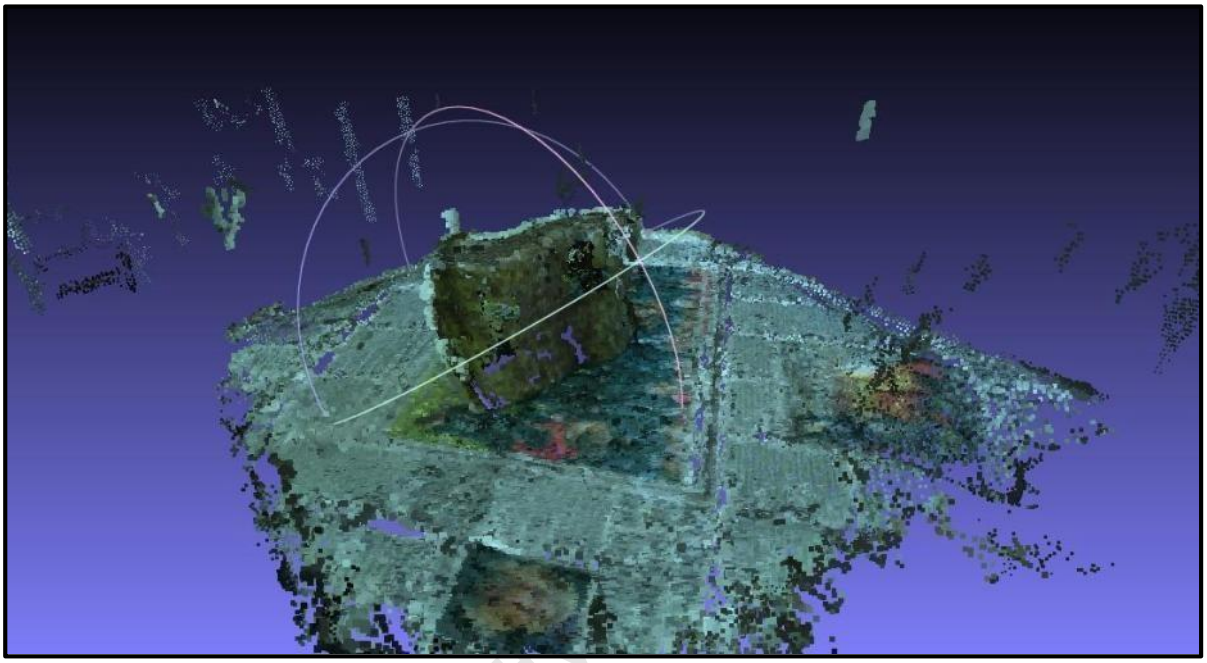

Figure 64. The point clouds imported into MeshLab from PPT, at reduced capacity, to produce a 3D copy of a burrow. The apparent poor result is because of the low processing power of the outdated computer used and early stage of the workflow.

6. Interpretations

6.1. Sedimentary facies interpretations

The steps taken during facies analysis include: (1) Description of facies and architectural elements; (2) Identification and interpretation of the processes that produce specific features; (3) Comparison of the facies, architectural elements, the processes that produced them and the fluvial styles that they represent; (4) The characterisation of the depositional environment and (5) Comparisons of this depositional environment with modern and ancient analogues. The first step is presented in the previous chapter (results), whereas the subsequent steps are presented in this section.

6.1.1. The sandstone facies assemblage

The dominance of laterally extensive, 15-90 cm thick tabular sandstone beds with erosional bases, water escape structures, the occurrence of intraformational mudclast and minor interbedded mudstones are indicative of high-energy conditions alternating with low-energy conditions. The dominance of facies such as massive bedding (Sm, Gmm), horizontal lamination (Sh, Gh), low-angle cross-bedding (Sl), planar and trough cross-bedding in gravelly lithofacies (Gp, Gt) are also characteristic of upper to transitional flow regime conditions.

The frequency of massive sandstone (Sm) beds in conjunction with the evidence for high energy processes suggests rapid deposition under high velocities (Miall, 1985; Collinson, 1996). The low-angle planar (Sl) and trough cross-bedding (St) in the sandstone and gravelly lithofacies indicate the occurrence of dunes, characteristic of upper flow regimes. Horizontal lamination (Sh) in the sandstones can form in two environments applicable to fluvial deposits (Miall, 1996; Neveling, 2004): (1) During lower flow-regimes when coarse to very coarse sand (> 0.6 mm) is deposited at low constant-flow speeds (< 0.4 $m.s^{-1}$). (2) Or during upper flow-regime conditions when fine- to

very fine-grained, sands are deposited at the transition between subcritical and supercritical flow (Miall, 1996; Neveling, 2004). Many of the Sh co-occur with other upper flow regime features (Sm where grain size changes and erosional contacts). Since most of the Sh sandstones are medium-grained, some are fine- to medium-grained (few are very fine to medium-grained) and none are coarse-grained, the upper-flow regime conditions are favoured (Figures 18, 22, 23, 24 and 25). Lower-flow regime bedforms and structures such as ripples and mudstone beds are in the minority (Figures 18, 22, 23, 24 and 25), and when present they occur in the upper parts of fining upward cycles or as in the case of the mudstones, paradoxically situated on upper flow regime deposits separated by an erosional contact. The fining upward cycles are truncated by erosional contacts (Figures 18 and 22). The truncated fining upward cycles indicate that the lower flow regime sediments were eroded by subsequent upper flow regime conditions. The fine-grained beds draped over the sandstone beds separated by erosional contacts can be explained by a similar process, with the fine-grained beds representing bedloads deposited during lower flow conditions after erosion during upper flow conditions.

The multilateral and multi-stacked arrangement of the beds may represent successive events but could be produced during more continuous sedimentary processes, such as with sandy bedforms (SB). The outcrops at Hobbs Hill preserve both foreset macroforms (FM) and SB architectural elements in the sandstone facies assemblage.

The almost exclusive occurrence of rip-up mud clast in the gravelly lithofacies at Hobbs Hill fits well with the above-described alternating conditions of upper and lower flow regimes.

With the mudstones being deposited during lower flow regime conditions, enough time must have passed between the next phases of upper flow conditions to allow the mudstones to become compacted or consolidated enough to form clasts during erosion and transportation.

Soft sediment deformation features in mudstones were also observed, preserved as isolated lenticular bodies, similar to the scour hollows (HO) element described by Miall (1996). During flooding events, scouring produced lenticular hollows, later they were filled by finer grained material during lower flow regimes because of channel abandonment or during the late stages of flooding (Miall, 1996). The soft sediment deformation of the fine-grained lenses and erosive contact with the overlying sandstone bed indicates that upper flow regime conditions resumed rapidly after the deposition of the finer grained material, while the sediment was still water saturated (Owen and Moretti, 2011). This type of feature is more likely to have occurred due to rapid migration of channels, than in between flooding events (three stages: erosion, quiet settling, erosion and deposition).

The soft sediment deformation features in the HO elements suggest that the discharge varied significantly during periods of flow, therefore the fluvial style was episodic, but at times more sustained with varying rates of discharge (Miall, 1996).

6.1.2. The fine-grained facies assemblage

The fine-grained facies assemblage consists of thick successions of mudstones and siltstone. The lithofacies are generally massive, with some patches of laminated siltstones, bone beds and water escape structures identifiable. The lack of sedimentary structures makes it difficult to determine which processes produced this assemblage. The water escape structures in the coarser horizons suggest periods of relatively rapid deposition of sediments, while the fine-grained nature of this assemblage suggests the contrary (Owen and Moretti, 2011). The water escape structures, association with erosive contacts at the base of the finer grained deposit, poorly sorted chaotic mix horizons (containing bone fragments) and massive nature of this facies could be evidence for reworked sand sized mud aggregates (Wright and Marriott, 2007). Some of the irregular features are clearly due to escaping pore waters prior to lithification (Figure 38), while others could be related to

or are poorly preserved forms of large burrows (Figures 21, 22 and 39). The massive nature of this assemblage could be because of the blocky weathering and bioturbation. Bioturbation and rhizocretions are rare in the mudstones only visible in the coarser grained horizon (Figures 41, 47 and 48), however large burrows were numerous in the Hobbs Hill outcrops and do occur in this assemblage in the northern sites. The preservation of surficial morphology and the incremental filling of the burrows bare testament to the firm nature of the fine-grained facies assemblage. This suggests that some level of pedogenesis took place before the burrows were produced, seemingly contrary to the lack of other features commonly associated with pedogenesis.

This assemblage may represent fine-grained over bank deposits that accumulated during the waning phase of flooding events. The erosion of the floodplain fines and incorporation into the channel lags is evidenced by the abundance of intraformational mudclast throughout the sandstones and gravels (Figures 22 and 33). The sandstone beds in the fine-grained facies assemblage are most likely crevasse splay deposits because of their position, relatively thin thickness and the way in which they thin out within finer grained sediments (Figures 18, 19 and 20).

6.1.3. Sedimentary interpretations of the burrow fill

The high carbonate content of burrows and some of the sandstone beds indicate that supersaturated fluids were interacting with the sediments between deposition and the present (Klappa, 1979). If this occurred above the water table (in the vadose zone) then precipitation of supersaturated carbonate fluids most likely occurred because of rapid surface evaporation during conditions that are more arid or after channel abandonment (Saigal and Walton, 1988). The coarse-grained nature of the carbonates (poikilotopic) suggests that the carbonates were precipitated in the phreatic zone or during deep diagenesis. Vadose zone diagenetic processes are preserved in fine-grained carbonates (> 40 μm) which are most commonly replaced by coarser grained carbonates

characteristic of deep burial and later stages of diagenesis (Quast *et al.*, 2006). Fortunately, the texture of vadose zone carbonates can be preserved and used to infer whether carbonate was precipitated in the vadose zone. Based on these, the texture seen in Figure 44 is poikilotopic carbonate and not floating grains.

Displacive texture

The displacive nature of the concretions suggests that the carbonate was precipitated in the vadose zone (Alonso-Zarza and Wright, 2010). The fine-grained feathery carbonate structures are also associated with vadose zone carbonates while the coarser grained radial-fibro carbonates minerals are more indicative of phreatic zone carbonates (Alonso-Zarza and Wright, 2010). The radial acicular needle-fibre calcite structures are considered to have been produced by precipitation and replacement of fungal mycelia and roots by calcite (Alonso-Zarza and Wright, 2010). These radial structures are generally micritic therefore the coarse-grained nature suggests later recrystallization. These features together indicate that carbonate was precipitated initially in the vadose zone during pedogenesis and then recrystallized later on during deep burial in the phreatic zone (Alonso-Zarza and Wright, 2010).

Since the Katberg Formation is not a carbonate deposit, the carbonate between clasts must have been precipitated from supersaturated fluids. Thus, floating grains must have occurred, further evidence for this is the low level of compaction of sediment in the burrows. The fine-grained carbonate minerals precipitated in the vadose zone (and the floating grains feature) must have been overprinted by later stages of diagenesis or during periods of increased rainfall. Where the water table can rise and the phreatic zone can move over the vadose zone. In both cases, carbonate supersaturated fluids are needed to precipitate locally ubiquitous carbonates, seen in the burrows.

The preferential occurrence of carbonate minerals in the burrows could be explained by two mechanisms. Firstly, the burrow fill is porous and permeable while the fine-grained host rocks are aquitards. Therefore, during water table fluctuations the burrows may have acted as conduits in the soil profile (similar to joints and fractures in non-porous, crystalline rocks). The carbonates then precipitated in these conduits when conditions were suitable (supersaturated fluids, high evaporation rates).

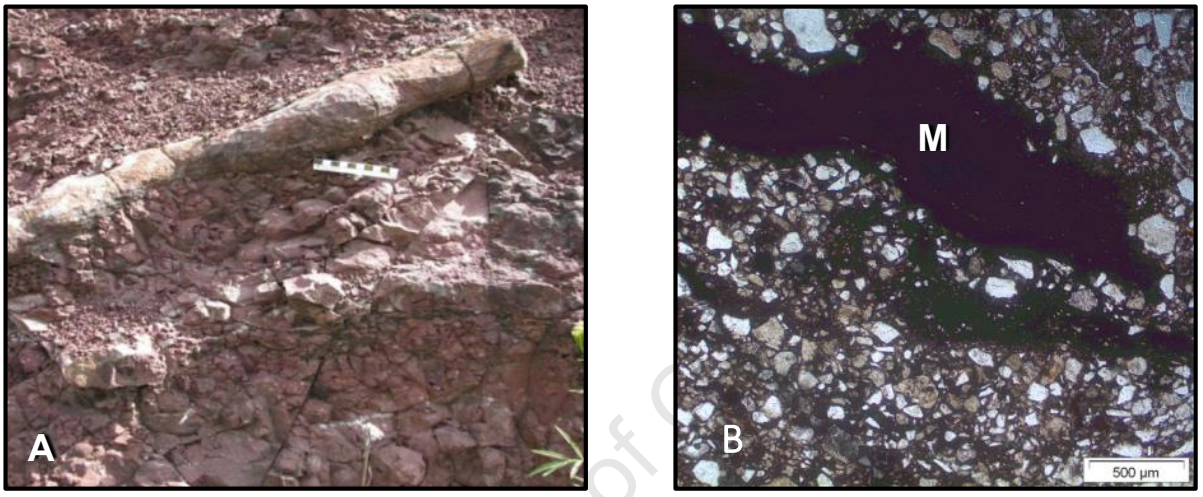

Figure 65. Burrow cast in mudstone host rock (A, scale = 10 cm) and a thin-section (B, 10x magnification) of the burrow fill material with a rip-up mudclast (M) to demonstrate the fine-grained nature of the host rock relative to the burrow fill (surrounding the clast M).

An additional explanation is that the burrows served as a kind of evaporation "pan". The fine-grained host rock surrounding the burrows was less porous; therefore, the burrows would hold water (Figure 65). The incremental filling of the burrows must have been associated with water (Figure 56). If evaporation occurred between filling increments then the remaining trapped fluids would have become increasingly saturated in dissolved salts. This supersaturated fluid would be localised to burrows and other depressions filled by coarse-grained material (such as potholes and scour fills). The supersaturated fluids then precipitate carbonate producing floating grains and later poikilotopic carbonate.

The latter explanation can also account for the irregular occurrence of carbonates in some of the sandstone beds. In all cases, the features imply fluctuating groundwater levels, alternating periods of dry and wet conditions possibly due to flooding in an overall semi-arid climate. An in-depth investigation of the precipitation of carbonates in the Katberg Formation could give further insight into the climate and groundwater behaviour during the Early Triassic. A detailed history of the diagenesis of the Katberg Formation is needed, with special attention to the interaction between diagenetic minerals, deep burial processes, low temperature metamorphic processes and later interactions of the Drakensberg Group associated hydrothermal interactions. This kind of study is necessary especially before the use carbon and oxygen isotopes as palaeoclimate indicators, because such post-depositional events may overprint primary climate signatures.

6.2. The Low sinuosity sand-bed River Fluvial Styles

The alternating flow regimes and the lack of well-defined channels interpreted for the LS successions are characteristic of the low sinuosity, flashy, ephemeral, sheetflood sand-bed river model described by Miall (1985, 1996). These beds were therefore produced during flash floods. During peak flooding, the "channel" floor is scoured, producing scours and gutter cast; the material deposited previously is eroded and transported. As the flow decreased, Sm, Sh, Sl, St, Sr and Fm facies were deposited in sequence, however subsequent flooding events removed the lower flow regime deposits, thus producing a preferential preservation of Sm, Sh and Sl facies. The upper flow regime facies would have been preserved at the base of flood cycles and thus has a higher preservation potential. When the subsequent flooding events occurred the lower flow regime facies, which occur at the top of the flood cycle, would have been eroded first. At Hobbs Hill the predominance of intraformational mudclasts in more gravelly facies and at the bases of LS elements, suggest that deposit related to lower flow regimes were eroded and redeposited as gravel lags.

The identified lateral accretion (LA) elements indicate that:

1) The fluvial style changed from sheetflood to more channelized , confined flow
2) The flow was not always episodic or that periods of sustained flow and rapid aggradation occurred during flooding
3) The channel migration occurred at a low frequency (low angle of accretion surfaces)

The LA and HO elements, the relative abundance of Sh and Sl correspond well with the low sinuosity high energy, sand bed braided river fluvial style described by Miall (1985, 1996). The sedimentation during this style occurs during high-energy discharge events, with significant scouring of the channel floor and macroforms (such as LA and DA) (Miall, 1985, 1996). The significant scouring may make the identification of DA and LA elements in the resulting deposits very difficult (Miall, 1985, 1996), which is the case in most of the outcrops at Hobbs Hill and

Katberg Formation in the area. The LA and the floodplain fines (FF) elements are not included in the low sinuosity, flashy, ephemeral, sheetflood sand-bed river model described by Miall (1985,1996), however the fluvial styles should be considered as a continuum. In this case, the LA elements are most likely to have been produced during the waning phase of the flooding, with LS elements representing overland flows which occur during peak flooding events.

The outcrops at Hobbs Hill therefore preserve features of fluvial styles that are gradational between the low sinuosity, flashy, ephemeral, sheetflood sand-bed river and the low sinuosity high energy, sand bed braided river models.

7. Burrow Producer Identification

The burrows described in the Ichnology Results chapter are referred to here as the Hobbs Hill type burrows. The type of producer is constrained based on burrow dimensions and characteristic features associated with certain types of organism (only terrestrial, relatively large organism need to be seriously considered). In order to determine the possible producer of the Hobbs Hill type burrows, their comparison to burrows from other studies with or without fossilised burrow producers "in life" position is undertaken (Smith, 1987; Groenewald, 1991; Groenewald *et al.*, 2001; Miller *et al.*, 2001; Damiani *et al.*, 2003; Sidor *et al.*, 2008; Modesto and Botha-Brink, 2010a; Bordy *et al.*, 2011). Good descriptions of burrow morphology are essential in the comparative process of burrow classification (ichnospecies or type) and burrow producer identification. For this purpose, 3D digital copies of the Hobbs Hill type burrows were produced and were presented above, as this is one of the first time that this technique has been used, for this purpose, direct digital comparisons are not yet possible.

7.1. Possible Producers

The large width or horizontal diameters and lengths of the Hobbs Hill type burrows are more characteristic of a tetrapod burrow producer than of invertebrate burrow producers. The surficial morphology (bioglyphs) preserves features, which are interpreted as scratch marks, similar to previous studies of comparable burrows (Smith, 1987; Groenewald *et al.*, 2001; Miller *et al.*, 2001).

7.1.1. Invertebrates (arthropods)

Modern and ancient flood plain environment host crayfish in relatively large burrows which are sub-vertical above the water table and become more horizontal below it (Hasiotis and Mitchell, 1993; Hasiotis *et al.*, 1993). Hobbs Hill type burrows are too large and have no vertical portions characteristic of crayfish burrows (Hasiotis and Mitchell, 1993; Hasiotis *et al.*, 1993). The

preservation of scratch marks on the surface of the burrows indicates that the substrate was not saturated with water. No bioglyphs diagnostic of crayfish such as imprints of claws were seen on the surfaces of the Hobbs Hill type burrows. Therefore, decapods (crayfish) are unlikely candidates for the Hobbs Hill type burrows. Other arthropods can be excluded on similar grounds (Hasiotis, 2004).

7.1.1. Lungfish

Lungfish produce burrows which are sub-vertical, generally circular to oval and sometimes preserving spiral surface markings produced by the tail fin (Dubiel *et al.*, 1987; Dziewa 1980 in Miller *et al.,* 2001). Although lungfish burrows have been reported for the Permian and Triassic deposits of the Clear Fork Group (Texas) and Chinle Formation respectively, the sub-horizontal tunnels and the scratch marks of the Hobbs Hill type burrows could not have been produced lungfish (Dubiel *et al.*, 1987; Dziewa 1980 in Miller *et al.*, 2001). It is impractical for lungfish to produce horizontal burrows like the one in this study (Table 5, Figures 49, 52, 53 and 54).

7.1.2. Tetrapods

Modern tetrapods (mammals, reptiles, amphibians) are known to produce and use burrows in semi-arid environments, vertebrates have been burrowing from as early as the Carboniferous (Kinlaw, 1999). The Hobbs Hill type burrows are similar to burrows studied in the last 3 decades found in the Permian to Triassic fluvial deposits in South Africa and Antarctica (Smith, 1987; Groenewald, 1991; Groenewald *et al.*, 2001; Miller *et al.*, 2001; Damiani *et al.*, 2003; Sidor *et al.*, 2008; Voigt *et al.*, 2011).

Studies of large penetrative terrestrial burrows have culminated in the development of criteria for identifying the burrow producer with different levels of confidence (Smith, 1987; Miller *et al.*, 2001) (Figure 14). The burrows in this study did not contain any fossil material and therefore the

identification of the burrow producer was done by comparison of burrow morphology with similar burrows in other studies (modern and ancient). A summary of the comparison with different studies is provided in Table 6.

7.2. Studies of fossils bearing-burrows

Smith (1987), Groenewald *et al.* (2001) and Damiani *et al.* (2003) described burrows similar to the Hobbs Hill type burrow which do contain tetrapod fossils. The Hobbs Hill type burrows are first compared to these burrows and then to other similar burrows where the possible burrow producers were inferred (Miller *et al.*, 2001).

7.2.1. Late Permian spiralling burrows

Smith (1987) described a burrow type based on numerous specimens (~50), consisting of an entrance, spiralling mid-section and terminal chamber from the *Pristerognathus* and *Tropidostoma* Assemblage Zones of the Permian Teekloof Formation (western equivalent of the Middleton Formation). Several burrows contained "in life position" fossilised *Diictodon* (from here on referred to as *Diictodon* burrows). The terminal chambers and entrances of the *Diictodon* burrows are superficially similar to the Hobbs Hill type burrows with respect to size, cross-sectional shape, surficial morphology, ramp (or inclination) and architectural morphology (Table 6). The major difference is the occurrence of a spiralling mid-section in the *Diictodon* burrows which is absent from the Hobbs Hill type burrows. Although no complete burrow systems were found of the Hobbs Hill type burrows, there is no evidence to suggest that such a section existed.

The diameters are similar but the *Diictodon* burrows' entrances are smaller and the terminal chambers are larger than the Hobbs Hill type burrows (Table 6). The diameters are similar in size with the spiral section, but the Hobbs Hill burrows do not spiral.

The more circular Hobbs Hill type burrows are similar to the *Diictodon* burrows with respect to cross-sectional shape; however, the variation in cross-sectional shape along the lengths of the two types of burrows is significantly different. The major differences include the Hobbs Hill type burrows commonly having a bilobate base and none with a flattened ceiling were observed (Table 6).

The dicynodont *Diictodon* went extinct during the Permian and therefore are unlikely to have produced the Hobbs Hill Type burrows which occur in the Triassic Katberg Formation (Smith, 1987; Smith and Ward, 2001). The burrows described by Smith (1987) share several similarities in morphology (i.e., similar aspect ratios in certain parts of the *Diictodon* burrows and similarly shaped scratch marks) with the Hobbs Hill type burrows and therefore a similar organism was most likely at work in both cases.

Features	Hobbs Hills type Burrows	*Diictodon* burrow Smith (1987)	Groenewald *et al.* (2001)	Damiani *et al.* (2003)	Modesto and Botha-Brink (2010)	Groenewald (1991) *Scoyenia* 1b	Large burrow Bordy *et al. (*2011)	Ichnogenus A Sidor *et al.* (2008)	Type G: Miller *et al.* (2001)
Diameter (width)	9.5 - 15 cm (~10 cm)	6 - 25 cm (increasing with depth)	6.3 – 15.4 cm (15.4; 10.9; 9.1-6.3 cm)	~17.5 cm (est. from figure and scale)	34 cm	20 - 45 cm	~ 20 – 40 cm	15.7 cm	8 - 19 cm (~12 cm)
Diameter (height)	5 – 10 cm (~7 cm)	3 - 12.5 cm (est. from horizontal diameter and width height ratio)	3 - 6.4 cm	~15 cm (est. from figures and scale)	12 cm	?	Similar (circular)	8.5 cm	9.6 – 62.7 cm*
Length	30 – 170 cm	N/A	N/A	~45 cm (estimated from figures and scale)	>25 cm (~100 cm ramp)	300 cm	~0.5 - 300 cm	34.8 cm	
Width: height ratio	1 – 3 (~1.8)	1.5 – 6	1.6 – 5.7 (~2.4 mode; ~3 average)	~1.16		Not reported	~1 (based on cross-sectional shape)	1.85	1.2 - 3.3 (~2.4) to 1
cross-sectional shape	Circular, ellipsoidal (oval), bilobate	Circular (entrance and spiral), more flattened ellipsoidal terminal camber	Bilobate base to flattened, bilobate ceiling also occurs	Circular with raised central peak at the base (bilobate)	Not reported (but described as flattened)	Not reported	Circular to slightly elliptical	Arched ceiling, Bilobate base	Ellipsoidal to bilobate
Architecture	Near horizontal, slightly curved to loose spiral, almost straight	Elongate to loose curvature (entrance, terminal chamber), dextral spiral (radius of curvature 8 - 9 cm)	Straight to broadly curving, branched	N/A	Single large burrow, no apparent coiling	Single large burrow, no apparent coiling, Overly each other at 90^{o}	Single large burrow, some near horizontal near terminus	N/A	Straight to slightly curved
Ramp	Gently inclined (~25°, 8°- 45°)	30-35 (entrance), 10-32 (spiral) Near horizontal (terminal chamber)	Gently inclined (≤ 8°) entrances, tunnels and terminal chambers (1° - 23°)	N/A	12^{o} to 0^{o} for chamber	0-10^{o}	~30^{o} to 0^{o} near terminus	“Gently inclined”	Gently inclined
Branching	Absent	Not reported	Several T-junctions	*N/A*		None	Absent	N/A	Rare
Bioglyphs	Scratch/scrape marks (1-15 cm long, 3 mm deep), tangential to long axis (on the sides and toward the “roof”), cross cutting (diamond) on the base and roof (often fading towards the roof)	Parallel to slightly curved ridges tangentially up the outer wall (spiral), chevron pattern on side and top (terminal chamber).(no bioglyphs reported for the entrance/upper-decline)	Scratch marks (3 mm deep) on the floor, sides and ceiling, converging on the axis (centre) of the burrow. Increasing quality of preservation with depth.	Scratch marks: low ridges parallel to each other along the sides and ceiling converging on the axis (described in text, but not really visible in the figure)	No obvious scratch marks	Grooves and ridges on sides (described as large scale *spongeliomorpha*, see Figure 13 and 69)	Only on the walls, vertical and horizontal scratch marks (relative to horizontal burrow axis) as parallel ridges, Λshapes and chevrons	Scratch marks on the sides at 20° from the floor or base (similar to Hobbs Hill type and Type G)	Scratch marks tangential to long axis with some extending to sides
Burrow linings	Rare, one possible occurrence	Non reported	Not reported	N/A	Not reported	None	Discontinuous clay flakes(~0.2 – 0.3 cm)	Not reported	Rare
Producer in burrow	Absent	*Diictodon*	20 *Trirachodon* (1 *Bauria Cynops:* King, 1996)	*Thrinaxodon*	Fragments inside burrow: *Lystrosaurus*	Fragments associated outside burrow (identity unconfirmed)	None	None	Absent
Calcite plagues	Present	Not reported	Not reported	Not reported	Not reported	Not reported	N/A	Present	Not reported
Burrow Fill	Sand, mudchips, incremental filling	Sand and silt (calichification of burrow fill, ascribed to original porosity)	Incremental filling, sandstone and mudchips, coprolites, bone fragments	N/A	grey mudstone	Sandstone	Siltstone to fine-grained sand and claystone clast para-breccia	Mudchips at base	Sands and some mudchips

Table 6. Summary and comparison the key ichnological features of the burrows described by Smith (1987), Groenewald *et al*. (2001), Damiani *et al*.(2003), Modesto and Botha-Brink (2010), Groenewald (2001), Bordy *et al*. (2011), Sidor *et al*. (2008) and Miller *et al*. (2001) (*Calculated range based on aspect ratio and width therefore most likely more extreme than actually observed).

The architectural morphological similarities include a gently inclined ramp (near horizontal to 30°), relatively simple structure (no intricate networks, suggesting invertebrate burrow producers) and relatively large size (diameter > 6 cm, length up to at least 170 cm). The surficial morphology is similar with parallel ridges of similar dimension interpreted in both burrow types as scratch marks (Table 6, Figure 66). The scratch marks on the *Diictodon* burrows are described as chevron shaped, produced by crosscutting scratches. This may in fact be the same shape observed on the Hobbs Hill type burrows, diamonds and chevrons produced by crosscutting scratch marks. However if the scratch marks are indeed different then the chevron indicates that the implement (claw or beak) was singular or only one part applied enough pressure to produce a scratch mark deep enough to be preserved. Similarly, the diamond-shaped scratch marks provide information on the nature of the implement creating the scratches. Multiple parallel scratches indicate that multiple points were in contact at the same time and that enough pressure was applied by at least 2 points to produce preferable scratch marks. Therefore if the chevrons are not at all diamonds then the organism that produced them would have used different tools (two claws or a beak) or with different dimensions (functional morphology).

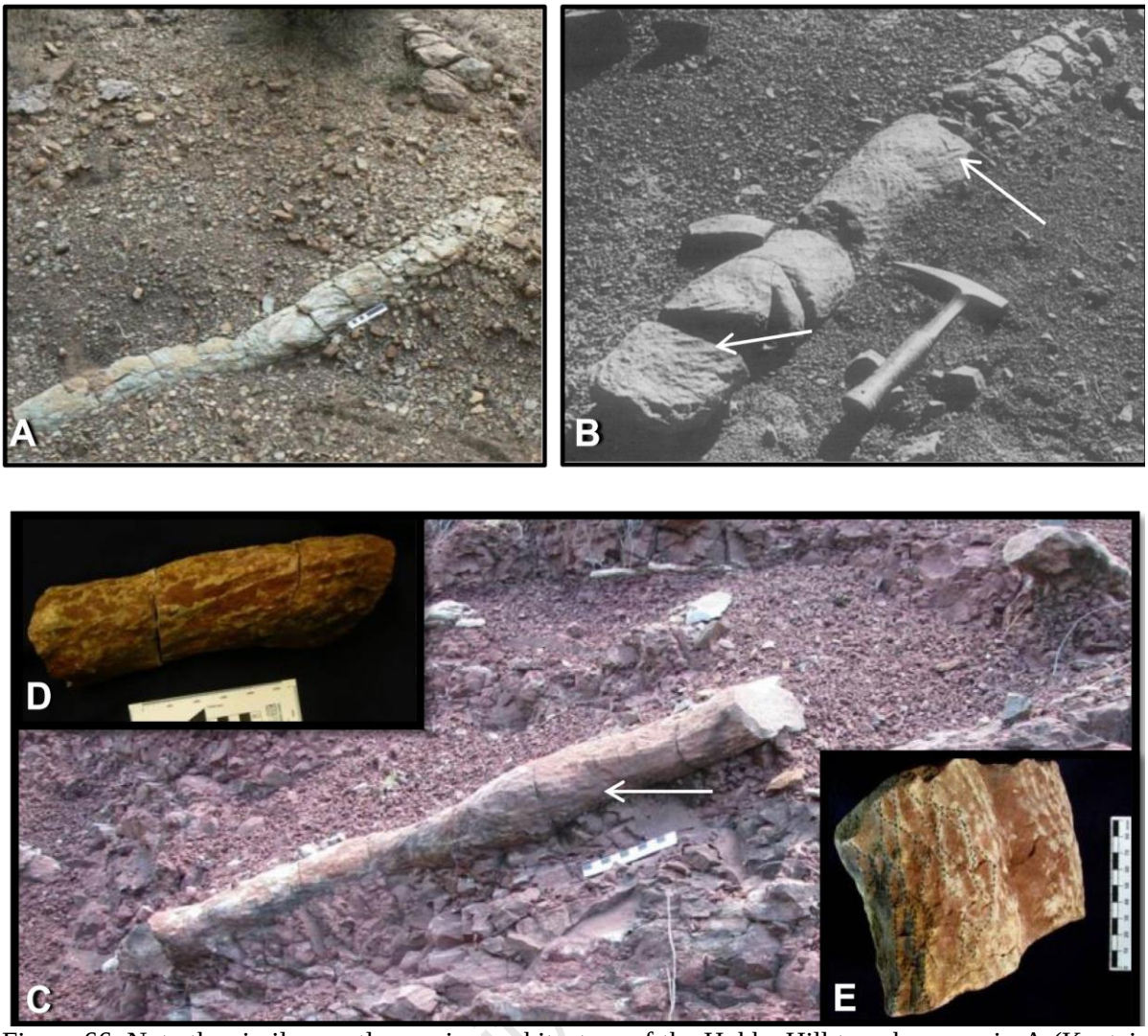

Figure 66. Note the similar gently curving architecture of the Hobbs Hill type burrows in A (Kapteinskraal), C (Hobbs Hill) and a terminal chamber of a *Diictodon* burrow in B (taken from Smith, 1987) (10 cm scale bar in A and geopick for scale in B). The scratch marks, which are oblique to the lengths of the burrows, are indicated in B (white arrows) and in C (white arrow); the insert D and E are close up views of the scratch marks on the opposite surface of the burrow in C. The scratch marks, which run tangentially parallel with the length, are visible in D, while the cross-cutting scratch marks that produce the diamond-shapes are outlined in E.

The chevron-shaped scratch marks on *Diictodon* burrows can be explained by a similar process that produced the diamond-shaped scratch marks (crosscutting linear scratch marks) (Figure 66). The production of these cross-cutting scratch marks indicate the burrows were both produced by an organism that could dig in two directions most by removing soil away from a central point in alternating directions (Figure 66). The diamond shaped scratch marks indicate that pressure was applied for a longer distance in both directions than for the chevron shaped scratch marks. It is also possible that more claws (at least 2) were in contact with the digging surface producing a diamond shapes, while only one claw (or other point e.g., beak) was used to produce the chevrons-shaped

scratch marks. The length of the digits in the hands need to be longer on the outside of the hand to maintain contact in an arched scraping movement. When all the digits are similar in length then only one finger would be in contact with the surface during a curved scraping movement. (Functional morphology studs and 3D modelling could explain this with more accuracy).

7.2.2. *Trirachodon* complex burrow systems

Groenewald *et al. (*2001) described a complex system of burrows with numerous branching, enlarged entrances and tapered terminal chambers, found at two localities in the Burgersdorp Formation. One well preserved burrow complex and the other complex poorly preserved but containing at least 20 *Trirachodon* (*Cynodontia*) fossils. The complex nature, large size of the burrows relative to the size of the *Trirachodon* and the occurrence of 20 *Trirachodon* fossils within indicates that the burrow complexes were inhabited and produced by communities of *Trirachodon* (Groenewald *et al.*, 2001).

The *Trirachodon* burrows are very different to the Hobbs Hill type burrows occurring as a system of tunnels where branching is numerous with multiple terminal chambers and an enlarged entrance (Groenewald *et al.*, 2001). These burrows are slightly younger (*Cynognathus* Assemblage Zone) than the Hobbs Hill type burrows which occur in the underlying Katberg Formation (*Lystrosaurus* Assemblage Zone) (Groenewald and Kitching, 1995).

The diameters of the entrances and tunnels are very similar to the “tunnels” of the Hobbs Hill burrows (~9-15 cm). The terminal chambers of the *Trirachodon* burrows taper off (6.5 down to 1 cm) and are less extensive (7.5 – 26.5 cm in length) than the single possible terminal chamber (~10 cm height) of the Hobbs Hill type burrows that is enlarged relative to the “tunnels” (Figure 54). Overall, the aspect ratios of the *Trirachodon* burrows (~2.4) are higher than the Hobbs Hill type burrows (~1.8) (Table 6).

The *Trirachodon* burrows are considerably smaller vertically than the Hobbs Hill type burrows. This could be because of compaction, because the burrow described for the Locality 2 has a higher aspect ratio (width 10.4 cm, height 6.3 cm = 1.65). Although it is clear that there are numerous burrows based on the photographs in Groenewald *et al.* (2001), there are measurements for very few burrows. Fortunately, many of the features are visible in the photographs. A second difficultly with using this paper for comparisons is the lack of descriptions for the Locality 2 burrows. It must be assumed that the difference in aspect ratios is due to compaction. A more detailed petrographic description texture and nature of cement of the burrow fill could have allowed for a more definitive conclusion as to whether compaction occurred or not.

The cross-sectional shape of the tunnels in both types is often bilobate (Figure 67). The roof of the *Trirachodon* burrows differs from the Hobbs Hill type burrows in that they are sometimes bilobate as well, while the later generally have an arched or flat roof (Table 6). Describing the roof as flattened may lead to the perception that the burrows were actually flattened; here flat is used instead to avoid such confusion. The scratch marks described for the *Trirachodon* burrows are similar to the *Diictodon* burrows and similar to the Hobbs Hill type burrows for the same reasons as outlined in the previous comparison (see *Diictodon* burrows above) (Table 6).

The complexity of the *Trirachodon* burrows is a major difference with no evidence of branching preserved in the Hobbs Hill type burrows. Social behaviour is required to produce large complex burrow systems, but the absence of large complex burrow systems does not necessarily indicate the absence of social behaviour. Groenewald *et al. (*2001) proposed that the bilobate base was formed by *Trirachodon* moving past each other along the length of the burrows. Parts of the burrow complex with the most traffic would are therefore wider and the bilobate feature more prominent. A similar explanation could be given for the bilobate base in the Hobbs Hill type burrows as illustrated in Figure 67.

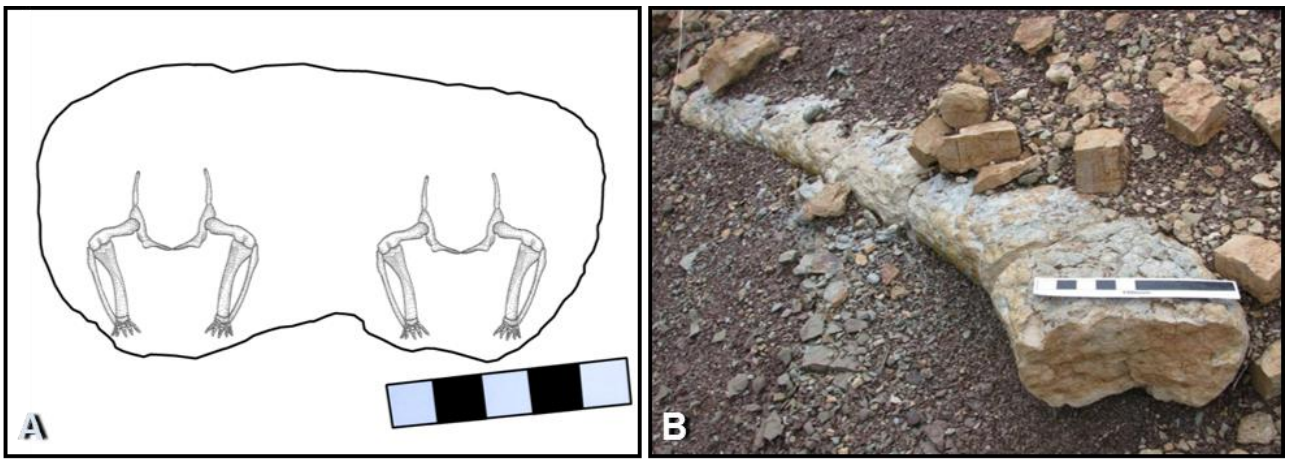

Figure 67. Two organisms may have moved inside a burrow as demonstrated in A, moving next to each other in opposite directions, wearing down the two lobes in the most used parts of the burrow. B is the burrow is the burrow that saw outline to create the cross-sectional view in A.

The complex burrow systems, large burrow size relative to burrow producer and the bilobate base of the burrows are evidence for the establishment of social behaviour by the Early Triassic in the Karoo Basin. This strategy may have been developing in other tetrapods during the deposition of the Katberg Formation. The similarities with respect to the bilobate base suggest that the Hobbs Hill burrows may have been produced and occupied by social organisms.

7.2.3. *Thrinaxodon* containing burrow

Damiani *et al.* (2003) described a single burrow containing a *Thrinaxodon* fossil, which was found close to three similar burrows which are not associated with it. The architectural morphology comparisons are limited due to the relatively small specimen size and lack of *in situ* examples (ramp). The burrows were found in the Palingkloof Member of the Balfour Formation, near Bethulie, which represents the PT boundary in South Africa. The burrow fill is sandstone while the host rock is fine-grained indicating that the burrow was filled during a flooding event in the flood plain environment in semi-arid conditions (Damiani *et al.*, 2003). The presence of bioturbation (invertebrate burrows) between burrow fill and host rock is an indication of moist soil and a close proximity to water during and soon after the burrows were filled (Damiani *et al.*, 2003).

The width, height, aspect ratio and length of the burrow are estimated from the figures (with scales) presented in Damiani *et al. (*2003). Based on these values the *Thrinaxodon* burrows are larger and taller, are circular than the Hobbs Hill type burrows (Table 6 and Figure 68).

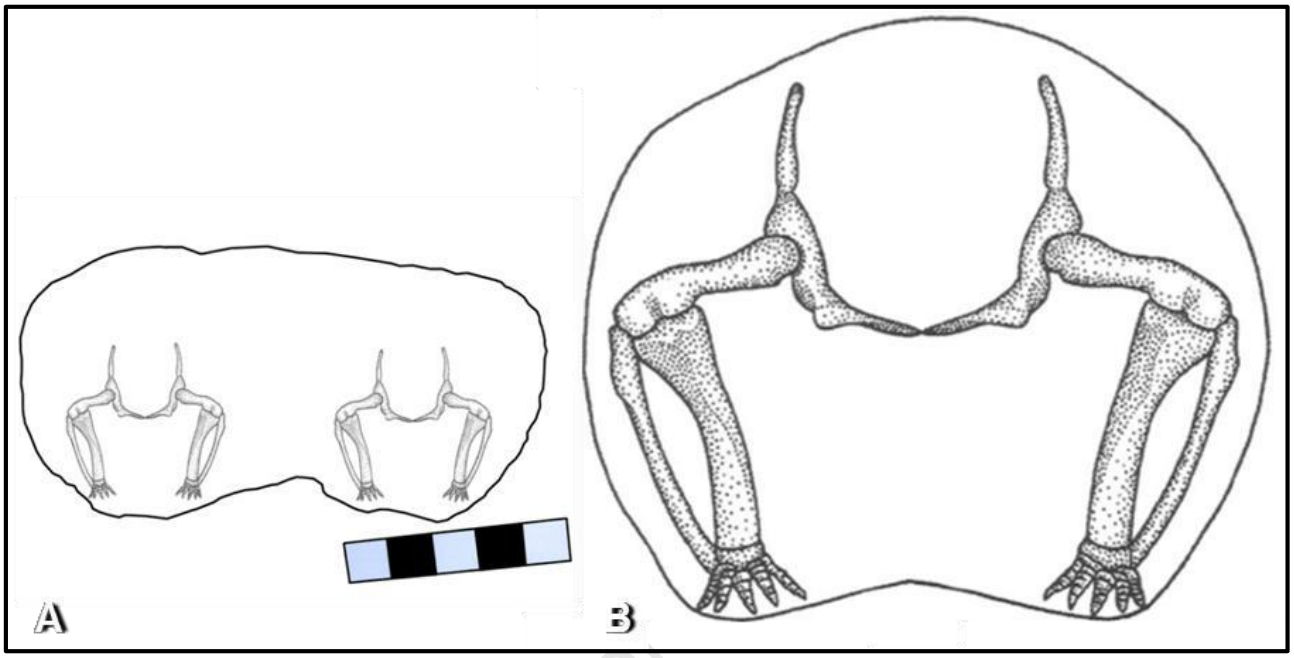

Figure 68. Thrinaxodon clearly could not have produce the Hobbs Hill type burrow (A) when compared at the same scale with *Thrinaxodon* burrow (B). *Thrinaxodon* is too large to have produced burrows which are generally less than 10 cm in height (Scale bar = 5 cm; skeleton was scaled down in order to fit inside the Hobbs Hill type burrow).

Figure 68 is a good example of how numbers alone are deceptive, they appear similar (in Table 6), but when put next to each other like this it is clear that they were produced by different organisms. The above comparison also demonstrates the importance of reporting both vertical and horizontal diameters as both have the same width, yet the height and therefore the entire burrow is very different. This illustrates one of the pitfalls of comparative analysis using limited data, something may appear similar with respect to certain aspects, but when the aspects are considered together the object described as a whole is not at all similar.

The surficial morphology of the *Thrinaxodon* burrow has parallel ridges that run along the length of the (tangentially) burrow walls and ceiling; these ridges are considered scratch marks. This is

similar to the scratch marks observed in the *Diictodon* (Smith, 1987), *Trirachodon* (Groenewald *et al.*, 2001) and Hobbs Hill type burrows. The diamond-and chevron-shaped bioglyphs are absent from the *Thrinaxodon* burrow, this may be indicative of a different excavation technique or a preservational bias relating to the nature of the substrate (different moisture levels in the original soil). Although *Thrinaxodon* is clearly not the same organism that produced the Hobbs Hill type burrows, the similarities indicate a tetrapod producer and that burrowing behaviour was practiced by several different tetrapods during the Triassic in the Karoo Basin.

Alternate explanation for the bilobate base

The burrowing techniques of tetrapods could be interpreted from the scratch marks and other features of burrow morphology. The burrowing techniques could then be compared to the range of movements possible by the different possible burrow producers based on the analysis of anatomy and functional morphology.

The comparison is interrupted here to propose a different mechanism for the origin of the bilobate base seen in many of the burrows. It is possible that the two depressions seen in the *Trirachodon*, *Thrinaxodon* and Hobbs Hill type burrows are not due to the compaction related to locomotion. The *Thrinaxodon* burrows could not have been produce by the same mechanism as proposed for the *Trirachodon* burrows because only one organism can fit inside it. If the locomotion of a single organism produces this bilobate base as proposed for the *Thrinaxodon* burrows by Damiani *et al. (*2003), then why do the *Diictodon* burrows not show any bilobate base?

Ray and Chinsamy (2003) describe the functional morphology of *Diictodon*. They describe the posture and locomotion by considering the range of movement of limbs away from the midline of

the body and not pigeon holing organisms into sprawling, semi-erect and erect postural grades (Ray and Chinsamy, 2003). According to them the *Diictodon* dug its burrows by rotation thrust.

It is possible that the bilobate base (in some if not all of the above) is because of the digging mechanism and not the type of locomotion or posture used by the organism that move inside the burrows. The scratch marks and functional morphology could be used to confirm this.

7.3. Studies on burrows not containing fossil in "life position"

7.3.1. Burrow resembling *Spongeliomorpha*

The paper by Groenewald (1991) briefly describes several burrows from the Katberg Formation and Palingkloof Member, the Kapteinskraal and Speelmanskop sites seemed to have burrows that are similar to the Hobbs Hill type burrows. These burrows were reinvestigated in this study (Chapter 3.2 study area). The surficial morphology (inferred from "large scale *Spongeliomorpha*", Figure 13 and 69), low ramp, 90^{o} orientation of burrows relative to each other, occurrence of desiccation cracks in the sandstone horizon just above the burrows, burrow architecture and fill material are essentially the same for the burrows described in this study at Kapteinskraal and those described by Groenewald (1991) (Scoyenia 1b).

Groenewald (1991) describes 60 cm diameter burrows as *Scoyenia* and 20 cm diameter burrows as *Gyrolithes*, both with a surficial morphology described as *Spongeliomorpha* at Kapteinskraal. In his Table 2 the Scoyenia b1 type burrows have diameters which range from 20-45 cm. Nowhere in the table does Groenewald mention a burrow of 60 cm diameter, thus it is very difficult to link the text to the tables in the article.

Several major problems make it very difficult to reconcile the burrows described for Kapteinskraal in Groenewald (1991) with the Hobbs Hill type burrows found at Kapteinskraal, despite the above described similarities. The major differences include: (1) a 150m distance separating the sites (based on the co-ordinates provided in Groenewald, 1991), (2) the smaller diameters of the Hobbs Hill type burrows, (3) the Hobbs Hill type burrows do not actually overlay each other and (4) no fossils were observed in association with the burrows at Kapteinskraal. Based on these differences the burrows are not considered to have been produced by the same organisms.

Figure 69. Scratch marks on the burrows found in this study at Kapteinskraal may be considered similar to the *Spongeliomorpha* described Groenewald (1991) for Scoyenia 1b illustrated in Figure 13. The burrow is seen from a distance and the the insert is a close up of the scratch marks.

7.3.2. Large burrow of the Palingkloof Member

Modesto and Botha-Brink (2010a) describe a burrow with a living chamber (terminal chamber) which they consider similar to the Scoyenia 1b type burrow described by Groenewald (1991). The diameter reported by Modesto and Botha-Brink (2010a) (Table 6) is for the terminal chamber, they later state that the chamber is not enlarged relative to the rest of the burrow. Therefore the "ramp" (tunnel between the entrance and terminal chamber) also has a diameter of 34 cm. Based on these dimensions, the burrows described by Modesto and Botha-Brink (2010a) are considerably larger than the Hobbs Hill type burrows (Table 6). This burrow is not considered the same as the Hobbs Hill type burrows and was most likely not the produced by the same organism that produced them.

Modesto and Botha-Brink (2010a) do not consider *Lystrosaurus* as the most likely candidate based on the fragmentary and disarticulated nature of the *Lystrosaurus* bones found inside the burrow in their study. They also contend that the bone fragments found inside the burrow belonged to a

Lystrosaurus that was too small to have produced that burrow. They concluded that the *Lystrosaurus* bones represent larded prey brought into the burrow by an akidnognathid *Olivierosuchus* or *Moschorhinus* predator (Modesto and Botha-Brink, 2010a).

7.3.3. Large Burrow in the Katberg Formation Bordy *et al*. (2011)

The burrows described by Bordy *et al.* (2011) are very similar to those described by Modesto and Botha-Brink (2010) and Groenewald (1991) (Scoyenia 1b) (Table 6) with respect to burrow widths, consisting of single relatively straight burrows with ramp decreasing with depth, lack of bilobate base and over 100 cm in length. They are so similar that they could be considered as being produced by the same or very similar organisms. With only one or two samples described for this type of burrow by Groenewald (1991) (Scoyenia 1b) and Modesto and Botha-Brink (2010) the Hobbs Hill type burrows could have been part of a burrow type with two extreme examples present. With the inclusion of the information provided by Bordy *et al. (*2011), it is clear that they represent a type of burrow that is larger than the Hobbs Hill type burrows and not a highly variable burrow type.

The producers that were considered for the Bordy *et al.* (2011) type burrows include *Lystrosaurus murrayi, Lystrosaurus declivis, Thrinaxodon liorhinus, Galesuarus* and *Progalesaurus* based on their anatomical features that allow for fossorial behaviour. The *Lystrosaurus murrayi* and *Lystrosaurus declivis* are considered the most likely burrow producers based on their size and the occurrence of their bone fragments in similar large burrows described briefly in previous studies (Groenewald, 1991; Retallack *et al.,* 2003). These burrows may also have been produced by a predator as suggested by Modesto and Botha-Brink (2010) based on the similarities in morphology and stratigraphic position.

7.3.4. Ichnogenus A

Sidor *et al. (*2008) described several large burrows from the Fremouw Formation (Early Triassic) and Lashly Formation (Member A) (early Middle Triassic) in Antarctica. The burrows from the Fremouw Formation are similar to *Thrinaxodon* containing burrows described by Damiani *et al. (*2003) and the Giant or Type G burrows described by Miller *et al. (*2003) and later Hasiotis *et al. (*2004). Sidor *et al. (*2008) called the burrow Ichnogenus A, its details are summarised in Table 6 for comparison with the Hobbs Hill type burrows.

Based on the similarities in burrow morphology of Ichnogenus A and the Hobbs Hill type burrows and the occurrence in Early Triassic deposit of Gondwana they could be considered the same type of burrow (Hobbs Hill type burrow therefore could be called Ichnogenus A). The width of the Ichnogenus A burrow is slightly larger than the Hobbs Hill type burrow, but the aspect ratio is the same (Table 6). One striking difference though is the surficial morphology of the specimen from the Fremouw Formation (Figure 70). The scratch marks appear to dip in one direction only while those on some of the Hobbs Hill burrows dip in two opposite directions producing the diamond-shape pattern described above (Figures 53, 61). This difference in scratch mark types may be a function of the variations in substrate (during construction), wear from use (by the burrow user) or weathering during filling of the burrow.

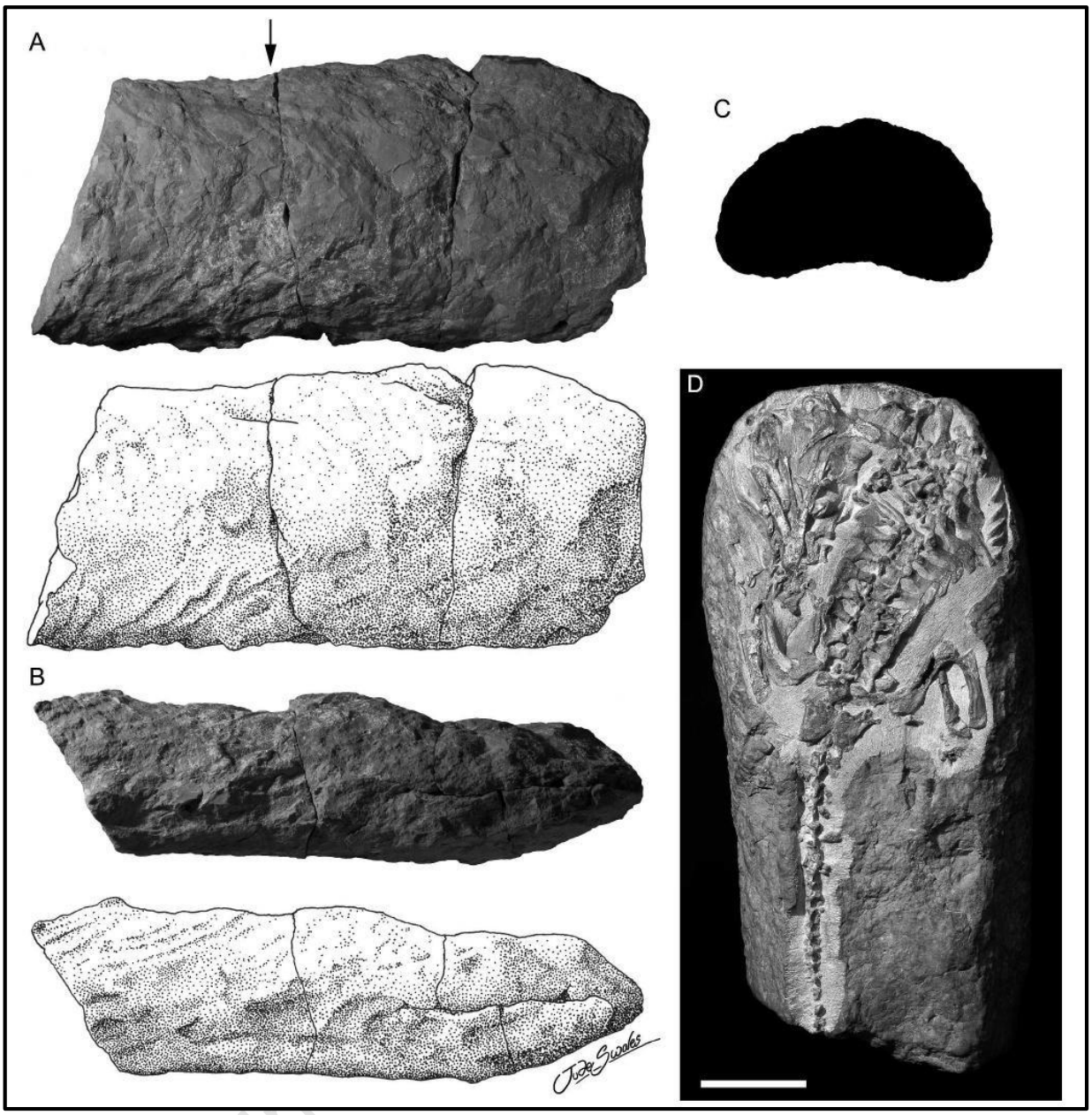

Figure 70. Scratch marks dipping in one direction on the surface of the burrow (UWBM 88617) and cross-sectional shape (at the arrow in A is indicated in C) from the Fremouw Formation Scale bar represents 5 cm (white line on black surface in D, that is a view of the *Thrinaxodon* inside the burrow described by Damiani *et al.*, 2003) (Taken from Sidor *et al.*, 2008).

Sidor *et al. (*2008) consider Ichnogenus A similar to the *Thrinaxodon* containing burrow described by Damiani *et al. (*2003), but point out that the surficial morphology seen in their burrows are lacking in the *Thrinaxodon* containing burrows and that the height of the burrow is different. The difference in aspect ratio (Ichnogenus A= almost 2 apposed just over 1 for *Thrinaxodon* containing burrow) is attributed to compression of the Antarctic burrows having some effect on the anatomy of the burrow greater than previously expected. The Ichnogenus A burrow is more similar to the

Hobbs Hill type burrows with respect to the aspect ratio than it is to the *Thrinaxodon* containing burrow (Figure 71). The apparent difference in shape may be of significance, the rough edges in Figure B are due to weathering, D another Hobbs Hill type burrow is smother and more similar in cross-sectional shape to Ichnogenus A.

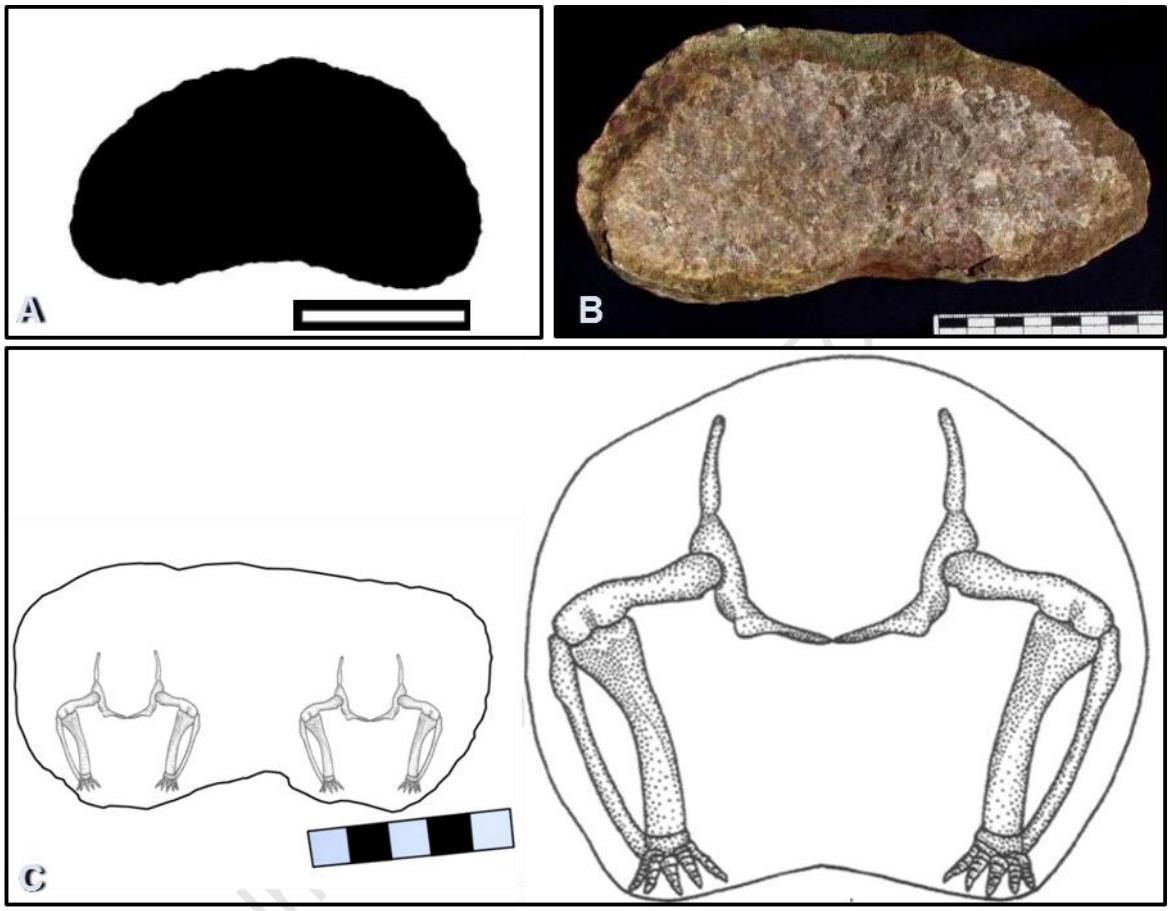

Figure 71. The similarities in aspect ratio and shape between the Hobbs Hill type burrows (B and C with two skeletons) and Ichnogenus A burrow (A). Note how very different the aspect ratio of the *Thrinaxodon* containing burrow (C with single skeleton) is relatvie to the other three. The cross-sectional shape is quite different between the burrows from three different studies. Scale bars in A and C are 5 cm, in B scale bar is 8 cm.

In conclusion, the Ichnogenus A burrow from the Fremouw Formation more similar to the Hobbs Hill type burrows than any of those compared above. It is however unfortunate that there is only one sample described, since the burrow morphology may change dramatically along the length of a single burrow [e.g., the *Diictodon* containing burrows of Smith, 1987 and the Holmsgrove burrow in this study (Figure 49)]. The possible burrow producers considered by the Sidor *et al. (*2008)

include *Procolophon* and *Thrinaxodon* or another similar sized tetrapod as the most likely candidates. These organisms were selected by Sidor *et al. (*2008) based on the burrow's similarity to the *Thrinaxodon* contain burrow (Damiani *et al.*, 2003) and the Type G burrows (Miller *et al.*, 2001).

7.3.5. Type G burrows of Miller

Miller *et al.* (2001) described numerous burrow samples from the Early Triassic Fremouw Formation, which they divided into two populations base on the diameters (width) namely Type L and Type G (Figure 72). Type L burrows are 2 to 6.5 cm in diameter and the Type G burrows are 8 to 19 cm in diameter (Table 6). The Type G burrows are most similar to the Hobbs Hill type burrows and are compared here, while the Type L burrows are more similar with respect to cross-sectional shape and surficial morphology they are considered too small to be the same as the Hobbs Hill type burrows.

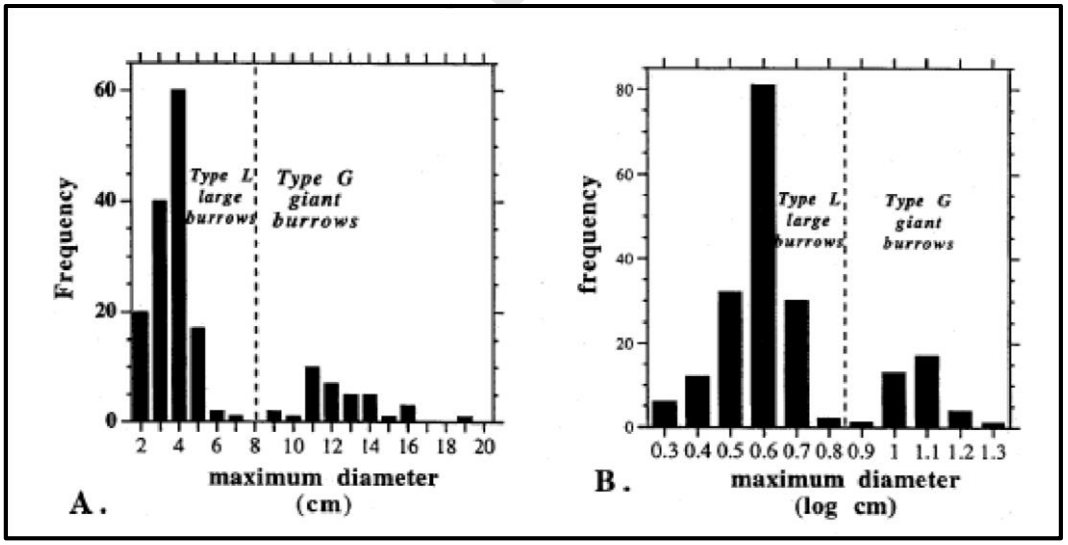

Figure 72. The frequency distribution of the large burrows studied by Miller *et al.* (2001) separating them into two groups, the Type L and Type G. The Type G burrows overlap very well with the Hobbs Hill type burrows (Taken from Miller et al., 2001).

Most of the Type G burrows have a width between 10 and 15 cm while the Hobbs Hill type burrows are mostly between 10 and 12 cm, therefore they overlap quite well with respect to frequency as well as the size range. The differences between the horizontal diameters of the Hobbs Hill type burrows and the Type G burrows could be related to the greater samples size of the Type G burrows (Figure 72 and Table 6). The average aspect ratio of the Type G burrows is higher than that of the Hobbs Hill burrows (therefore they are generally wider than the Hobbs Hill type burrows). If the difference in aspect ratios is attributed to compression of the Type G burrows, then the larger diameters could also be a function of compression depending on the type of compression. The other features such as surficial morphology and architecture are quite similar with minor difference most likely related to variations in the substrate and the larger sample size of the Type G burrows respectively. Therefore, the Type G burrows described by Miller *et al.* (2001) are considered the same as the Hobbs Hill type burrows.

The organisms that produced the Hobbs Hill type burrows are most likely the same organism that produced the Type G burrows. Both types of burrows occur in Early Triassic fine-grained floodplain deposit in braided fluvial systems (Miller *et al.*, 2001). The paleoclimate was highly seasonal in the Karoo Basin and in the Transantarctic Mountain Range (Miller *et al.*, 2001). All these similarities allow for the consideration of the same organisms that were considered by Miller *et al.* (2001) for the potential burrow producers of the Hobbs Hill type burrows as well.

Lystrosaurus is considered a possible semi-fossorial organism based on its anatomical similarities to *Diictodon*, a proven semi-fossorial organism (Smith, 1987; Miller *et al.*, 2001). *Lystrosaurus* is excluded as a possible trace maker by Miller *et al. (*2001) because the adult organism is too large to have produced them, similarly the Hobbs Hill type burrows are too small to have been used or produced by *Lystrosaurus*. *Thrinaxodon* and *Procolophon* are also considered possible producers of

the Type G burrows based on their occurrence in the Fremouw Formation. However, *Thrinaxodon* is already excluded as likely producer of the Hobbs Hill type burrow based on the different aspect ratios, with the *Thrinaxodon* contain burrow being more circular. The Type G burrow have a higher aspect ratio than the Hobbs Hill type burrows and are therefore even less likely to have been produce by *Thrinaxodon*.

According to Miller *et al.* (2001) *Procolophon trigoniceps* is considered a likely candidate for the Type G burrows based on five lines of evidence (Miller *et al.*, 2001):

1) The occurrence of *Procolophon* bones in burrow resembling Type G [Referring to the *Thalassinoides*-like burrows in Groenewald, (1991)] (Stanistreet and Turner, 1979, Groenewald, 1991, 1996 in Miller *et al.*, 2001).
2) Branching in some of the Type G and in the *Thalassinoides*-like burrow (Groenewald *et al*., 2001).
3) *Procolophon trigoniceps* had anatomical features which are characteristic of burrowing organisms and was considered a burrowing organism by J. W. Kitching (personal communication with Miller *et al.*, 2001 in 1998) (Colbert and Kitching, 1975; Miller *et al.*, 2001).
4) *Procolophon trigoniceps* was the appropriate size, an immature skull and rib width of ~5-6 cm and limb span of 8 cm.
5) The only known Type G burrow bearing location was Kitching Ridge, which is also, where most of the *Procolophon* fossils were found in the Shackleton Glacier area at the time.

The likelihood of *Procolophon trigoniceps* being the producer of the Type G burrows appears high and is also considered here to be the most likely candidate. Point 1) above however is not strong evidence for *Procolophon* because of the precarious link between the *Procolophon* fossil containing

burrows and the Type G burrows. Groenewald (1991) states that his *Thalassinoides* burrows are similar to burrows that contain *Procolophon* fossil according to personal communication with J.W. Kitching (in 1990).

The points made by Miller *et al. (*2001), however circumstantial, present a strong case for *Procolophon* which is known to occur in burrows (Kitching 1990 pers. comm. with Groenewald, 1991). Studies on the functional morphology and bone histology of *Procolophon* indicate that it was capable of digging and had a bone density commonly associated with fossorial and semi-fossorial organisms respectively (Colbert and Kitching, 1975; deBraga, 2003; Botha-Brink and Smith, 2012). Furthermore the lack of growth rings indicate that *Procolophon trigoniceps* did not suffer seasonal stress and most likely employed burrowing as a survival strategy, unless the lack of growth rings is because this species reaching adulthood in less than one year. *Procolophon trigoniceps* has also been found in association with the Hobbs Hill type burrows (at Hobbs Hill) (Cisneros, 2006).

Another candidate for the Hobbs Hill type burrows is *Kitchingnathus untabeni*, which was previously considered a juvenile *Procolophon trigoniceps* (Cisneros, 2008). The holotype (BP/1/1187) for *Kitchingnathus untabeni* was collected from the Hobbs Hill locality by Kitching between 1952 and 1966 and initially classified by Gow (1977) as a juvenile *Procolophon trigoniceps*. While there are no reports of *Kitchingnathus untabeni* in Antarctica the possibility remains.

7.4. Fossils found in association with burrows

The best-case scenario is the occurrence of fossils in life position inside the burrow; however, this is a relatively rare occurrence. Many studies of large tetrapod burrows from the Mesozoic use circumstantial evidence to infer what the most likely burrow producer was (Groenewald, 1991; Miller *et al.*, 2001; Sidor *et al.*, 2008; Modesto and Botha-Brink, 2010a; Bordy *et al.*, 2011). This ranges from disarticulated fossils, fossil fragments, scales and other biogenic remains within the burrows to more complete to fragmentary remains preserved in the same beds and in the extreme case to remains in the same stratigraphic unit (Dubiel *et al.*, 1987; Sidor *et al.*, 2008; Modesto and Botha-Brink, 2010b). Fortunately, the Hobbs Hill type burrows are associated with fragmentary fossil remains discovered in this study (Figure 42) and more complete specimens discovered in previous studies at Hobbs Hill (Kitching 1952 and 1966 in Cisneros, 2008).

As outlined in section 2.2.6. the Early Triassic is dominated by the dycynodon *Lystrosaurus* but also records the period when procolophonoids radiated (Neveling, 2004; Botha *et al*., 2007). The Hobbs Hill site specifically contains fossils of *Lystrosaurus*, *Procolophon trigoniceps* and *Kitchingnathus untabeni* (Groenewald and Kitching, 1995; Neveling, 2004; Cisneros, 2008). The skull width of *Procolophon trigoniceps* is always equal to or greater than the length based on descriptions and measurements in several publications (Colbert and Kitching, 1975; deBraga, 2003). The largest skull length for *Procolophon trigoniceps* is 78 mm (BP/1/4248) (Botha-Brink and Smith, 2012), therefore the width is most likely equal to or greater than 78 mm. Assuming that the skull width is the greatest width along the length of *Procolophon trigoniceps* and that most are smaller than 78 mm then most adult *Procolophon trigoniceps* would fit comfortably inside the Hobbs Hill type burrows.

However, the adult *Procolophon trigoniceps*, reconstructed by deBraga (2003), is up to 30 cm in length and has a skull diameter of at least 7 cm and a height of about 10 cm. The Hobbs Hill type

burrows (9.5-15 cm wide, ≤10 cm high) would be a very tight fit for *Procolophon trigoniceps*. Since the Type G and Ichnogenus A burrows are the same as the Hobbs Hill type burrows then the size range increases to 8 – 19 cm width and a height which comfortably accommodates even the largest of *Procolophon trigoniceps*. *Kitchingnathus untabeni* was smaller than *Procolophon trigoniceps* (Cisneros, 2008). *Kitchingnathus untabeni* is therefore also a very good candidate producer of the Hobbs Hill type Burrows.

Therefore, the most likely burrow producer candidates for the Hobbs Hill type burrows are *Procolophon trigoniceps* and *Kitchingnathus untabeni*.

7.5. 3D digital burrows

The reproduction of digital 3D copies of burrows is easily achievable using photogrammetry, as demonstrated here and in other studies (Falkingham, 2012). Photogrammetry is preferred over most other 3D scanning technologies due to inexpensiveness and ubiquity of its hardware requirements (Yilmaz *et al.*, 2008). With multiple free and open source software available, this technique is well suited for research purposes even at graduate level. The accuracy of photogrammetry has been demonstrated in a comparative study by Falkingham (2012) and a review by Gruen (2012) suggests photogrammetry may be superior to 3D laser scanning techniques (Figure 73).

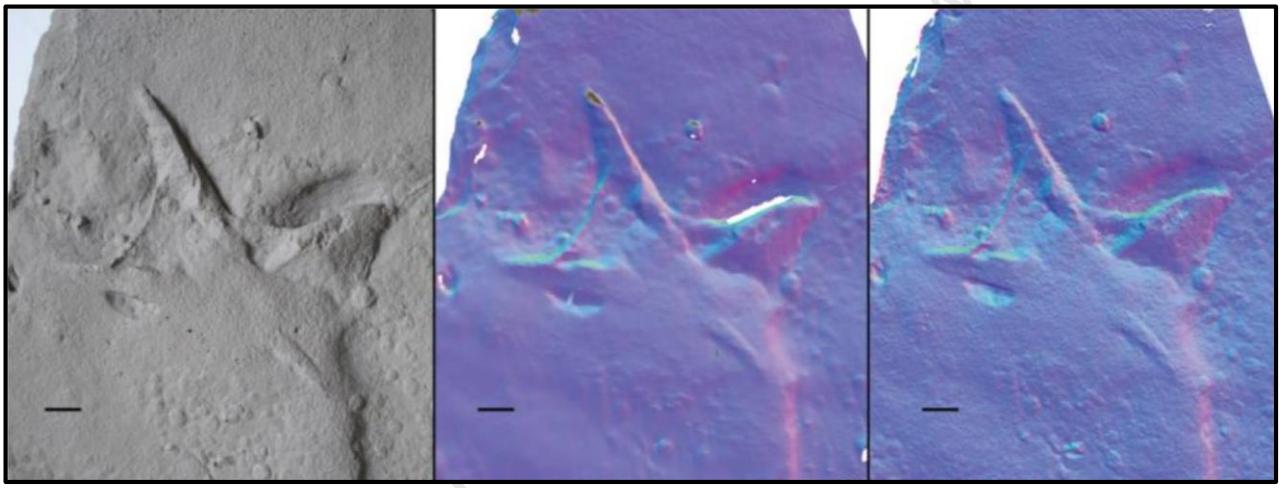

Figure 73. A comparison of a cast of a bird track in the form of a photograph (A), a laser scan (B) (using NextEngine scanner) and a photogrammetric model (C) (from 75 photographs) (Scale = 10 mm). A higher resolution 3D model has been produced in C at a fraction of the cost of producing B (taken from Falkingham, 2012).

PPT vs. 123D

While the quality of 123D is great, several issues make PPT more suited for research purposes for the following reasons. In 123D,

1) The file size is limited;
2) The number of photographs are limited;
3) The security of the uploaded data is limited;
4) The potential for loss of data and time (being internet based) is high;
5) No guarantees that it will remain free in the future as well;

6) There are unclear copyright issues;
7) There are uncertainties related to a free product offered by a commercial entity.

Together these issues are most likely to produce less accurate results than PPT, which is customizable, limited only by the users' ability and the processing power of the hardware used.

The PPT is the result of a growing community that seeks to improve FLOSS (Free/Libre and Open Source Software) technology, its usability and applications (Lerner and Tirole, 2000; Moulon and Bezzi, 2011). PPT has been used in archaeological and anthropological studies producing great results (Figures 73 and 74) (Falkingham, 2012; Moraes, 2012c). The relatively raw results in this study of the PPT software should not be considered a true reflection of the software's potential. High quality digital 3D copies of objects have been produced in other studies using the same software that is in PPT (Figures 73 and 74). To make this technology work in the field of ichnology, palaeontology and other earth sciences, it should be adopted more frequently.

In addition to enhancing the comparative and recording capacity of ichnological studies, 3D models can be used to determine whether possible candidates were capable of moving inside the burrows. This would require the 3D modelling of the fossil remains, determination of the range of movements using functional morphology and modelling these movements in a virtual 3D space. Once this has been done, the possible movements of the organism can be placed inside the virtual model; this could exclude or confirm possible potential burrow makers as the producers of a specific burrow.

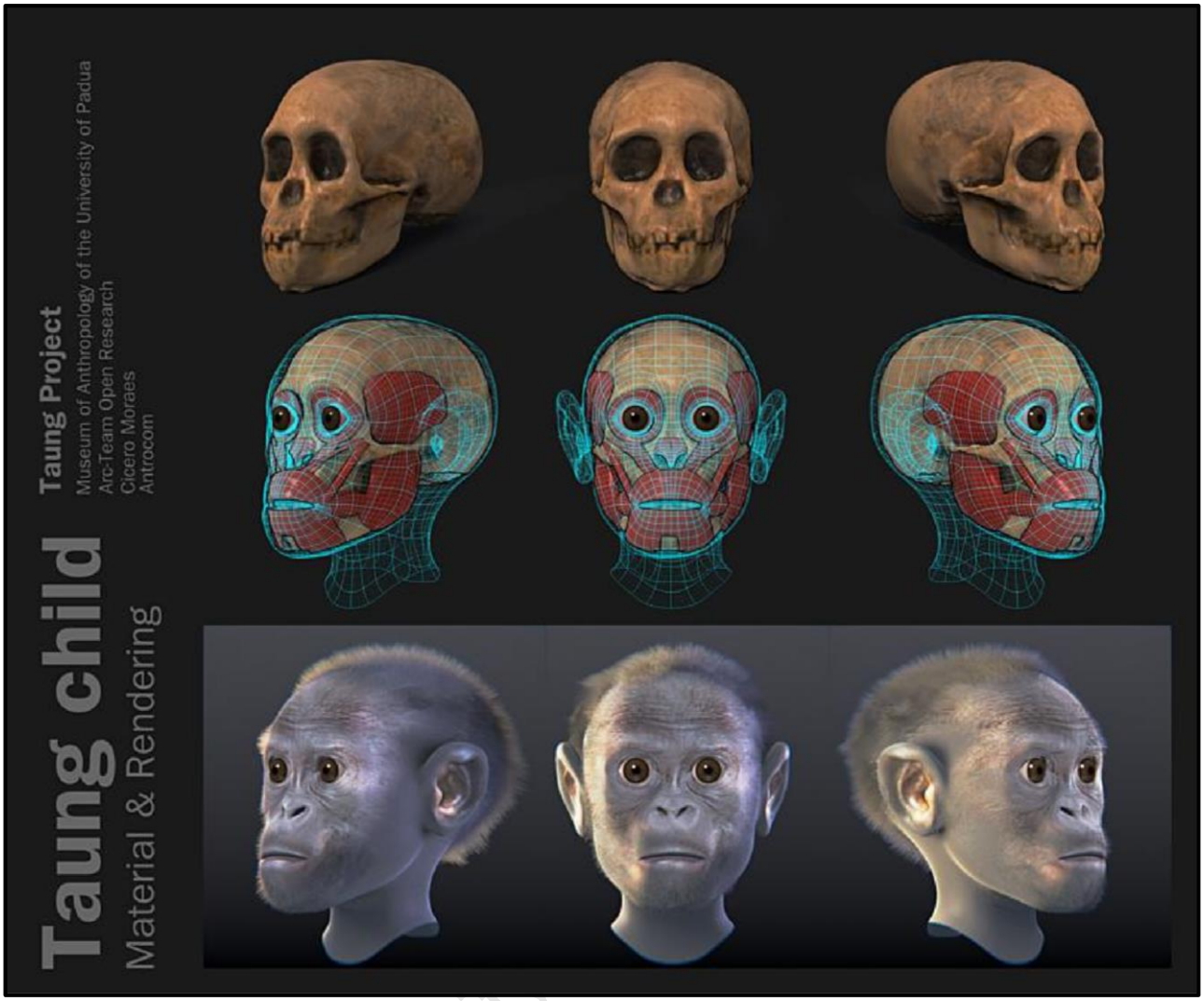

Figure 74. Demonstrating the potential of PPT to produce high quality 3D models using photogrammetry and the potential modelling that can be done using a 3D model (taken from Moraes, 2012).

The importance of accurate and unambiguous descriptions of trace fossils cannot be over emphasised. Unfortunately the description of a 3D object in a 2D results in a loss of information and generalisations are often necessary (Remondino *et al.*, 2010). By using averages and reporting only certain measurements, the researcher can give the reader an idea of the burrow morphology. This is not the ideal situation as many of the morphological properties of the burrows change along the length of the burrow. The surficial morphology, which can make the difference between identifying the producer or not, is often inadequately recorded in 2D photographs and sketches, even less so when described in words only. The exact points at which measurements such as diameter are made are generally not reported. These are a few examples of the limitations of conventional methods of recording the dimensions and morphology of burrows. If a feature such as

the cross-sectional shape was consistent along the length of a burrow, then it would be possible the make accurate generalisations, this is often not the case with biological structures such as vertebrate burrows. While these methods can be used to compare and thereby determine the sameness of burrows, and possibly a common producer, the potentially more accurate method of photogrammetry is advocated here.

The use of photogrammetry in scientific fields is rapidly developing with the goal of increasing accuracy and precision (Remondino *et al.*, 2010; Falkingham, 2012). The advent of 3D printing and the subsequent increase in affordability of 3D printing and rapid prototyping have resulted in the development of user-friendly, low-cost scanning techniques. 123D is one of these which uses photogrammetry, cloud servers and free software to allow users to create 3D copies and convert them into printable file formats. Online 3D printing services and rapid prototyping allow almost anyone to print out 3D objects saved in the appropriate file format. In this study, several sections of a burrow were converted into a 3D digital copy using photogrammetry and 123D. The result was then converted to the printing format to illustrate one of the potential uses of 3D scanning and processing.

By using 3D scanning or photogrammetry to produce a 3D digital copy of a burrow, the morphological characteristics are more accurately described. Even if the accuracy of the technique is not at the level where an exact replica can be produced, it is still much better than written and 2D graphical representations alone. Therefore, 3D copies of scanned burrows should be produced when possible in conjunction with conventional descriptions. Using both techniques will greatly assist in the comparison of burrow and the identification of the burrow producers.

8. Conclusions

The Early Triassic was a uniquely harsh period on Earth: the ocean temperatures reached 40° C in the equatorial Tethys creating a dead zone along the equator; the polar regions did not have permanent ice caps; and the seasonal climate was exacerbated by global megamonsoon conditions (Scotese and McKerrow, 1990; Parrish, 1993; Scotese *et al.*, 1999; Chumakov and Zharkov, 2002; Wang, 2009; Preto *et al.*, 2010; Sun *et al.*, 2012). Geological studies of the Lower Triassic, Katberg Formation indicate harsh and semi-arid conditions in the main Karoo Basin (Hiller and Stavrakis, 1984; Smith, 1990; Smith and Botha, 2005; Catuneanu *et al.*, 2005). Life struggled to recover from the Permo-Triassic mass extinction event and biodiversity remained low throughout the Early Triassic (Payne *et al*., 2004; Smith and Botha, 2005; Botha *et al*., 2007; Retallack *et al*., 1996, 2011). The Beaufort Group records the response and evolution of tetrapods on land before and after the PT extinction. It is within this framework that the burrows and their potential producers are considered.

A range of methods were used to identify the burrow producers, their environmental conditions and to produce affordable and useful digital 3D burrow copies, including standard sedimentological techniques, ichnological descriptions, comparisons and the use of photogrammetry.

Based on facies and architectural element analysis the Katberg Formation at the Hobbs Hill site has characteristics that are in agreement with those observed in other studies of the Katberg Formation. The exception to this is the occurrence of Lateral Accretion surfaces (albeit low angle) that are not often reported for the Formation. The HO or scour hollow element observed at Hobbs Hill is also a feature that is not frequently reported for the Katberg Formation. The occurrence of carbonate cement in medium- or larger grained sandstone (with or without intraformational rip-up mudclasts) Hobbs Hill site is difficult to explain, apart from being associated with burrows and beds containing fossils.

The Hobbs Hill type burrows occur as simple un-branched, gently curving tunnels with an aspect ratio of ~1.8, a ramp of ~25°, a bilobate to oval cross-sectional shape and crosscutting scratch marks on the surface. The burrows are hosted in the fine-grained facies assemblage, made up of casts that were passively and incrementally filled by coarser medium-grained sandstones with intraformational rip-up mudchips.

The facies assemblages at Hobbs Hill indicate alternating periods of upper to intermediate flow regimes with lower flow regimes in channels and overland sheetflood deposits (thick sandstone packages). The preponderance of sharp and/or erosive contacts between sandstone beds, preferential preservation of upper flow regime facies (Sh, Sl and Sm), common occurrence of intraformational rip-up mudclast in thick successions of sandstone beds interbedded with minor mudstone beds (mud drapes) indicate alternating upper and lower flow regime conditions. The architectural element analysis together with the facies analysis indicate a fluvial style which was transitional between the low sinuosity, flashy, ephemeral, sheetflood sand-bed river and the low sinuosity high energy, sand bed braided river described by Miall (1985, 1996).

The thick purple brown mud and siltstone successions represent flood plain and overbank deposits. They contain evidence of periods of rapid deposition in the form of water escape structures and fragmentary fossilised bone horizons. The lack of sedimentary features in this facies assemblage may be a function of the blocky weathering or a combination of bioturbation and weathering. The burrows that are the focus of this study occur exclusively in the mudstone dominated facies assemblage.

The morphological features of the Hobbs Hill type burrows are characteristic of burrows produced by tetrapods rather than invertebrates or lungfish. Features that infer a tetrapod burrow producer include the low ramp, simple architecture, relatively large size (excludes invertebrates), cross-

sectional shape, scratch marks on the surface, occurrence in floodplain deposits (terrestrial) and association with tetrapod fossils. In addition to having features more characteristic of tetrapod burrows, the Hobbs Hill type burrows share many similarities with tetrapod burrow containing "in life position" fossils from the Permian and Triassic of Gondwana basin deposits. The Hobbs Hill type burrows, Type G burrows and Ichnogenus A (of Sidor *et al.*, 2008) are considered here to have been produced by the same organism based on the very similar burrow morphology.

Possible burrow producers include: *Procolophon trigoniceps* (often referred to as *Procolophon*), the procolophonoid *Kitchingnathus untabeni*, *Trirachodon*, *Galesaurus* (cynodont), *Progalesaurus* (cynodont), *Thrinaxodon liorhinus*, *Lystrosaurus* (dicynodont) and the akidnognathid *Olivierosuchus* or *Moschorhinus* (therocephalian). Based on biostratigraphy, the Hobbs Hill site is in the *Procolophon* subzone zone of the *Lystrosaurus* Assemblage Zone, in the Katberg Formation (Beaufort Group) which is Early Triassic, Olenekian ICS Stage (249.5-245.9 Ma) (Neveling, 2004; Cisneros, 2008; ICS and IUGS, 2012).

Based on the age ranges of the candidate burrow producers, it is possible to exclude *Trirachodon* as a trace maker. *Thrinaxodon liorhinus, Olivierosuchus* or *Moschorhinus* (therocephalian) and *Lystrosaurus* are too large to have produced the Hobbs Hill type burrows. *Galesaurus* and *Progalesaurus* (cynodont) may have been small enough to have used the Hobbs Hill type Burrows. Juvenile *Procolophon trigoniceps* is small enough to fit in the Hobbs Hill type burrows, Type G burrows and the Ichnogenus A (of Sidor *et al.*, 2008). The smaller procolophonid *Kitchingnathus untabeni* is an even more likely producer/user of the Hobbs Hill type burrows, Type G burrows and Ichnogenus A (of Sidor *et al.*, 2008), when considering size alone. While *Kitchingnathus untabeni* is a strong candidate based on its size and association with the Hobbs Hill site, the lack of this species at Kitching Ridge makes it less attractive than *Procolophon trigoniceps.*

In addition to the morphological similarities between the Hobbs Hill burrows and the Type G burrows, both occur in association with relatively concentrated occurrences of *Procolophon* fossils. Smaller taxa dominate the majority of the *Lystrosaurus* Assemblage Zone with larger taxa limited to the base of the biozone (Neveling, 2004). Fossil abundances decrease towards the top of the biozone with the exception of isolated occurrences of *Procolophon* dominated deposits. As an arid, hot climate favours the decrease in organism size (Lilliput effect), the fauna Karoo Basin became smaller during the Early Triassic (Neveling, 2004; Twitchett, 2007; Harries and Knorr, 2009; Sun *et al.*, 2012). The ability to burrow would have provided protection from the extreme Early Triassic climate. Therefore, the reason why the relatively large *Procolophon* was able to survive when most other large fauna disappeared from the Karoo Basin is most likely because of its fossorial lifestyle. The occurrence of *Procolophon* in un-described burrows (Groenewald, 1991) and the close association between *Procolophon* dominated deposits with burrows (at Hobbs Hill and at Kitching Ridge) provide supporting evidence for *Procolophon* as the producer of the Hobbs Hill and Type G burrows (and therefore also the Ichnogenus A type burrows).

Histological and functional morphological studies on *Procolophon trigoniceps* bone tissues provide evidence that *Procolophon trigoniceps* was able to burrow and did not suffer seasonal stress (Colbert and Kitching, 1975; deBraga, 2003; Botha-Brink and Smith, 2012). In particular, the lack of growth rings in the *Procolophon trigoniceps* fossils is considered an indicator of the lack of environmental stress because they were protected from the harsh seasonal conditions in their burrows (Botha-Brink and Smith, 2012). However, the lack of growth rings could also be because the animal reached adulthood within one season (most likely less than a year) (Botha-Brink and Smith, 2012).

The use of 3D digital copies for better comparison/accuracy.

The importance of accurate and unambiguous descriptions of trace fossils cannot be over emphasised. Unfortunately the description of a 3D object in a 2D results in a loss of information and generalisations are often necessary (Remondino *et al.*, 2010). By using averages and reporting only certain measurements, the researcher can give the reader an idea of the burrow morphology. This is not the ideal situation as many of the morphological properties of the burrows change along the length of the burrow. The surficial morphology which can make the difference between identifying the producer or not is also not adequately the recorded in 2D photographs and sketches, even less so when described in words only. The exact points at which measurements such as diameter are made are generally not reported. These are a few examples of the limitations of conventional methods of recording the dimensions and morphology of burrows. If a feature such as the cross sectional shape was consistent along the length of a burrow then it would be possible the make accurate generalisations, this is often not the case with biological structures such as burrows. While these methods can be used to compare and thereby determine the sameness of burrows and possibly a common producer a more accurate method is possible.

The use of photogrammetry in scientific fields is rapidly developing with the goal of increasing accuracy and precision (Remondino *et al.*, 2010; Falkingham, 2012). The advent of 3D printing and subsequent increase in affordability of 3D printing and rapid prototyping has resulted in the development of user-friendly low cost scanning techniques. 123D is one of these which uses photogrammetry, cloud servers and free software to allow users to create 3D copies and convert them into printable file formats. Online 3D printing services and rapid prototyping allow almost anyone to print out 3D objects saved in the appropriate file format. In this study, several sections of a burrow were converted into a 3D digital copy using photogrammetry and 123D. The result was then converted to the printing format to illustrate one of the potential uses of 3D scanning and processing.

By using 3D scanning or photogrammetry to produce a 3D digital copy of a burrow the morphological characteristics are more accurately described. Even if the accuracy of the technique is not at the level where an exact replica can be produced, it is still much better than written and 2D graphical representations alone. Therefore, 3D copies of scanned burrows should be produced when possible in conjunction with conventional descriptions. Using both techniques will greatly assist in the comparison of burrows and the identification of the burrow producers.

9. Acknowledgements

I would like to thank my supervisor Dr Emese Bordy for her guidance in all aspects of postgraduate studies and life, her work ethic, perseverance and ability is inspirational. I would like to thank everyone for their advice and comments at Geosynthesis 2011 (Cape Town), the Palaeo-Discussion Group (Zoology Department UCT), PSSA conference (2010 and 2012) and subsequent communications, although our communications may have been limited many of your words echoed through my mind in the last 2 years undoubtedly influencing the path of this project. I would like to thank all the members of the Department of Geological Sciences UCT (2011-2013), your support, interest, encouragement, advice and work (in both professional and personal capacities) made this project possible and my transition into the department and Cape Town easier. I would like to thank Pierre Moulon, Robert Nagy and Chloe Adams for their help with the Python Photogrammetry Toolbox, photography and understanding 3D software respectively. Without funding, I would not have been able to pursue this degree; the funding provided by the NRF Free-Standing Masters Scholarship (2011, 2012), Emese Bordy's NRF Incentive and URC Funds, the KW Johnstone Bursary and the GSSA WCB Geosynthesis Sponsorship were greatly appreciated and essential.

10. References

Abdala F, Cisneros JC and Smith RMH (2006) Faunal Aggregation in the Early Triassic Karoo Basin: Earliest Evidence of Shelter-Sharing Behaviour Among Tetrapods? *Palaios* **21:** 507–512.

Alonso-Zarza AM and Wright VP (2010) Calcretes. In Developments in Sedimentology, Volume **61**, Alonso-Zarza, AM & Tanner, LH (ed.) *Carbonates in Continental Settings: Facies, Environments, and Processes.* Elsevier, pp.225–267.

ALOOPINICON (2009) Meshing Point Clouds. *meshlastuff.blogspot.com* Available at: http://meshlabstuff.blogspot.com/2009/09/meshing-point-clouds.html [Accessed December 17, 2012].

Bangert B, Stollenhofen H, Lorenz V and Armstrong R (1999) The geochronology and significance of ash-fall tuffs in the glaciogenic Carboniferous-Permian Dwyka Group of Namibia and South Africa. *Journal of African Earth Sciences* **29:** 33–49.

Baucon A (2010) Da Vinci's Paleodictyon: the fractal beauty of traces. *Acta Geologica Polonica* **60:** 3–17.

Beerling DJ, Harfoot M, Lomax B and Pyle JA (2007) The stability of the stratospheric ozone layer during the end-Permian eruption of the Siberian Traps. *Philosophical Transactions of the Royal Society A: Mathematical, Physical and Engineering Sciences* **365:** 1843–1866.

Boggs S (2006) Principles of Sedimentology and Stratigraphy 4th edition. New Jersey: Pearson Prentice Hall. 662pp.

Bordy EM, Buchanan G and Krummeck W (2010) Recent sedimentological and palaeontological discoveries in the Lower to Mid-Triassic Tarkastad Subgroup (Beaufort Group, Karoo Supergroup), Transkei, Eastern Cape, South Africa. In Mostovski MB and Ovechkina MN (eds.): Proceedings of the 16th Biennial Conference of the Palaeontological Society of Southern Africa (Howick, 5-8 August, 2010). Pietermaritzburg, South Africa. p. 9.

Bordy EM, Sztano O, Rubidge BS and Bumby AJ (2011) Early Triassic vertebrate burrows from the Katberg Formation of the south-western Karoo Basin, South Africa. *Lethaia* **44:** 33–45.

Botha J and Smith RMH (2007) *Lystrosaurus* species composition across the Permo-Triassic boundary in the Karoo Basin of South Africa. *Lethaia* **40:** 125–137.

Botha-Brink J and Smith RMH (2012) Palaeobiology of Triassic *Procolophonids*, inferred from bone microstructure. *Comptes Rendus Palevol* **11:** 419–433.

Bromley RG and Frey RW (1974) Redescription of the trace fossil *Gyrolithes* and taxonomic evaluation of *Thalassinoides*, *Ophiomorpha* and *Spongeliomorpha*. *Bulletin of the Geological Society of Denmark* **23:** 311– 335.

Carlson KJ (1968) The Skull Morphology and Estivation Burrows of the Permian Lungfish, *Gnathorhiza serrata*. *The Journal of Geology* **76:** 641–663.

Catuneanu O (2004a) Basement control on flexural profiles and the distribution of foreland facies: The Dwyka Group of the Karoo Basin, South Africa. *Geology* **32:** 517.

Catuneanu O (2004b) Retroarc foreland systems—evolution through time. *Journal of African Earth Sciences* **38:** 225–242.

Catuneanu O and Elango HN (2001) Tectonic control on fluvial styles: the Balfour Formation of the Karoo Basin, South Africa. *Sedimentary Geology* **140:** 291–313.

Catuneanu O, Hancox PJ, Cairncross B and Rubidge BS (2002) Foredeep submarine fans and forebulge deltas: orogenic off-loading in the underfilled Karoo Basin. *Journal of African Earth Sciences* **35:** 489–502.

Catuneanu O, Hancox PJ and Rubidge BS (1998) Reciprocal flexural behaviour and contrasting stratigraphies: a new basin development model for the Karoo retroarc foreland system, South Africa. *Basin Research* **10:** 417–439.

Catuneanu O, Wopfner H, Eriksson PG, Cairncross B, Rubidge BS, Smith RMH and Hancox PJ (2005) The Karoo basins of south-central Africa. *Journal of African Earth Sciences* **43:** 211–253.

Chumakov NM and Zharkov MA (2002) Climate during Permian–Triassic Biosphere Reorganizations: Climate of the Early Permian. *Stratigraphy and Geological Correlation* **10:** 586–602.

Chumakov NM and Zharkov MA (2003) Climate during the Permian – Triassic Biosphere Reorganizations: Climate of the Late Permian and Early Triassic - General Inferences. *Stratigraphy and Geological Correlation* **11:** 361–375.

Cisneros JC (2006) A taxonomic revision of the genus *Procolophon* and the phylogenetic relationships of the procolophonoid reptiles. Unpublish Ph.D. thesis. University of the Witwatersrand, Johannesburg, 178.

Cisneros JC (2008) New basal Procolophonid reptile from the Katberg Formation (Lower Triassic) of the South African Karoo. *Palaeoworld* **17:** 126–134.

Colbert EH and Kitching JW (1975) The Triassic Reptile *Procolophon* in Antarctica. *American Museum Novitates***:** 1–23.

Cole DI (1992) Evolution and Development of the Karoo Basin. In *Inversion Tectonics of the Cape Fold Belt, Karoo and Cretaceous Basins of Southern Africa*, De Wit MJ and Ransome IG (eds.) pp 87–89. Rotterdam: Taylor and Francis, 1992.

Colombera L, Mountney NP and Mccaffrey WD (2012) A Relational Database for the Digitization of Fluvial Architecture: Toward Quantitative Synthetic Depositional Models, *AAPG* #40933 (2012).

Damiani R, Modesto S, Yates A and Neveling J (2003) Earliest evidence of cynodont burrowing. *Proceedings of the Royal Society of London: Biological sciences* **270:** 1747–51.

deBraga M (2003) The postcranial skeleton, phylogenetic position, and probable lifestyle of the Early Triassic reptile *Procolophon trigoniceps*. *Canadian Journal of Earth Sciences* **40:** 527–556.

DeCelles PG and Giles KA (1996) Foreland basin systems. *Basin Research* **8:** 105–123.

Dubiel RF, Blodgett RH and Bown TM (1987) Lungfish Burrows in the Upper Triassic Chinle and Dolores Formations, Colorado Plateau. *Journal of Sedimentary Petrology* **57**: 512-521.

Dubiel RF, Parrish JT, Parrish JM and Good SC (1991) The Pangaean megamonsoon; evidence from the Upper Triassic Chinle Formation, Colorado Plateau. *Palaios* **6:** 347– 370.

Duncan RA, Hooper PR, Rehacek J, Marsh JS and Duncan AR (1997) The timing and duration of the Karoo igneous event, southern Gondwana. *Journal of Geophysical Research* **102:** 18127–18138.

Efremov JA (1940) Taphonomy: New Branch of Paleontology. *Pan-American Geologist* **74:** 81–93.

Ekdale AA and De Gibert JM (2010) Paleoethologic Significance of Bioglyphs: Fingerprints of the Subterraneans. *Palaios* **25:** 540–545.

Ennex Corporation (2013) The StL Format. *Fabbers* Available at: http://www.ennex.com/~fabbers/StL.asp.

Erwin DH (1998) The end and the beginning: recoveries from mass extinctions. *Trends in Ecology and Evolution* **13:** 344–349.

Falkingham PL (2012) Acquisition of high resolution three-dimensional models using free, open-source, photogrammetric software. *Palaeontologia Electronica* **15:** 15.

Frey RW and Pemberton SG (1985) Biogenic Structures in Outcrops and Cores. 1. Approaches to Ichnology. *Bulletin of Canadian Petroleum Geology* **33:** 72–115.

G.S.I (2013) The Basics of Photogrammetry V-Stars. *Geodetic Systems* Available at: http://www.geodetic.com/v-stars/what-is-photogrammetry.aspx [Accessed February 14, 2013].

Gastaldo RA and Rolerson MW (2008) *Katbergia* Gen. Nov., a New Trace Fossil from Upper Permian and Lower Triassic Rocks of the Karoo Basin: Implications for Palaeoenvironmental Conditions at the P/Tr Extinction Event. *Palaeontology* **51:** 215– 229.

De Gibert JM and Ekdale AA (2010) Paleobiology of the Crustacean Trace Fossil *Spongeliomorpha iberica* in the Miocene of Southeastern Spain. *Acta Palaeontologica Polonica* **55:** 733–740.

Gradstein FM, Ogg JG and Smith AG (2005) Triassic Period. In Gradstein FM, Ogg JG and Smith AG (eds) *A Geologic Time Scale.* Cambridge University Press, pp. 271–306.

Groenewald GH (1991) Burrow casts from the *Lystrosaurus-Procolophon* Assemblage-zone, Karoo Sequence, South Africa. *Koedoe - African Protected Area Conservation and Science* **34:** 13–22.

Groenewald GH (1996) *Stratigraphy and sedimentology of the Tarkastad subgroup, Karoo Supergroup, South Africa.* Unpublished PhD Thesis, University of Port Elizabeth, pp.145.

Groenewald GH and Kitching JW (1995) Biostratigraphy of the *Lystrosaurus* Assemblage Zone. In Rubidge BS (ed) *Biostratigraphy of the Beaufort Group (Karoo Supergroup)*, South African Committee for Stratigraphy, pp. 25–39.

Groenewald GH, Welman J and MacEachern JA (2001) Vertebrate Burrow Complexes from the Early Triassic *Cynognathus* Zone (Driekoppen Formation, Beaufort Group) of the Karoo Basin, South Africa. *Palaios* **16:** 148.

Gruen A (2012) Development and Status of Image Matching in Photogrammetry. *The Photogrammetric Record* **27:** 36–57.

Hasiotis ST (2003) Complex ichnofossils of solitary and social soil organisms: understanding their evolution and roles in terrestrial paleoecosystems. *Palaeogeography, Palaeoclimatology, Palaeoecology* **192:** 259–320.

Hasiotis ST and Mitchell CE (1993) A comparison of crayfish burrow morphologies: Triassic and Holocene fossil, paleo- and neo-ichnological evidence, and the identification of their burrowing signatures. *Ichnos* **2:** 291–314.

Hasiotis ST, Mitchell CE and Dubiel RF (1993) Application of morphologic burrow interpretations to discern continental burrow architects: Lungfish or crayfish? *Ichnos* **2:** 315–333.

Hasiotis ST (2004) Reconnaissance of Upper Jurassic Morrison Formation ichnofossils, Rocky Mountain Region, USA: paleoenvironmental, stratigraphic, and paleoclimatic significance of terrestrial and freshwater ichnocoenoses. *Sedimentary Geology* **167:** 177–268.

Hasiotis ST, Wellner RW, Martin AJ, Demko TM and Taylor P (2004) Vertebrate Burrows from Triassic and Jurassic Continental Deposits of North America and Antarctica: Their Paleoenvironmental and Paleoecological Significance. *Ichnos* **11:** 103–124.

Hembree DI and Hasiotis ST (2007) Biogenic Structures Produced by Sand-Swimming Snakes: A Modern Analogue for Interpreting Continental Ichnofossils. *Journal of Sedimentary Research* **77:** 389–397.

Hiller N and Stavrakis N (1984) Permo-Triassic fluvial systems in the southeastern Karoo Basin, South Africa. *Palaeogeography, Palaeoclimatology, Palaeoecology* **45:** 1–21.

ICS and IUGS (2012) International chronostratigraphic chart. *International Commission on Stratigraphy***: 541** Available at: http://www.stratigraphy.org/column.php?id=Chart/Time Scale [Accessed January 20, 2013].

ISPRS (2008) STATUTES of International Society for Photogrammetry and Remote Sensing, **Amended 2008:** 1–6.

Jefferson H (1983) Permian and Triassic woods from the Transantarctic Mountains : Paleoenvironmental indicators. *Antarctic Journal* **114:** 55–57.

Johnson MR (1976) Stratigraphy and sedimentology of the Cape and Karoo Sequences in the Eastern Cape Province. Unpublished Ph.D. thesis. Rhodes University**:** 351.

Johnson MR, Van Vuuren CJ, Hegenberger WF, Key R and Shoko U (1996) Stratigraphy of the Karoo Supergroup in southern Africa: an overview. *Journal of African Earth Sciences* **23:** 3–15.

Johnson MR, Van Vuuren CJ, Visser JNJ, Cole DI, De Wickens H, Christie ADM, Roberts DL and Brandl G (2006) Sedimentary rocks of the Karoo Supergroup. In Johnson MR, Anhaeusser CR and Thomas RJ (eds) *The Geology of South Africa*, Johannesburg: Geological Society of South Africa/Council for Geoscience.

Kalloniatis M and Luu C (2007) Space Perception. *Webvision: The Organization of the Retina and Visual System* Available at: http://webvision.med.utah.edu/book/part-viiigabac-receptors/space-perception/ [Accessed February 8, 2013].

Kidder DL and Worsley TR (2004) Causes and consequences of extreme Permo-Triassic warming to globally equable climate and relation to the Permo-Triassic extinction and recovery. *Palaeogeography, Palaeoclimatology, Palaeoecology* **203:** 207–237.

Kidder DL and Worsley TR (2010) Phanerozoic Large Igneous Provinces (LIPs), HEATT (Haline Euxinic Acidic Thermal Transgression) episodes, and mass extinctions. *Palaeogeography, Palaeoclimatology, Palaeoecology* **295:** 162–191.

Kiehl JT and Shields CA (2005) Climate simulation of the latest Permian: Implications for mass extinction. **Geology 33:** 757–760.

Kinlaw A (1999) A review of burrowing by semi-fossorial vertebrates in arid environments. *Journal of Arid Environments* **41:** 127–145.

Klappa CF (1979) Comment and Reply on "Displacive calcite: Evidence from recent and ancient calcretes" : COMMENT. *Geology* **7**: 420-421.

Lerner J and Tirole J (2000) The Simple Economics of Open Source. *Working Paper* **7600:** 38.

Lock BE (1978) The Cape Fold Belt of South Africa; tectonic control of sedimentation. *Proceedings of the Geologists' Association* **89:** 263–281.

Lucas SG (1998) Global Triassic tetrapod biostratigraphy and biochronology. *Palaeogeography, Palaeoclimatology, Palaeoecology* **143:** 347–384.

Lucas SG (2010a) The Triassic timescale: an introduction. *Geological Society, London, Special Publications* **334:** 1–16.

Lucas SG (2010b) The Triassic timescale based on nonmarine tetrapod biostratigraphy and biochronology. *Geological Society, London, Special Publications* **334:** 447–500.

Martin AJ, Rich TH, Poore GCB, Schultz MB, Austin CM, Kool L and Vickers-Rich P (2008) Fossil evidence in Australia for oldest known freshwater crayfish of Gondwana. *Gondwana Research* **14:** 287–296.

Mathews NA (2008) Aerial and Close-Range Photogrammetric Technology: Providing Resource Documentation, Interpretation, and Preservation. Technical Note 428. Denver, Colorado.

Merry B and Held C (2011) MLS reconstruction from noisy point sets. *Technical report, University of Cape Town, Department of Computer Science,* **CS11-04-00**: 15.

Miall AD (1985) Architectural-element analysis: A new method of facies analysis applied to fluvial deposits. *Earth-Science Reviews* **22:** 261–308.

Miall AD (1996) The geology of fluvial deposits: Sedimentary facies, basin analysis, and petroleum geology. Berlin and New York: Springer Verlag. 582pp.

Miall AD (2000) Principles of Sedimentary Basin Analysis. 3rd ed. Berlin and New York: Springer Verlag. 616pp.

Miller MF, Hasiotis ST, Babcock LE, Isbell JL and Collin (2001) Tetrapod and large burrows of uncertain origin in Triassic high paleolatitude floodplain deposits, Antarctica. *Palaios* **16:** 218–232.

Mitrovica JX, Beaumont C and Jarvis GT (1989) Tilting of continental interiors by the dynamical effects of subduction. *Tectonics* **8:** 1079–1094.

Modesto SP and Botha-Brink J (2010a) A Burrow Cast with *Lystrosaurus* Skeletal Remains from the Lower Triassic of South Africa. *Palaios* **25:** 274–281.

Modesto SP and Botha-Brink J (2010b) Problems of correlation of South African and South American tetrapod faunas across the Permian–Triassic boundary. *Journal of African Earth Sciences* **57:** 242–248.

Moraes C (2012a) Converting pictures into a 3D mesh with PPT, MeshLab and Blender. *ArcTeam Open Research* Available at: http://arc-team-openresearch.blogspot.com/2012/09/converting-pictures-into-3d-mesh-with.html.

Moraes C (2012b) How to make 3D scan with pictures and the PPT GUI. *Arc-Team Open Research* Available at: http://arc-team-open-research.blogspot.com/2012/12/how-tomake-3d-scan-with-pictures-and.html [Accessed February 6, 2013].

Moraes C (2012c) Taung Project: 3D Forensic Facial Reconstruction. *Arc-Team Open Research* Available at: http://arc-team-open-research.blogspot.com/2012/11/taungproject-3d-forensic-facial.html [Accessed December 17, 2012].

Moulon P and Bezzi A (2011) Python Photogrammetry Toolbox: A free solution for Three-Dimensional Documentation. In *ArcheoFoss 6-Workshop Open Source, Free Software e Open Format nei processi di ricerca archeologica VI Workshop (Napoli, 9/10 giugno 2011)* Napoli, Italy, pp 1–12.

Neveling J (2004) Stratigraphic and sedimentological investigation of the contact between the *Lystrosaurus* and the *Cynognathus* Assemblage Zones (Beaufort Group : Karoo Supergroup). *Bulletin of the Council for Geoscience* **137:** 164 pp.

Newby PRT (2012) Photogrammetric Terminology: 2nd Edition. *The Photogrammetric Record* **27:** 360–386.

Noursalehi E (2012) 123D Catch - How to Make 3D Models from Pictures. *YouTube* Available at: http://www.youtube.com/watch?v=NsBg-m2hrIM [Accessed February 8, 2013].

Owen G and Moretti M (2011) Identifying triggers for liquefaction-induced soft-sediment deformation in sands. *Sedimentary Geology* **235:** 141–147.

Pace DW, Gastaldo RA and Neveling J (2009) Early Triassic Aggradational and Degradational Landscapes of the Karoo Basin and Evidence for Climate Oscillation Following the P-Tr Event. *Journal of Sedimentary Research* **79:** 316–331.

Parrish JT (1993) Climate of the Supercontinent Pangea. *The Journal of Geology* **101:** 215–233.

Payne JL, Lehrmann DJ, Wei J, Orchard MJ, Schrag DP and Knoll AH (2004) Large perturbations of the carbon cycle during recovery from the end-permian extinction. *Science* **305:** 506–9.

Peel MC, Finlayson BL and McMahon TA (2007) Updated world map of the Koppen-Geiger climate classification. *Hydrology and Earth System Science* **11:** 1633–1644.

Pemberton SG, Spila M, Pulham AJ, Saunders T, MacEachern JA, Robbins D and Sinclair LK (2001) Ichnology and sedimentology of the shallow to marginal marine systems: Ben Nevis and Avalon reservoirs, Jeanne D' Arc Basin. Geological Association of Canada. *Short Course Notes* **15.** pp.

Platt BF, Hasiotis ST and Hirmas DR (2010) Use of Low-Cost Multistripe Laser Triangulation (MLT) Scanning Technology for Three-Dimensional, Quantitative Paleoichnological and Neoichnological Studies. *Journal of Sedimentary Research* **80:** 590–610.

Preto N, Kustatscher E and Wignall PB (2010) Triassic climates — State of the art and perspectives. *Palaeogeography, Palaeoclimatology, Palaeoecology* **290:** 1–10.

ProtoCAM (2012) Acceptable CAD Formats. *ProtoCAD* Available at: http://www.protocam.com/html/stl.html [Accessed February 8, 2013].

Quast A, Hoefs J and Paul J (2006) Pedogenic carbonates as a proxy for palaeo-CO_2 in the Palaeozoic atmosphere. *Palaeogeography, Palaeoclimatology, Palaeoecology* **242:** 110–125.

Ray S and Chinsamy A (2003) Functional aspects of the postcranial anatomy of the Permian dicynodont Diictodon and their ecological implications. *Palaeontology* **46:** 151–183.

Remondino F, Rizzi A, Girardi S, Petti FM and Avanzini M (2010) 3D Ichnology — Recovering Digital 3D Models of Dinosaur Footprints. *The Photogrammetric Record* **25:** 266–282.

Retallack GJ, Smith RMH and Ward PD (2003) Vertebrate extinction across Permian-Triassic boundary in Karoo Basin, South Africa. *GSA Bulletin* **115:** 1133–1152.

Retallack GJ, Veevers JJ and Morante R (1996) Global coal gap between Permian-Triassic extinction and Middle Triassic recovery of peat-forming plants. *Geological Society of America Bulletin* **108:** 195–207.

Retallack GJ, Sheldon ND, Carr PF, Fanning M., Thompson C, Williams ML, Jones BG And Hutton A (2011). Multiple Early Triassic greenhouse crises impeded recovery from Late Permian mass extinction. *Palaeogeography, Palaeoclimatology, Palaeoecology*, **308:** 233–251.

Riese DJ, Hasiotis ST and Odier GP (2011) Synapsid Burrows and Associated Trace Fossils in the Lower Jurassic Navajo Sandstone, Southeastern Utah, U.S.A., Indicates a Diverse Community Living in a Wet Desert Ecosystem. *Journal of Sedimentary Research* **81:** 299–325.

Royer DL, Berner RA, Montañez IP, Tabor NJ and Beerling DJ (2004) CO_2 as a primary driver of Phanerozoic climate. *GSA Today* **14:** 4.

Rubidge BS (2005) 27th Du Toit Memorial Lecture Re-uniting lost continents – Fossil reptiles from the ancient Karoo and their wanderlust. *South African Journal of Geology* **108:** 135–172.

Rubidge BS, Johnson MR, Kitching JW, Smith RMH, Keyser AW and Groenewald GH (1995) An introduction to the Biozonation of the Beaufort Group. In Rubidge, B.S. (ed) *Biostratigraphy of the Beaufort Group (Karoo Supergroup)*, Geological Survey of South Africa, pp, 1–2.

Rubidge BS, Erwin DH, Ramezani J, Bowring SA and de Klerk WJ (2013) High-precision temporal calibration of Late Permian vertebrate biostratigraphy: U-Pb zircon constraints from the Karoo Supergroup, South Africa. *Geology*-published online 4 January 2013; doi: 10.1130/G33622.1

Saigal GC and Walton EK (1988) On the Occurrence of Displacive Calcite in Lower Old Red Sandstone of Carnoustie, Eastern Scotland. *SEPM Journal of Sedimentary Research* **58:** 131–135.

Scheidegger C, Fleishman S and Silva C (2005) Triangulating point set surfaces with bounded error. In Desbrun M and Pottmann H (eds) *Proceedings of the third Eurographics Symposium on Geometry,* pp. 63–72.

Scotese CR (2004) A Continental Drift Flipbook. *The Journal of Geology* **112:** 729–741.

Scotese CR (2008) Climate History. *PALEOMAP Project* Available at: http://www.scotese.com/climate.htm [Accessed December 17, 2012].

Scotese CR, Boucot AJ and Mckerrow WS (1999) Gondwanan palaeogeography and palaeoclimatology. *Journal of African Earth Sciences* **28:** 99–114.

Scotese CR and McKerrow WS (1990) Revised World maps and introduction. *Geological Society, London, Memoirs* **12:** 1–21.

Seilacher A (1967) Bathymetry of trace fossils. *Marine Geology* **5:** 413–428.

Seilacher A (2007) Trace Fossil Analysis. Berlin: Springer. p. 241.

Shen S, Crowley JL, Wang Y, Bowring S, Erwin DH, Sadler PM, Cao C, Rothman DH, Henderson CM, Ramezani J, Zhang H, Shen Y, Wang X, Wang W, Mu L, Li W, Tang Y, Liu X, Liu L, Zeng Y, Jiang Y, Jin Y (2011). Calibrating the end-Permian mass extinction. *Science* **334 (6061)**: 1367–72.

Sidor CA, Miller MF, Isbell JL and Museum B (2008) Featured Article Tetrapod Burrows From the Triassic of Antarctica. *Journal of Vertebrate Paleontology* **28:** 277–284.

Smith C (2006) On Vertex-Vertex Systems and Their Use in Geometry and Biological Modelling. Unpublished Ph.D. dissertation. University of Calgary**:** 216.

Smith RMH and Botha J (2005) The recovery of terrestrial vertebrate diversity in the South African Karoo Basin after the end-Permian extinction. *Comptes Rendus Palevol* **4:** 623– 636.

Smith RMH (1987) Helical burrow casts of therapsid origin from the Beaufort Group (Permian) of South Africa. *Palaeogeography, Palaeoclimatology, Palaeoecology* **60:** 155–169.

Smith RMH (1990) A review of stratigraphy and sedimentary environments of the Karoo Basin of South Africa. *Journal of African Earth Sciences (and the Middle East)* **10:** 117–137.

Smith RMH (1993) Vertebrate Taphonomy of Late Permian Floodplain Deposits in the Southwestern Karoo Basin of South Africa. *Palaios* **8:** 45–67.

Smith RMH (1995) Changing fluvial environments across the Permian-Triassic boundary in the Karoo Basin, South Africa and possible causes of tetrapod extinctions. *Palaeogeography, Palaeoclimatology, Palaeoecology* **117:** 81–104.

Smith RMH, Eriksson PG and Botha WJ (1993) A review of the stratigraphy and sedimentary environments of the Karoo-aged basins of Southern Africa. *Journal of African Earth Sciences* **16:** 143–169.

Smith RMH and Ward PD (2001) Pattern of vertebrate extinctions across an event bed at the Permian-Triassic boundary in the Karoo Basin of South Africa. *Geology* **29:** 1147.

Stouffer R, Yin J and Gregory J (2006) Investigating the causes of the response of the thermohaline circulation to past and future climate changes. *Journal of Climate* **19:** 1366–1387.

Sun Y, Joachimski MM, Wignall PB, Yan C, Chen Y, Jiang H, Wang L and Lai X (2012) Lethally hot temperatures during the Early Triassic greenhouse. *Science* **338:** 366–70.

Svensen H and Jamtveit B (2010) Metamorphic Fluids and Global Environmental Changes. *Elements* **6:** 179–182.

Svensen H, Planke S, Chevallier L, Malthe-Sørenssen A, Corfu F and Jamtveit B (2007) Hydrothermal venting of greenhouse gases triggering Early Jurassic global warming. *Earth and Planetary Science Letters* **256:** 554–566.

Svensen H, Planke S, Polozov AG, Schmidbauer N, Corfu F, Podladchikov YY and Jamtveit B (2009a) Siberian gas venting and the end-Permian environmental crisis. *Earth and Planetary Science Letters* **277:** 490–500.

Svensen H, Schmidbauer N, Roscher M, Stordal F and Planke S (2009b) Contact metamorphism, halocarbons, and environmental crises of the past. *Environmental Chemistry* **6:** 466.

Tamura N (2007) *Cynognathus crateronotus*. *Spinops*. Available at: http://spinops.blogspot.com/2012/05/cynognathus-crateronotus.html [Accessed December 17 2012].

Tankard A, Welsink H, Aukes P, Newton R and Stettler E (2009) Tectonic evolution of the Cape and Karoo basins of South Africa. *Marine and Petroleum Geology* **26:** 1379–1412.

Tankard A, Welsink H, Aukes P, Newton R and Stettler E (2012) Geodynamic interpretation of the Cape and Karoo basins, South Africa. In Roberts DG and Bally AW (eds) *Regional Geology and Tectonics: Phanerozoic Rift Systems and Sedimentary Basins: Phanerozoic Rift Systems and Sedimentary Basins*, Elsevier Science, pp. 869–932.

Tankard AJ, Jackson MPA, Eriksson KA, Hobday DK, Hunter DR and Minter WEL (1982) Crustal evolution of southern Africa: 3.8 billion years of earth history New York: Springer Verlag.

Thomson GH (2010) Digital Camera Performance Where Spatial Resolution is Determined by the Optical Component. *The Photogrammetric Record* **25:** 42–46.

Trouw R and De Wit M (1999) Relation between the Gondwanide Orogen and contemporaneous intracratonic deformation. *Journal of African Earth Sciences* **28:** 203– 213.

Turner BR (1999) Tectonostratigraphical development of the Upper Karoo foreland basin: Orogenic unloading versus thermally-induced Gondwana rifting. *Journal of African Earth Sciences* **28:** 215–238.

Veldhuis H and Vosselman G (1998) The 3D reconstruction of straight and curved pipes using digital line photogrammetry. *ISPRS Journal of Photogrammetry and Remote Sensing* **53:** 6–16.

Visser JNJ (1989) The Permo-Carboniferous Dwyka Formation of Southern Africa: Deposition by Predominantly Subpolar Marine Ice Sheets. *Palaeogeography, Palaeoclimatology, Palaeoecology* **70:** 377–391.

Visser JNJ, Von Brunn V and Johnson MR (1990) Dwyka Group Catalogue of South African Lithostratigraphic Units. *SA committee for Stratigraphy***:** 1–3.

Voigt S, Schneider JW, Saber H, Hminna A, Lagnaoui A, Klein H, Brosig A and Fischer J (2011) Complex Tetrapod Burrows From Middle Triassic Red Beds of the Argana Basin (Western High Atlas, Morocco). *Palaios* **26:** 555–566.

Wang P (2009) Global monsoon in a geological perspective. *Chinese Science Bulletin* **54:** 1113–1136.

Ward P, Montgomery D and Smith R (2000) Altered river morphology in South Africa related to the Permian-Triassic extinction. *Science* **289:** 1740–3.

Wignall PB (2001) Large igneous provinces and mass extinctions. *Earth-Science Reviews* **53:** 1–33.

De Wit MJ and Ransome IGD (1992) Regional inversion tectonics along the southern margin of Gondwana. In *Inversion Tectonics of the Cape Fold Belt, Karoo and Cretaceous Basins of Southern Africa: Proceedings of a Conference, Cape Town, South Africa, 2-6 December 1991* pp 15–32.

Wright VP and Marriott SB (2007) The dangers of taking mud for granted: Lessons from Lower Old Red Sandstone dryland river systems of South Wales. *Sedimentary Geology* **195:** 91–100.

Yilmaz M.H., Yakar M. and Yildiz F. (2008) Digital Photogrammetry in Obtaining of 3D Model Data of Irregular Small Objects. *The International Archives of the Photogrammetry, Remote Sensing and Spatial Information Science* **37:** 125–130.

Ziegler A, Eshel G, Rees PM, Rothfus T, Rowley D and Sunderlin D (2003) Tracing the tropics across land and sea: Permian to present. *Lethaia* **36:** 227–254.

Ziegler AM, Parrish JMIT, Jiping YAO, Gyllenhaal ED, David B, Shangyou NIE, Bekker A, Hulver ML and Rowley DB (1993) Early Mesozoic Phytogeography and Climate. *Philosophical Transactions: Biological Sciences* **341:** 297–305.